STRUCTURAL OPTIMIZATION USING MATLAB PARTIAL DIFFERENTIAL EQUATION TOOLBOX AND RADIAL BASIS FUNCTION BASED RESPOSNE SURFACE MODELS

by

FAISAL TANVEER MOSHARROF

Presented to the Faculty of the Graduate School of

The University of Texas at Arlington in Partial Fulfillment

of the Requirements

for the Degree of

MASTER OF SCIENCE IN MECHANICAL ENGINEERING

THE UNIVERSITY OF TEXAS AT ARLINGTON

August 2008

This work is dedicated to my parents,

Mr. Mosharrof Hossain and Mrs. Shaheen Mosharrof

who have been always there for me and for their love, support and inspiration without which my graduate study at UT Arlington could not be possible.

ACKNOWLEDGEMENTS

First, I would like to express my deepest gratitude and admiration to my supervisor Dr. Bo Ping Wang for his help and patience through out my Masters studies. His excellent guidance and support made my working and learning experience a very special one. This thesis would not have been completed without his constant inspiration and encouragement.

I want to extend my sincere appreciation and special thanks to Dr. Wen S. Chan and Dr. Kent L. Lawrence for their support and time in serving as my committee members and providing valuable suggestions regarding this thesis.

Special thanks and love to my parents, my wife Tashfee, my sister Deniz, my brother Saikat, other family members and all of my friends for their endless inspiration, love and support through out my graduate studies.

And last but not the least, I thank the Almighty Allah for giving me the strength to overcome all the difficulties and for being with me in all walks of my life.

July 17, 2008

ABSTRACT

STRUCTURAL OPTIMIZATION USING MATLAB PARTIAL DIFFERENTIAL EQUATION TOOLBOX AND RADIAL BASIS FUNCTION BASED RESPOSNE SURFACE MODELS

Faisal Tanveer Mosharrof, M.S.

The University of Texas at Arlington, 2008

Supervising Professor: Bo Ping Wang

As a decision making tool, optimization has become an inseparable part of the modern design process. However, in spite of the advances in computer capacity and speed, the computational time for some complex problems is too high to use conventional solution approach. In order to reduce the computational effort and the cost associated with such type of problems, approximation methods such as response surface methodology (RSM) along with design of experiments (DOE) are used in engineering design optimization. The main idea involves replacing the expensive simulation model during the design and optimization process with a simplified mathematical approximation of the original problem. This method is applicable where the calculation

of the design sensitivity information is difficult or impossible to compute, and also in the cases with noisy functions, where the sensitivity information is not reliable. Although a variety of optimization techniques are already in use, researchers are working to figure out more efficient and improvised techniques for design optimization.

In this research, an efficient and simple structural optimization method based on response surface methodology and design of experiments has been developed and implemented using MATLAB for solving computationally expensive design optimization problems. Four different radial basis function models known as Multiquadric Interpolation, Multiquadric Regularization, Gauss Interpolation, and Gauss Regularization were utilized for constructing the response surface models and three different low discrepancy sequencing methods known as Halton sequence, Faure sequence, and Sobol sequence were used to generate the design of experiments. MATLAB Partial Differential Equation Toolbox was used for finite element model development and determining the true response of the design problems. Several design optimization problems have been solved using the proposed optimization scheme. The results thus obtained have been compared to that attained by solving the same problems using MATLAB optimization function *fmincon*. The comparison of the results demonstrates the effectiveness and applicability of the proposed optimization scheme.

TABLE OF CONTENTS

LIST OF ILLUSTRATIONS

LIST OF TABLES

CHAPTER 1

INTRODUCTION

In today's competitive world, engineers and manufacturers are under enormous pressure for the reduction of production cost and time, but at the same time improving the product quality. Design of complex engineering systems includes a wide variety of activities whose objective is to determine the optimum characteristics of a product even before it is manufactured. Nowadays, as a decision making tool, optimization has become an integral part of the design process. Design optimization intends to minimize or maximize the objective functions by selecting properly the design variables and by satisfying the constraints [1]. The application of design optimization both shortens design-cycle time and identifies new designs that are not only feasible, but also increasingly optimal with respect to pre-specified design criterion.

Today's advanced finite element analysis (FEA) techniques, efficient computational algorithms and high power computers have enabled mechanical and structural design engineers to apply optimization techniques to find best possible solutions for complex engineering problems. Although a large variety of optimization techniques are currently being used in almost every discipline of engineering, researchers around the globe are working constantly to develop more efficient and improvised methods for design optimization. Since design optimization is an inherently nonlinear problem, there is no single method to solve all optimization problems

efficiently. Hence, the design engineer has to choose the most appropriate optimization method to solve his design problem by properly recognizing the nature of the problem and understanding the pros and cons of the optimization method he is intended to use.

1.1 Response Surface Approximation for Design Optimization

In structural optimization, the computational time for some complex problems is too high to use conventional solution approach. It can take several hours to get a finite element solution of one variant in order to obtain a response of the structure. Some times it is necessary to perform calculations of several thousand variants for the optimum design problem. For example, a single crash testing simulation can require 10 to 15 hours even when performed in a parallel processing environment [2]. Such complexity can severely limit comprehensive exploration of design alternatives. Consequently approximation methods such as response surface methodology are used in engineering design to minimize the computational expense of running such analysis and simulations, which is nothing but a simplified mathematical approximation of the actual problem.

Response surface methodology (RSM) is a method for constructing global approximations to system behavior based on results calculated at various points in the design space [3]. The strength of the method is in applications where the calculation of the design sensitivity information is difficult or impossible to compute, as well as in cases with noisy functions, where the sensitivity information is not reliable, or when the function values are inaccurate. Response surface methodology is associated with design of experiment (DOE). The selection of points in the design space where the response

must be evaluated is commonly known as design of experiment. The choice of experimental design can have a large influence on the accuracy of the approximation and the cost of constructing the response surface.

A variety of applications of the approximation methods in engineering design and optimization are found in the literature. These applications ranged from space station power systems, to fluid flow problems and oil tanker design, to structural design and automotive crash worthiness [4]. However, researches are going on for the development of new algorithms for applying approximation techniques for structural optimization more efficiently. In this research, a response surface approximation method based on radial basis function is employed for structural optimization.

1.2 Objective and Approach

The main objectives of this research are:

1. Development of an effective, simple and easy to apply structural optimization scheme using MATLAB Partial Differential Equation Toolbox and radial basis function (RBF) based response surface model for solving computationally expensive simulation based optimization problems.
2. Implementation of the developed scheme by solving various application problems.

These objectives are achieved by writing a design optimization code in MATLAB. Four different radial basis function models namely, Multiquadratic Interpolation, Multiquadratic Regularization, Gauss Interpolation and Gauss Regularization are used for constructing response surfaces, where as three different low discrepancy sequences namely, Halton, Faure and Sobol sequence are employed for

design of experiments creation. MATLAB Partial Differential Equation Toolbox is used for finite element analysis and obtaining true response of the problem. MATLAB built-in optimization function *fmincon* is used for response surface optimization.

The results obtained from the response surface optimization are then compared to those obtained by optimizing the actual problem using *fmincon* directly.

1.3 Contributions

This research contributed substantially to the following developments presented in this thesis:

1. Developed and implemented an effective, simple and easy to use response surface based optimization scheme for solving computationally expensive simulation based optimization problems.
2. Demonstrated the possibility of using four different forms of radial basis function for response surface approximation based structural optimization.
3. Systematically explored the possibility of using three different low discrepancy sequences for the generation of design of experiments (DOE) to be used for structural optimization.
4. Successfully employed MATLAB Partial Differential Equation Toolbox for solving simulation based structural optimization problems.

1.4 Outline of the Thesis

This thesis is documented into six chapters.

The general idea of structural optimization is presented in Chapter 2. Application of optimization in the field of engineering design, formulation of general

optimization problem, classifications of available optimization methods, the use of sequential quadratic programming for optimization are also discussed in this chapter.

In Chapter 3, a detailed discussion is presented on structural optimization based on response surface methodology (RSM), use of radial basis functions (RBF) for problem approximation, use of quasi Monte Carlo techniques for design of experiments (DOE) creation and use of MATLAB Partial Differential Equation Toolbox for structural optimization.

Chapter 4 explains the proposed algorithm for structural optimization using radial basis function based response surface model and MATLAB Partial Differential Equation Toolbox.

Chapter 5 presents the implementation of the proposed optimization scheme by solving ten different application problems.

Finally, the conclusions and recommendations for future research are presented in Chapter 7.

CHAPTER 2

STRUCTURAL OPTIMIZATION

2.1 Introduction

Optimization is the process of maximizing or minimizing a desired objective function while satisfying the prevailing constraints [5]. The ever-increasing competition and a growing dearth of the raw materials resulted in a demand for light weight and low cost structures. The weight or cost optimization of structures is the major means of existence for modern design and manufacturing industries. Hence, the motivation of optimization is to exploit the available limited resources in a manner that maximizes the utility. The objective of optimal design is to achieve the best feasible design according to a preselected measure of effectiveness [6].

2.2 Applications of Optimization

Optimization is not a new phenomenon in human life. In our daily life, we come across innumerable examples of optimization in nature. The honeycomb structure is an example of one of the most compact packaging arrangement. In metals and alloys, the atoms take positions of least energy to form unit cells that define the crystalline structure of materials. Optimization techniques are currently being used in a wide variety of industries like automobile, aerospace, electrical, chemical, MEMS and many other manufacturing industries. Over the last decades, design optimization theory has advanced rapidly and now it is a part and parcel of modern engineering design process.

Some examples of the diversified industrial applications of optimization technique are listed below:

1. Weight, vibration, and noise optimization of automobile for maximum fuel efficiency, reduction of manufacturing cost, and improving ride quality.
2. Design of aircraft and aerospace structures for minimum weight.
3. Design of structures like bridges, towers, dams for minimum cost.
4. Optimal design of various mechanical components like linkages, cams, machine tools etc.
5. Optimal design of electrical networks.
6. Optimization in production, planning, and control, etc.

2.3 Formulation of Optimization Problem

The optimization problem is stated as [7],

Find the set of design variables, $\mathbf{X} = \{X_1, X_2, X_3, \ldots..,X_n\}$, that will –

$$\text{Minimize} \quad F(\mathbf{X}) \tag{2.1}$$

$$\text{Subject to:} \quad g_j(\mathbf{X}) \leq 0 \qquad j = 1,\ldots,m \tag{2.2}$$

$$X_i^L \leq X_i \leq X_i^U \qquad i = 1,\ldots,n \tag{2.3}$$

The function, $F(\mathbf{X})$, is referred to as the objective or merit function and is dependent on the values of the design variables, $\mathbf{X}$, which themselves include member dimensions or shape variables of a structure as examples. The limits on the design variables, given in Eq. (2,3), are referred to as side constraints and are used to limit the region of search for the optimum. For maximization of $F(\mathbf{X})$, one has to simply minimize the negative of $F(\mathbf{X})$.

The $g_j(\mathbf{X})$ are referred to as constraints and they provide bounds on various response quantities. Some typical constraints for structural optimization include stress, displacement, frequency, local buckling, system buckling load factor, dynamic response, aeroelastic divergence and aeroelastic flutter, etc.

X* constitutes the optimum solution for the problem in k-dimensional space. Any optimization problem as stated above is known as constrained optimization problem. If there is no constraint present, that is known as unconstrained optimization problem.

2.4 Type of Optimization Methods

Over the years, optimization techniques have been studied extensively and have evolved considerably and many algorithms and implementations are now used by the engineering community. Optimization methods can be broadly classified into three categories [8]: (1) Conventional numerical optimization methods, (2) stochastic optimization methods, and (3) hybrid methods. These methods are briefly described below:

1. Conventional Numerical Optimization Methods:

These methods are also known as mathematical programming methods and are used to find the minimum of a function of several variables under a prescribed set of constraints. For these methods, it is now standard practice for computationally inexpensive approximate models to be used in lieu of exact models to reduce computational cost. One important reason these methods have been widely accepted and used is attributed to the theoretical guarantee of convergence to a local optima of the

exact problem. Some of the conventional numerical methods commonly used in engineering design are, steepest-descent methods, conjugate-gradient, quadratic programming, pattern search methods, linear approximation methods, etc.

2. Stochastic Optimization Method:

Conventional numerical optimization methods are very sensitive to the starting point selection and associated with the possibilities of stopping at local optima. The search for algorithms that are capable of avoiding local optima has led to the development of stochastic optimization techniques, where the probabilistic factors in the search process encourage global exploration. Stochastic techniques produce new design points that do not use information about the local slope of the objective function and are thus not prone to stalling at local optima as in the case with conventional numerical optimization methods. Examples of some modern stochastic optimization methods are simulated annealing, tabu search, genetic algorithms, particle swarm optimization, ant colony optimization, differential evolution etc.

3. Hybrid Methods:

The design of global search methods is governed by two competing goals: first one is the exploration, which is important to ensure global reliability; i.e., every part of the domain is searched enough to provide a reliable estimate of the global optimum. The second one is exploitation, which is also important as it concentrates the search effort around the best solutions found so far by searching their neighborhoods to produce better results. Many recent search algorithms achieve these two goals using a combination of dedicated global and local searches. These are commonly known as

hybrid methods. Such hybrids have been used successfully to solve a wide variety of engineering design problems and often proved to be more efficient to find better solutions than other techniques. Examples of such method are Hybrid Evolutionary Algorithm-Local Search methods (EA-LSs).

2.5 Finite Element based Optimization

Structural design process has been dramatically changed with the introduction of finite element method (FEM). Mathematically, finite element method may be viewed as a numerical tool to analyze problem governed by partial differential equations describing the behavior of the system. Finite element method can be used to determine the deformations and stresses in structure, to analyze dynamic response, heat conduction, fluid flow, and other phenomenon of a system. Considering the importance and wide usage of optimization techniques in structural design, various optimization tools have become a major feature of today's commercial finite element codes.

Optimization problem based on finite elements can generally be expressed as [5]:

$$\text{Minimize} \qquad f(\mathbf{x}, \mathbf{U}) \tag{2.4}$$

$$\text{Subject to} \qquad g_i(\mathbf{x}, \mathbf{U}) \leq 0 \qquad i = 1,\ldots,m \tag{2.5}$$

$$\text{and} \qquad h_j(\mathbf{x}, \mathbf{U}) = 0 \qquad j = 1,\ldots,l \tag{2.6}$$

Where, **U** is an (*ndof* ×1) nodal displacement vector from which the displacement field **u**(x, y, z) is readily determined. '*ndof*' is the number of degrees of freedom in the structure. It is to be noted here that **U** is implicitly a function of **x**, i.e. any change in the element parameter x_i will affect the displacement. The relation between **U** and **x** is

governed by partial differential equations of equilibrium. Finite element discretization of these differential equations can be expressed as:

$$\mathbf{K(x)\ U = F(x)} \tag{2.7}$$

Where, **K** is a (*ndof* × *ndof*) square stiffness matrix and F is a (*ndof* ×1) load vector. The functions f, g_i, h_j are implicit functions of design variables **x**. They depend explicitly on **x**, and also implicitly through **U** as given by Eq. (2.7). The objective function f is typically the weight of the structure, and g_i are constraints commonly reflecting limits on stresses at various points within the structure. Then if $\bar{\sigma}$ is the upper bound allowed on stress, the constraint function would be written as,

$$\frac{\sigma_{ijk}}{\bar{\sigma}} - 1 \leq 0 \tag{2.8}$$

Where, i = element, j = stress component, k = load condition

A general outline of the finite element based optimization process is shown in Figure 2.1. The process starts with by specifying the analysis and design models of the problem, which includes providing an initial geometric description of the component along with a definition of the physics of the problem (i.e. loads, boundary conditions, material properties, etc.), the design variables, objective and constraint requirements as a function of the geometry. In the next step, the component geometry is meshed using an automatic mesh generator and the specified problem physics and design requirements are mapped from the geometry to the finite element data. A finite element analysis is performed to compute the desired responses, which is in turn used for computing the design objectives and constraint functions. These design functions are

then passed on to the optimizer, which based on design sensitivity coefficients determines what changes in design parameters are required in order to achieve an optimal design. The process is continued until convergence is obtained.

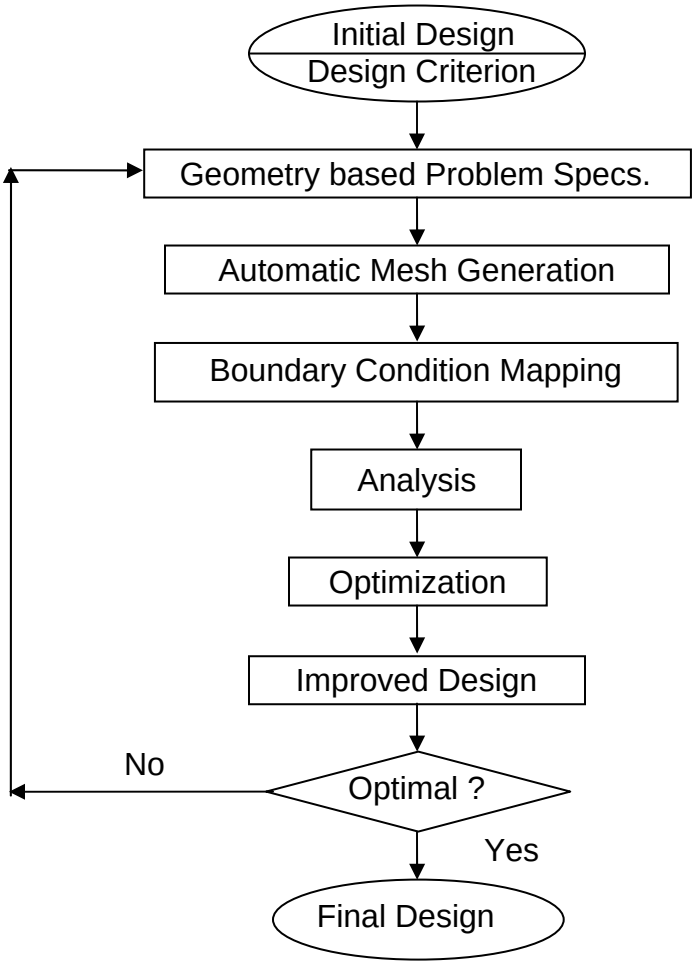

Figure 2.1 General outline of structural design optimization [9]

2.6 Sequential Quadratic Programming for Optimization

In this research, MATLAB built-in optimization function *fmincon* has been used to optimize both the proposed response surface model of the application problems and the actual problems of study to compare the results and performance of the two approaches. *fmincon* uses sequential quadratic programming (SQP) method for optimization purpose. Sequential quadratic programming (SQP) methods represent the state of the art nonlinear programming methods. As the name implies, sequential quadratic programming methods are iterative methods which solve at each iteration a quadratic programming problem (QP). The formulation of sequential quadratic programming is based on Newton's method and Karush-Kuhn-Tucker (KKT) equations. KKT equations based algorithms attempt to compute the Lagrange multipliers directly. Constrained quasi-Newton methods guarantee super-linear convergence by accumulating second-order information regarding the KKT equations using a quasi-Newton updating procedure [10].

Consider a general problem of the form,

$$\min_{x} \quad f(x) \tag{2.9}$$

Subject to $G_i(x) = 0 \qquad i = 1,\ldots,m_e, \tag{2.10}$

$$G_i(x) \leq 0 \qquad i = m_e+1,\ldots,m \tag{2.11}$$

For the problem given as in the Eq. (2.9), a quadratic programming sub problem is formulated based on a quadratic approximation of the Lagrangian function as bellow:

$$L(x,\lambda) = f(x) + \sum_{i=1}^{m} \lambda_i . g_i(x) \tag{2.12}$$

At the *k*th iteration, the following quadratic programming sub problem is solved for the next search direction:

$$\min_{d} \quad \frac{1}{2} d^T H_k d + \nabla f(x_k)^T d \tag{2.13}$$

Subject to $\nabla g_i(x_k)^T d + g_i(x_k) = 0, \quad i = 1,\ldots,m_e$ (2.14)

And $\nabla g_i(x_k)^T d + g_i(x_k) \le 0, \quad i = m_e+1,\ldots,m$ (2.15)

This sub problem can be solved using any quadratic programming algorithm. The solution procedure involves two phases. The first phase involves the calculation of a feasible point (if one exists) and the second phase involves the generation of an iterative sequence of feasible points that converge to the solution. The solution of the sub problem is used to form a new iterate as follows:

$$x_{k+1} = x_k + \alpha_k d \tag{2.16}$$

Where, d is the direction vector at the given point x_k and α_k is the step size. The step size parameter α_k is determined by an appropriate line search procedure so that a sufficient decrease in the objective function is obtained. A number of iterations are performed before the optimal result is obtained.

The main disadvantage of sequential quadratic programming is that it is a local method. So the finding of global minima is influenced by the starting point that must be close to the global solution.

CHAPTER 3

DESIGN OF EXPERIMENTS AND RADIAL BASIS FUNCTION FOR RESPONSE SURFACE BASED STRUCTURAL OPTIMIZATION

3.1 Introduction

In many areas of modern design and manufacturing industries, the design process has been transformed by the introduction of enormous computing power and advances in information technology, computational sciences and artificial intelligence. These advances are leading to new ways of managing the design process, reducing the design cycle times, cost savings and improvement in product quality. In spite of the advancement of computer capacity and speed, the massive computational cost of complex engineering simulations makes it impractical to rely exclusively on simulation codes for the purpose of design optimization. In order to reduce the computational efforts, alternative methods based on approximation concepts are evolved, which involve replacing the expensive simulation model during the design and optimization process.

Response Surface Methodology (RSM) based optimization refers to the idea of speeding optimization process by using approximate models for the objective and constraint functions. Generally response surface means any function that represents the trends of a response over the range of the design variables. The basic approach of RSM based optimization is to construct a simplified mathematical approximation of the computationally expensive simulation and analysis code, which is then used in place of

the original code to facilitate design optimization process. Since the approximation model acts as a surrogate for the original code, it is also referred as a surrogate model, surrogate approximation, approximation model, or metamodel [4].

The quality of the response surface model is extremely crucial as a poor model will be misleading, causing the optimization process to diverge and increasing the design cycle time. Hence, an important objective of the response surface construction is to achieve an acceptable level of accuracy while attempting to minimize the number of function evaluations [3]. The accuracy of the response surface is based on two important issues: a) the choice of the approximation function, and b) the selection of the design points on the design space where the design will be evaluated, i.e. the design of experiments. Increasing the number of experimental points could improve the accuracy. However, using a large number of points is expensive and the potential accuracy may be inhibited by other factors like the order of the approximating functions, the sub region size under investigation etc.

Generally, response surface based optimization method involves the following steps:

1. Choose an experimental design to sample the region of interest.
2. Perform analysis (or simulations) based on the selected sample data.
3. Construct the response surface model to the observed sample data.
4. Perform approximate optimization to find the predicted optimal design.
5. Validate the predicted optimal design by conducting an analysis on the actual model.

6. Check for convergence (stop if within convergence tolerance).
7. Update response surface model using new data points and iterate until converge.

3.2 Response Surface Methodologies

To meet the challenge of ever increasing model complexity, the process of building response surfaces has gained wide acceptance from the design community. So far, a wide variety of metamodeling techniques have been used, but still newer and improved techniques are being proposed by the researchers. The most popular form of the RSM involves fitting second-order polynomial functions using least-squares regression over a set of data points [2]. An interpolation method known as Kriging is widely used by the design and analysis of computer experiments. Recently, statistical techniques, such as Multivariate Adaptive Regression Splines and radial basis function approximation are getting attention from the designers and researchers.

A detailed review of early RSM developments and applications (from 1966 to 1988 period) is presented by Myers et al. [11]. Barthelemy et al. [12] identified three general categories of approximation according to their ranges of applicability in the design space. These are local, medium range, and global approximations. They also distinguished between function approximation, in which an alternate and explicit expression is sought for the objective and /or constraints of the problem, and problem approximation where the focus is on replacing the original statement of the problem by one which is approximately equivalent but easier to solve. Jin et al. [13], and Auzins et al. [14] performed systematic comparative studies about the performance of various modern response surface methods and reported that the radial basis function based

response surface model out performs other methods. Simpson et al. [4] discussed about some of the practical implementations of RSM in multidisciplinary analysis and optimization and pointed out the future research directions in approximation methods. In another paper, Simpson et al. [15] presented survey reports and recommendations for the use of statistical techniques to build approximations of expensive computer analysis codes. After reviewing various metamodeling techniques they proposed some selection criterion for choosing right metamodeling scheme to represent a specific problem.

The knowledge of the performance of different metamodeling techniques with respect to different modeling criteria is of utmost importance to designers when trying to choose an appropriate technique for a particular application. Various factors contribute to the success of a given metamodeling technique such as, nonlinearity of the model behavior, the dimensionality and data sampling technique, the internal parameter settings of the various techniques etc. So, it is not prudent to conclude that a particular RSM technique is suitable for all kinds of problems.

3.3 Radial Basis Function (RBF)

Multiquadrics (MQ) functions (RBF) have been developed for scattered multivariate data interpolation by Hardy [16] in 1971, which is a special case of Radial Basis Functions. A radial basis function model uses a series of basis functions that are symmetric and centered at each sampling point. The method uses linear combinations of a radially symmetric function based on Euclidean distance of other such metric to approximate response function. Let $f(\mathbf{x})$ be the true response function and $\widetilde{f}(\mathbf{x})$ be the approximate obtained using RBF. Then in general form,

$$\tilde{f}(\mathbf{x}) = \sum_{i=1}^{n} C_i \phi(\|\mathbf{x} - \mathbf{x_{ci}}\|) \tag{3.1}$$

Where, n is the number of center points, $\mathbf{x}$ is the vector of design variables, $\mathbf{x_{ci}}$ is the vector of center points at the i^{th} center point, $\|\mathbf{x} - \mathbf{x_{ci}}\|$ is the Euclidean distance, ϕ is the basis function, and C_i is the unknown coefficient. Figure 3.1 shows the 1-D Gauss and Multiquadric basis function (see Table 3.1) centered at 0 and with h = 1. Note that h is known as shift or smooth parameter for Multiquadric function. The parameter h controls the width of the Gauss basis.

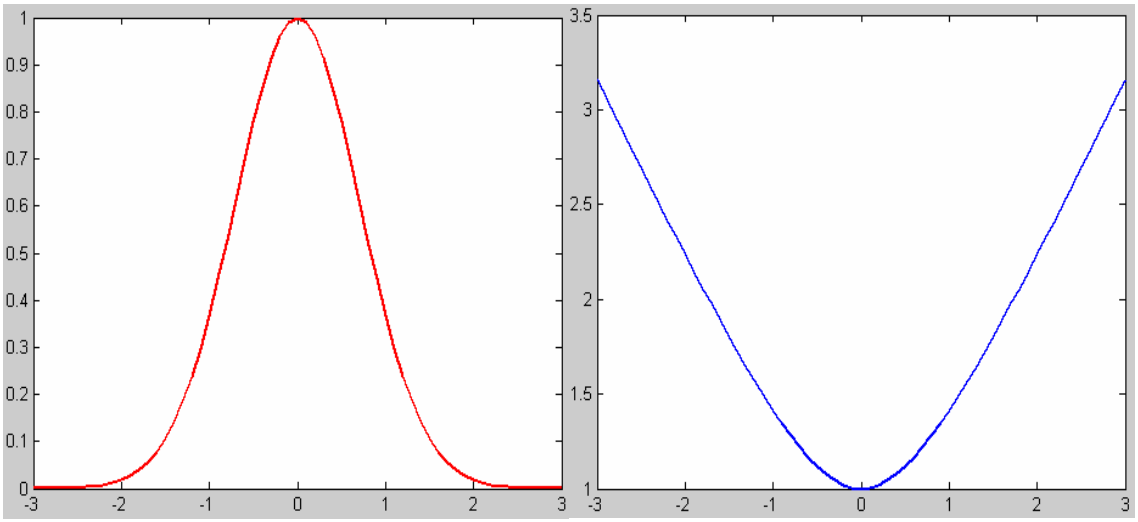

(a) (b)

Figure 3.1 (a) Guassian and (b) Multiquadric RBF with centers at 0 and h = 1

In real world applications, radial basis function techniques have become extremely useful, ranging from geodesy, geophysics, surveying and mapping, photogrammetry, remote sensing, signal processing, artificial intelligence, geography,

digital terrain modeling, hydrology, to the solution of elliptic, parabolic and hyperbolic partial differential equations [17]. A list of common radial basis functions is presented in Table 3.1. Nevertheless the most popular radial basis functions are the Thin-Plate Spline, Gaussian and Multiquadrics (MQ). Among these common functions, the Multiquadrics (MQ) appears to be the overall best performing RBF [18, 20, 2].

Table 3.1 Common Radial Basis Functions ($r = r_i = \|\mathbf{x} - \mathbf{x}_i\|$) [20]

Name	$\phi(r)$	Parameters
Thin-plate spline	$r^2 \ln r$	$\mathbf{x} \in \mathbf{R}^2$
Cubic spline	r^3	$\mathbf{x} \in \mathbf{R}^3$
Polyharmonic splines	$r^{2n} \ln r$	$n \geq 1,\ \mathbf{x} \in \mathbf{R}^2$
Polyharmonic splines	r^{2n-1}	$n \geq 1,\ \mathbf{x} \in \mathbf{R}^3$
Sobolev spline	$r^{\nu} K_{\nu}(r)$	$\nu > 0$, K_{ν} : spherical Bessel function
Matern spline	$e^{-hr} K_{\nu}(hr)$	$\nu > 0$, $h > 0$
Exponential spline	e^{-hr}	$h > 0$
Gaussians	e^{-hr^2}	$h > 0$
Multiquadrics	$\sqrt{r^2 + h^2}$	$h > 0$
Inverse multiquadrics	$(r^2 + h^2)^{-1/2}$	$h > 0$
Compactly supported	$(1-r)^m + p(r)$	$m \geq 2,\ p(r)$: polynomial of Wendland

3.4 Radial Basis Functions for Response Surface Methodology

Radial basis function approximations have been shown to produce good fits to arbitrary contours of both deterministic and stochastic response functions. Jin, et al. [13] observed that in terms of accuracy and robustness of the various techniques for different types of problems (i.e., different orders of nonlinearity and problem scales), RBF shows the best performance among different metamodeling techniques. However, Harpham et al. [21] demonstrated that the optimal choice of basis function is problem dependent.

In this research, four different models for two of the most popular radial basis functions have been used for response surface generation. These are,

(a) Multiquadric Interpolation (MQI),

(b) Multiquadric Regularization (MQR),

(c) Gauss Interpolation (GuassI), and

(d) Guass Regularization (GuassR)

To determine the unknown coefficient C_i in Eq. (3.1), let us replace $\mathbf{x}$ and $\widetilde{f}(\mathbf{x})$ in equation Eq. (3.1) with m vectors of design variables and their corresponding function values at the sampling points. We obtain the following series of m equations,

$$\widetilde{f}(\mathbf{x}_1) = \sum_{i=1}^{n} C_i \phi(\|\mathbf{x}_1 - \mathbf{x}_{\mathbf{ci}}\|),$$

$$\widetilde{f}(\mathbf{x}_2) = \sum_{i=1}^{n} C_i \phi(\|\mathbf{x}_2 - \mathbf{x}_{\mathbf{ci}}\|), \tag{3.2}$$

….

$$\tilde{f}(\mathbf{x}_m) = \sum_{i=1}^{n} C_i \phi(\|\mathbf{x}_m - \mathbf{x_{ci}}\|)$$

The matrix form of the Eq. (3.2) is

$$\mathbf{f} = \mathbf{AC} \tag{3.3}$$

Where, $\mathbf{f} = \left[\tilde{f}(\mathbf{x}_1), \tilde{f}(\mathbf{x}_2), .. \tilde{f}(\mathbf{x}_m)\right]^T$, $\mathbf{C} = [C_1, C_2, ... C_n]^T$

And, $\mathbf{A}_{ji} = \phi(\|\mathbf{x}_j - \mathbf{x_{ci}}\|)$, ($i = 1, 2, ..., n$, $j = 1, 2, ..., m$)

Now, if $n = m$, Eq. (3.1) is an interpolation model and if $m > n$, Eq. (3.1) becomes a regression model. Interpolating metamodels are capable of yielding globally accurate response surface [13, 2]. Generally for RBF interpolation models, while calculating the Euclidean distance, the set of sampling/data points and the set of center points for the RBF are same [2, 22]. Hence the RBF passes through all the sampling points exactly. This means that function values from the approximate function are equal to the true values at the sampling points. The unknown coefficient C_i can easily be found by solving Eq. (3.3),

$$\mathbf{C} = \mathbf{A}^{-1}\mathbf{f} \tag{3.4}$$

In this research, for the Multiquadric Interpolation and Guass Interpolation, the unknown coefficient C_i is determined using Eq. (3.4). With Multiquadric Regularization and Gauss Regularization model, for determining the optimum value of the unknown coefficient C_i (the weight vector), the sum of error square is used to measure the accuracy of fit of the response surface model and an additional weight penalty term is introduced as follows:

$$e = \sum_{j=1}^{m} (f(\mathbf{x}_j) - \tilde{f}(\mathbf{x}_j))^2 + r\sum_{i=1}^{n} C_i^2 \tag{3.5}$$

Where r is the regularization parameter, which controls the balance between fitting error and the smoothness of the fitting function. A small value of r means the data can be fit tightly without causing a large penalty. A value of $r = 0.001$ is used for all the test problems solved in this research.

The objective of introducing Eq. (3.5) is to find the minimum error function that would give a good approximation of the response function. To do that, we have to differentiate Eq. (3.5) with respect to C (which is the free variable), equate the result to zero, and then solve the resulting equations. For i^{th} weight optimization, differentiating Eq. (3.5) with respect to C gives,

$$\frac{\partial e}{\partial C_i} = 2\sum_{j=1}^{m} (\tilde{f}(\mathbf{x}_j) - f(\mathbf{x}_j)) \frac{\partial \tilde{f}(\mathbf{x}_j)}{\partial \mathbf{C}_i} + 2rC_i \tag{3.6}$$

The derivative of $\tilde{f}(\mathbf{x}_j)$ can be obtained from Eq. (3.3),

$$\frac{\partial \tilde{f}(\mathbf{x}_j)}{\partial C_i} = A_i(x_j) \tag{3.7}$$

Substituting this into Eq. (3.6) and equating the result to zero leads to the equation,

$$\sum_{j=1}^{m} \tilde{f}(x_j) A_i(x_j) + rC_i = \sum_{j=1}^{m} f(x_j) A_i(x_j) \tag{3.8}$$

There are n such equations, for $1 \leq i \leq n$, each representing one constraint on the solution. Since there are exactly as many constraints as there are unknowns, the system of equations has a unique solution. The above equation can be written in the matrix form as,

$$\mathbf{A}_i^T \mathbf{f} + rC_i = \mathbf{A}_i^T \hat{Y} \tag{3.9}$$

Where,

$$\mathbf{A}_i = \begin{bmatrix} A_i(x_1) \\ A_i(x_2) \\ .... \\ A_i(x_m) \end{bmatrix},\ \mathbf{f} = \begin{bmatrix} \widetilde{f}_i(x_1) \\ \widetilde{f}_i(x_2) \\ .... \\ \widetilde{f}_i(x_m) \end{bmatrix},\ \hat{\mathbf{Y}} = \begin{bmatrix} f_i(x_1) \\ f_i(x_2) \\ .... \\ f_i(x_m) \end{bmatrix}$$

Since there is one of these equations for each value of *i* form 1 up to n, it is possible to stack them one on top of the other to create a relation between two vector quantities as given below,

$$\begin{bmatrix} \mathbf{A}_1^T \mathbf{f} \\ \mathbf{A}_2^T \mathbf{f} \\ .... \\ \mathbf{A}_n^T \mathbf{f} \end{bmatrix} + \begin{bmatrix} rC_1 \\ rC_2 \\ .... \\ rC_n \end{bmatrix} = \begin{bmatrix} \mathbf{A}_1^T \hat{\mathbf{Y}} \\ \mathbf{A}_2^T \hat{\mathbf{Y}} \\ .... \\ \mathbf{A}_n^T \hat{\mathbf{Y}} \end{bmatrix} \tag{3.10}$$

This is equivalent to

$$\mathbf{A}^T \mathbf{f} + r\mathbf{I}_n \mathbf{C} = \mathbf{A}^T \hat{\mathbf{Y}} \tag{3.11}$$

Where $\mathbf{A} = [\mathbf{A}_1 \mathbf{A}_2 .... \mathbf{A}_n]$ and $\mathbf{I}_n$ is and identity matrix of length n.

Substituting for vector **f** in the above equation from Eq. (3.3),

$$\begin{aligned} \mathbf{A}^T \hat{\mathbf{Y}} &= \mathbf{A}^T \mathbf{f} + r\mathbf{I}_n \mathbf{C} \\ &= \mathbf{A}^T \mathbf{A}\mathbf{C} + r\mathbf{I}_n \mathbf{C} \\ &= (\mathbf{A}^T \mathbf{A} + r\mathbf{I}_n)\mathbf{C} \end{aligned}$$

Hence, $\mathbf{C} = (\mathbf{A}^T \mathbf{A} + r\mathbf{I}_n)^{-1} \mathbf{A}^T \hat{\mathbf{Y}}$ (3.12)

As all the values on the right hand side of the above equation is known, from this equation, optimal value of the unknown coefficient, **C** (the weight matrix) that gives a good approximation of the response function can be found. Using Eq. (3.12), the optimal coefficient matrix **C** is determined for Multiquadric Regularization and Gauss Regularization model in this research. Once the coefficient matrix **C** is known, the approximate function can be found using Eq. (3.3). It is to be noted here that for interpolation model, $r = 0$ in Eq. (3.12).

3.5 Choosing the Optimal Shift Parameter for Radial Basis Function

The parameter h in the radial basis function is known as the shift parameter. It is sometimes also called the smooth or shape parameter of the radial basis function. It is well known that the accuracy of the multiquadric interpolants depends heavily on the choice of shift parameter [23]. It is verified that, this is true for the Gaussian interpolants also [17]. The proper choice of the shift parameter is of great importance because by adjusting the shift parameter, the accuracy of the approximation can be considerably increased. By increasing the shift parameter, the root mean square (RMS) error of the fit drops to a minimum and then grows rapidly thereafter [24]. Thus there exists an optimal shift parameter that will yield minimum RMS for the fitted function. Effective methods for selecting optimal shift parameter have been developed by Wang [18, 19] and Rippa [17].

To select the optimal shift parameter, number of experiments were performed with different values of the shift parameter h, at the initial stage of this research. The results are not presented here as they are beyond the scope of this thesis. However, at

the end of the experimentations, a shift parameter value of 1 is selected for solving the problems in this research.

3.6 Design of Experiments

Design of Experiments (DOE) is a procedure for choosing a set of samples in the design space, with the general goal of maximizing the amount of information gained from a limited number of samples [25]. One of the goals of a design of experiments study is to estimate and predict the trends in the response data.

In general, the design of experiments techniques can be classified as classical and modern design of experiments techniques. The classical techniques were developed for laboratory and field experiments while the modern DOE techniques pertain to deterministic computer simulations. Both classical and modern design of experiments technique share the common goal of extracting as much information as possible from a limited set of laboratory or computer experiments. Examples of classical DOE techniques are central composite design, Box-Behnken design, full- and factorial-factorial design etc. The examples of modern DOE techniques are Latin hypercube sampling, Orthogonal array sampling, Quasi-Monti Carlo sampling etc. that are also known as space filling techniques as they put the sampling points in the interior as compared to the extremes of the design space in order to accurately extract the response trend information.

The fundamental difference between classical and modern DOE stems from the assumption that random error exists in a laboratory experiment, but does not exist in a computer experiment. Another feature that distinguishes classical DOE from modern

DOE is the choice of probability distribution functions associated with design parameters. Classical DOE typically assumes that the possible values of a design parameter are uniformly distributed between a lower and upper bound. On the other hand, modern DOE methods are intended to handle design parameters that have both uniform and non uniform probability distributions. In classical DOE, the goal of minimizing the effects of random error has the affects of placing the samples on the boundaries or vertices of the design space and placing very few samples in the interior of the design space. This causes the interior of the design space to be largely unexplored. In contrast, for modern DOE, there is no notion of random errors, i.e. for a specific input data, computer simulation always produces the exact same response irrespective of the number of simulation run. Apart from the assumption that there is no random error in a computer simulation, an additional assumption is made in modern DOE that the true response trend is unknown. Due to this reason, modern DOE methods tend to place samples on the interior of the design space which is preferred in an effort to minimize bias error. Bias error arises when there is a difference between the functional form of the true response trend, and the functional form of the estimated trend.

For dealing with large and complex design space, it is not possible to estimate the number of design points in advance to resolve key features with a response surface. Incrementally adding data can create an opportunity to monitor resolution convergence, provided the design sites are appropriately chosen. Ideally the addition of any points would improve the predictive capabilities of a response surface. However, new points

that are chosen very near existing points can produce little or no improvement. On top of that, clustered points that are too close together can cause the response surface ill-conditioned. Moreover, adding unnecessarily more points would increase the cost of computation. Hence, in order to get the maximum amount of information out of a minimum number of design points with no prior knowledge of the design space requires a uniform sampling. The ideal sampling method would create a uniform sample and maintain that uniformity regardless of the number of points added in each incremental update. Literature survey reveals that among the modern DOE techniques, Quasi-Monte Carlo sampling attracted the researchers most due to its better uniformity properties, which reduces the computational intensity of the optimization problem considerably. Guinta et al. [25], Simpson, et al. [26], and Diwekar, et al. [27] presented the comparative results of the performance of different modern DOE techniques and reported that the Hammersley sampling sequence, a variant of Quasi-Monte Carlo sampling out performs the other DOE methods for accurate approximation globally as the root mean square error associated with it is consistently low.

In this research, three different Quasi-Monte Carlo techniques, namely Halton sequence, Faure sequence and Sobol sequence are used for generating the design of experiments for response surface.

3.7 Quasi-Monte Carlo Sampling for Design of Experiments

Quasi-Monti Carlo (QMC) sampling is a deterministic sampling procedure that uses low discrepancy sequences. The concept of low discrepancy is associated with the property that the successive numbers are added in a position as far away as possible

from the others numbers, this is, avoiding clustering. The sequence is constructed based in the scheme that each point is repelled from the others. Hence, if the idea for the points is "maximally avoiding of each other", the job for the numbers generated sequentially is to fill in the larger gaps between the previous numbers of the sequence. The deterministic nature of the Quasi-Monti Carlo method results in best possible spread of data through out the design space, but does not employ a regular grid or a Cartesian lattice of sample sites [9]. Some of the well known low discrepancy sequences are van der Corput sequence (1935), Halton sequence (1960), Sobol sequence (1967), Faure sequence (1982) and Niederreiter sequence (1987). But this is a growing research area and new sequences and the improvement of the previous sequences are being proposed [28]. According to the knowledge of this author, only a limited number of papers exist referring to the use of Halton and Sobol sequence for DOE generation for optimization of mechanical systems. Levi et al. [29] introduced an innovative structural design optimization method for optimizing stochastic systems where they used Sobol sequence for the DOE generation. Nelson, et al. [30] studied four well known Quasi-Monte Carlo sampling methods and suggested that Sobol sequence produces the most uniform samples on an incremental basis compared to the other sequences. Wang, et al. [31] proposed an optimization algorithm for solving real-world crashworthiness problems to enhance the structural impact performance, where they used Halton sequencing method for creating the design of experiments.

In this research, an already developed MATLAB code for generating Halton sequence, Faure sequence and Sobol sequence is used. The design of experiments

generated by these sequences are then employed for response surface creation. Brief discussions on these sequences are given in the following subsections.

3.7.1 Halton Sequence

The Halton sequence is a low discrepancy sequence which uses one different prime base for each dimension. For the first dimension it uses base 2, for the second dimension it uses base 3, for the third dimension uses base 5, and so on. Higher base means higher cycle and higher computational time.

The Halton sequence in relatively prime bases $b_1, b_2,\ldots,b_s$ is defined as sequence [28]:

$$x_n = \left(\Phi_{b_1}(n), \Phi_{b2}(n), \ldots \Phi_{b_s}(n)\right) \tag{3.13}$$

Where, $\Phi_b\ (n)$ is the radical inverse function:

$$\Phi_b(n) = \sum_{j=0}^{m} a_j(n) b^{-j-1} \tag{3.14}$$

This sum is coming from the digit expansion of the integer n in base b_j:

$$n = \sum_{j=0}^{m} a_j(n) b^j \tag{3.15}$$

Where, m is the lowest integer that makes $a_j(n) = 0$ for all $j > m$.

To illustrate this algorithm, consider the expansion of $n = 46_{10}$ using base $b = 5$:

$$n = 46_{10} = 141_5 = 1 \times 5^2 + 4 \times 5^1 + 1 \times 5^0$$

Now using the radical inverse function (Eq. 3.14):

$$\Phi_5(46_{10}) = 0.141_5 = \frac{1}{5} + \frac{4}{5^2} + \frac{1}{5^3} = 0.368_{10}$$

Table 3.2 shows some sampling generated by Halton sequence.

Table 3.2 First Five Sampling of Different Base by Halton Sequence

	b = 2	b = 3	b = 5
n = 1	0.5	0.3333	0.2
n = 2	0.25	0.6667	0.4
n = 3	0.75	0.1111	0.6
n = 4	0.125	0.4444	0.8
n = 5	0.625	0.7778	0.04

The major problem for the Halton sequence is its degradation when the dimension is large. It gives uniform distributions for lower dimensions from 1 to 10. As the number of dimensions increases, the quality of the Halton sequence rapidly decreases because the two-dimensional planes within the hypercube are sampled in cycles with increasing period due to the large prime number base. Due to the correlation between dimensions, Halton sequence becomes unsatisfactory after dimension 14 [32]. Many researchers proposed permutations of the radical inverse function in order to overcome the correlation problems and reported improvement over the original Halton sequence for larger values of dimensions [28].

In this research an externally developed MATLAB code for Halton sequence generation is used which uses “Leaping” technique to eliminate the correlation problem in higher dimensions [28]. Halton sequence leaped technique uses only every *L*th Halton number subject to the condition that *L* is a prime different from all bases

$b_1,\ldots\ldots,b_s$ used. This gives a formula for generation of the Halton points leaped – namely, n in Eq. (3.13) is replaced by mL, where L is the leap, and m = 1, 2, 3,…. The effect of leaping a Halton sequence is to choose a subset that progressively fills all parts of the unit cube in a similar manner to the original sequence.

3.7.2 Faure Sequence

The Faure sequence is like the Halton sequence, but with two differences: (1) it uses only one base for all dimensions, and (2) it uses a permutation of the vector elements for each dimension. The base of a Faure sequence is the smallest prime number that is larger than or equal to the number of dimensions in the problem. As in the case with Halton sequence, there is the problem of low speed at which the Faure sequence generates increasing finer grid points to cover the unit hypercube. However, this problem is not too sever as the Halton sequence. For example, if the dimension of the problem is 50, the last Halton sequence uses the 50th prime number that is 229, whereas the Faure sequence uses the first prime number after 50, that is a base 53, which is much smaller that 229.

By reordering the sequence within each dimension, Faure sequence prevents some problem of correlation for sequential high-dimensions that occurred with the Halton sequence. The algorithm for the Faure sequence uses eq. (3.14) and Eq. (3.15). But before using the eq. (3.14), there are a combinatorial rearrange of the a_j, which is performed using a recursive equation, from dimension (d-1) to the new dimension d:

$$a_i^d(n) = \sum_{j \geq i}^{m} \frac{j!}{i!(j-i)!} a_j^{d-1}(n) \bmod b \qquad (3.16)$$

Faure sequence exhibits high-dimensional degradation at approximately the 25th dimension. [32].

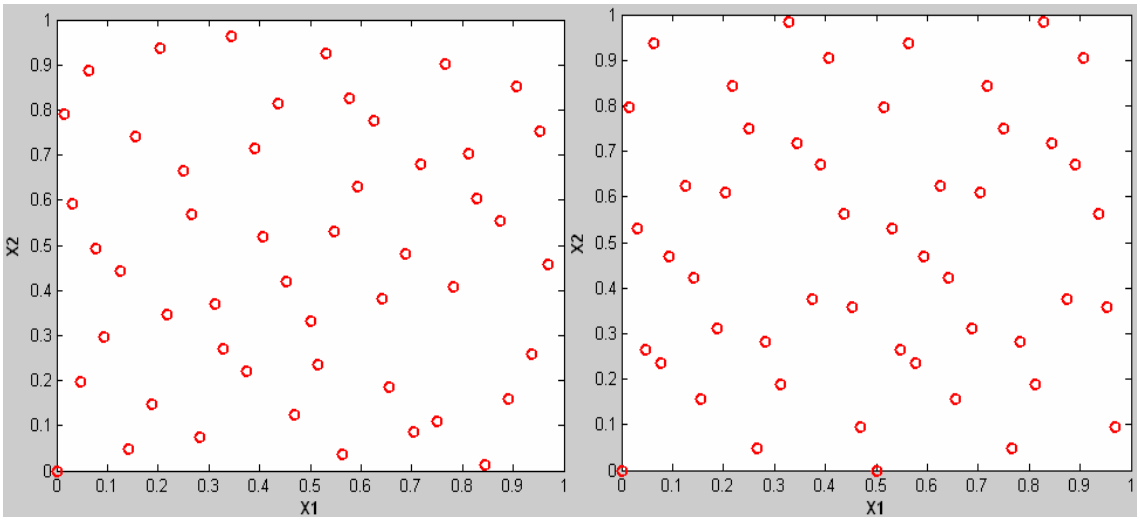

Figure 3.2 Fifty DOE points by (a) Halton, (b) Faure, and (c) Sobol sequence

3.7.3 Sobol Sequence

The sobol sequence, like the Faure sequence, has the same base for all dimensions and proceeds a reordering of the vector elements within each dimension.

The Sobol sequence is simpler and faster than the Faure sequence in the aspect that Sobol sequence uses base 2 for all dimensions. But Sobol uses a more complex reordering algorithm. Its reordering is based on a set of direction numbers, $\{v_i\}$. The v_i numbers are given by the equation,

$$v_i = \frac{m_i}{2^i} \tag{3.17}$$

Where, m_i are odd positive integers less than 2^i, and v_i are chosen so that they satisfy a recurrence relation using the coefficients of a primitive polynomial in the Galois field of order 2. A primitive polynomial is irreducible (i.e. can not be factored into polynomials of smaller degree) and does not divide the polynomial $x^r + 1$ for $r < 2^p - 1$. Thus, the Sobol sequence can be expressed as,

$$\Phi_b(n) = \sum_{i=0}^{j} d_i v_i b^{-i-1} \tag{3.18}$$

Sobol sequence does not show any degradation through the 260th dimension [32]. So, it outperforms both Halton and Faure sequences. Figure 3.2 shows the first fifty DOE points generated by Halton, Faure and Sobol sequence.

3.8 Scaling of Data Points

It is often desirable to eliminate wide variations in the magnitudes of design variables and the value of constraints by normalization. Design variables may be normalized to the order 1 by scaling. This operation may enhance the efficiency and reliability of the numerical optimization process [6].

For example, consider the variables X_1 and X_2 limited by side constraints,

$$0 \le X_1 \le 0.1$$

$$0 \leq X_2 \leq 100$$

The original variables can be replaced by new variables Y_1 and Y_2 defined by,

$$Y_1 = 10X_1$$

$$Y_2 = X_2/100$$

And the side constraints become,

$$0 \leq Y_1 \leq 1$$

$$0 \leq Y_2 \leq 1$$

In this research, the data points, i.e. the design variables generated by the low discrepancy sequences are scaled between 0 and 1 and that scaled data have been used for response surface training, evaluation and optimization purposes. The equations used for the scaling purpose are:

$$Xs = a + b \times X \tag{3.19}$$

Where, X and Xs is the value of the design variables in physical and scaled unit.

$$b = \frac{1}{XU - XL} \tag{3.20}$$

And, $$a = - b \times XL \tag{3.21}$$

XU is the maximum upper bound value of the design variables and XL is the minimum lower bound value of the design variables.

3.10 MATLAB Partial Differential Equation Toolbox for Structural Optimization

MATLAB Partial Differential Equation (PDE) Toolbox has been chosen for the modeling and FEM study in this research. The MATLAB Partial Differential Equation Toolbox contains tools for the study and solution of Partial Differential Equations in

two dimensions and time, using the finite element method. Some of the key features of PDE Toolbox are:

- Complete Graphical User Interface for pre- and post-processing of 2-D PDEs.
- Automatic and adaptive meshing.
- Geometry creation using constructive solid geometry paradigm.
- Boundary condition specification: Dirichlet, generalized Neumann, and mixed.
- Flexible coefficient and PDE problem specification using MATLAB syntax.
- Nonlinear and adaptive solvers for handling systems with multiple dependent variables.
- Simultaneous visualization of multiple solution properties, FEM-mesh overlays, and animation.

The PDEs implemented in the toolbox are used as a mathematical model for a wide variety of phenomena in different branches of engineering and science. The following is a list of examples that can be solved using MATLAB PDE Toolbox [33]:

1. The elliptic and parabolic equations are used for modeling:
    - Structural mechanics – plain stress, plain strain problems.
    - Steady and unsteady heat transfer in solids.
    - Flows in porous media and diffusion problems.
    - Electrostatics in dielectric and conductive media.
    - Potential flow.
2. The hyperbolic equation is used for modeling:

- Transient and harmonic wave propagation in acoustics and electromagnetics.
- Transverse motions of membranes.

3. The eigenvalue problems are used for determining natural vibration states in membranes and structural mechanics problems.

MATLAB is one of the well known packages that perform mathematical and engineering computation. The capabilities of MATLAB and some of its powerful toolbox are beyond any doubts. They provide engineers, scientists, mathematicians, and educators with an environment for technical computing applications. These products serve a broad range of tasks for a variety of industries from automotive and electronics to industrial equipment and telecommunications.

However, it is to be noted here that, MATLAB PDE Toolbox does not have a wide history as a structural analysis tool. Literature survey reveals only a few instances where the MATLAB PDE Toolbox has been used as the principal investigation tool and they are not even in the field of structural analysis. MATLAB PDE Toolbox user's guide [33] presented some examples of solving plain stress and plain strain problems using PDE Toolbox. Min, et al. [34] performed numerical simulation of straight fins heat conduction based on PDE tool and showed that MATLAB PDE Tool is convenient and highly efficient for numerical simulation, and applicable to practical engineering design optimization of heat exchanger. Makarov [35] presented a MoM antenna simulation code which was implemented using MATLAB PDE Toolbox. Magistris [36] reported the realization of a MATLAB PDE Toolbox based electromagnetic-fields

virtual laboratory. So, at the beginning of this research, some of the problems were also solved using ANSYS and the results were found to be very identical with MATLAB PDE Toolbox. Hence it can be claimed that the results obtained using MATLAB PDE Toolbox in this research are correct and valid.

CHAPTER 4

ALGORITHM FOR STRUCTURAL OPTIMIZATION USING RADIAL BASIS FUNCTION BASED RESPONSE SURFACE MODEL

4.1 Introduction

The core objective of this research is to construct and implement a design optimization code in MATLAB, which is based on response surface methodology, and design of experiment technique and uses radial basis function as approximation model. MATLAB Partial Differential Equation Toolbox is used for the finite element modeling and analysis. An already developed external MATLAB code is used for the generation of design of experiments. All the experiments are performed on Personal Computer with Intel Pentium 3.4 GHz processor and 2 GB memory in Windows XP environment. The MATLAB version used is MATLAB 7.4 (R 2007a).

The following sections describe the process and algorithm involved in the implementation of the optimization scheme presented in this research. The solution procedures are summarized in the flowchart in Figure 4.1.

4.2 Modeling the Problem in MATLAB PDE Toolbox

For each of the problem solved in this research, the pre-optimization step involved is to model the problem in MATLAB PDE Toolbox. The geometry is built for a specific set of design values, material properties are specified, and boundary conditions are applied. The problem is then solved and various responses such as displacement, stress and frequency are obtained. The whole finite element analysis is

then saved as an M-file and later converted into the parametric model of the problem. This MATLAB M-file parametric model is then ready to be used with the automated design optimization process.

4.3 Algorithm for Optimization Scheme

The stages involved in the optimization algorithm are described below:

1. Definition of the problem:

The first stage involves the definition of the design problem. Problem definition includes, specifying the actual analysis /response function, actual constraints function, method (sequencing technique) for generating the DOE points (sets of input design variables), the upper limit (XU) and lower limit (XL) of the input design variables, number of total DOE points to be generated (nPoints), number of initial DOE points to be taken (Ninit) out of the nPoints for obtaining the initial responses, the RSM model to be used for function approximation, and the shift parameter h, and regularization parameter r. The coefficient matrices of the objective functions (**Ax** and **Ay**) and constraints functions (**Cx**, **Cy**, **Cb**) are also specified in this stage.

2. Generation of Design of Experiments:

In this stage, based on the user specified sequencing method, 'nPoints' number of data points (DOE) are generated within the design space. These data points are scaled data within 0 to 1 limit and stored in a matrix called 'XQMC'. It is to be noted here that scaled data have been used for all cases of response surface training and evaluation purposes. But for the creation of the initial data base, these scaled data have been converted into physical unit within the predefined upper limits (XU) and lower limits

(XL) and have been stored in the matrix named 'XData'. Then the elements of the XData matrix have gone under a filtration process and only those data points which satisfy the geometric constraints of the problem have been kept in the XData matrix leaving all the other data points out.

3. Creating the initial data base:

This stage consists of calling the response function 'Ninit' number of times and evaluating it for the first 'Ninit' data points taken from 'XData' and storing the response into 'YC' matrix. Note that this response is the true response (stress, frequency etc.) which is obtained from the finite element analysis of the parametrically modeled problem in MATLAB PDE Toolbox. The first 'Ninit" data points are stored into the 'XC' matrix, which is later converted into scaled data and stored into 'XCs' matrix. The required initial database is now ready for the response surface creation.

4. Training of Response Surface Model:

In this stage, based on the database information, i.e. the scaled data points XCs, the true response YC, the name of the response surface model, shift parameter h, and regularization parameter r, response surface approximation is done and the coefficient 'C_i' of the radial basis function approximation is determined. For interpolation model, Eq. (3.4) and for regularization model, Eq. (3.12) is used for the determination of C_i. Note that, in this stage the Euclidean distance for the radial basis function is calculated for each of the scaled data points XCs using built-in MATLAB function *dist*.

5. Optimization Stage:

In this stage, the approximate response, 'Y_{app}' is obtained for different set of evaluation points 'Xes' using the Eq (3.3). Here, the elements of Xes are scaled within 0 to 1 and determined by MATLAB built-in optimization function *fmincon* with the initial set of values fixed at 0.5 for each element. In this case, the Euclidean distance for the radial basis function is calculated for each Xes to XCs using built-in MATLAB function *dist*. The elements of Xes are then converted to physical unit and stored into Xe matrix. Then the MATLAB built-in optimization function *fmincon* solves the following optimization problem, which is just a linear combination of the design variables and responses:

Find Xe to minimize, $\mathbf{f} = \mathbf{Ax} * [Xe] + \mathbf{Ay} * [Y_{app}]$ (4.1)

Subject to the constraint, $\mathbf{g} = \mathbf{Cx} * [Xe] + \mathbf{Cy} * [Y_{app}] - \mathbf{Cb} \leq 0$ (4.2)

Where, **Ax** and **Ay** are the coefficient matrices that define the input and output objectives respectively and **Cx**, **Cy** and **Cb** are the coefficient matrices that define the input and output constraints of the design problem.

After this first phase of the optimization stage is over, the optimal Xe is stored into scaled matrix 'XSQP' and then transformed into physical unit and stored into 'Xsqp' matrix.

In the second phase of the optimization stage, a *while* loop is initiated setting 'Iter' = 1, for Iter $\leq$ $Iter_{max}$, where $Iter_{max}$ are pre-specified number which should be chosen by the user based on the nature of the problem. For each of the iteration, two new data points, one is Xsqp and the second one is (Ninit + Iter)th data point from

XData are added to XC matrix. True responses (YC) for these points are also obtained and YC matrix is updated accordingly. Then the following objective and constraints functions are formulated:

Objective function: $\mathbf{ff} = \mathbf{Ax} * [XC] + \mathbf{Ay} * [YC]$ (4.3)

Constraint function: $\mathbf{gg} = \mathbf{Cx} * [XC] + \mathbf{Cy} * [YC] - \mathbf{Cb} \leq 0$ (4.4)

Then for each element along the length of XC, the maximum values of Eq. (4.4) is obtained and stored into 'g**'** matrix. Next, the indices of only those elements of g, that are less than gEPS (tolerance for constraints; gEPS = 0.001 used in this research) i.e. g < gEPS are determined and stored into the matrix 'Ifeasible'. The values of the objective and constraint functions for those Ifeasible elements are then stored into 'ff' and 'gg' matrices respectively. Then the minimum ff is determined and stored into 'fBEST' and the corresponding gg is stored into 'gBEST' metrix.

If Iter is greater or equal to $Iter_{min}$ (a pre-defined number), convergence check is started, otherwise Iter is incremented by 1 and stage 4 and 5 are repeated.

6. Convergence Check:

In this stage, the database just before the final optimization call, i.e. before the last implementation of the 5th stage is fed to the convergence check function which determines the optimal objective function value following the same procedure as in the case of the second phase of the 5th stage and stored into the matrix named 'fBest'. Then the values of fBEST and fBest are compared. If fBest is less or equal to fBEST, the optimization loop is terminated and the optimum result is published. Otherwise Iter is incremented by 1 and the stages from 4 to 6 are repeated until the convergence is

achieved. If the maximum number of iterations is reached the pre-defined upper level $Iter_{max}$, and yet the problem is not converged, then the design parameters need to be checked and redefined if necessary.

A flow chart for this optimization algorithm is presented in Figure 4.1.

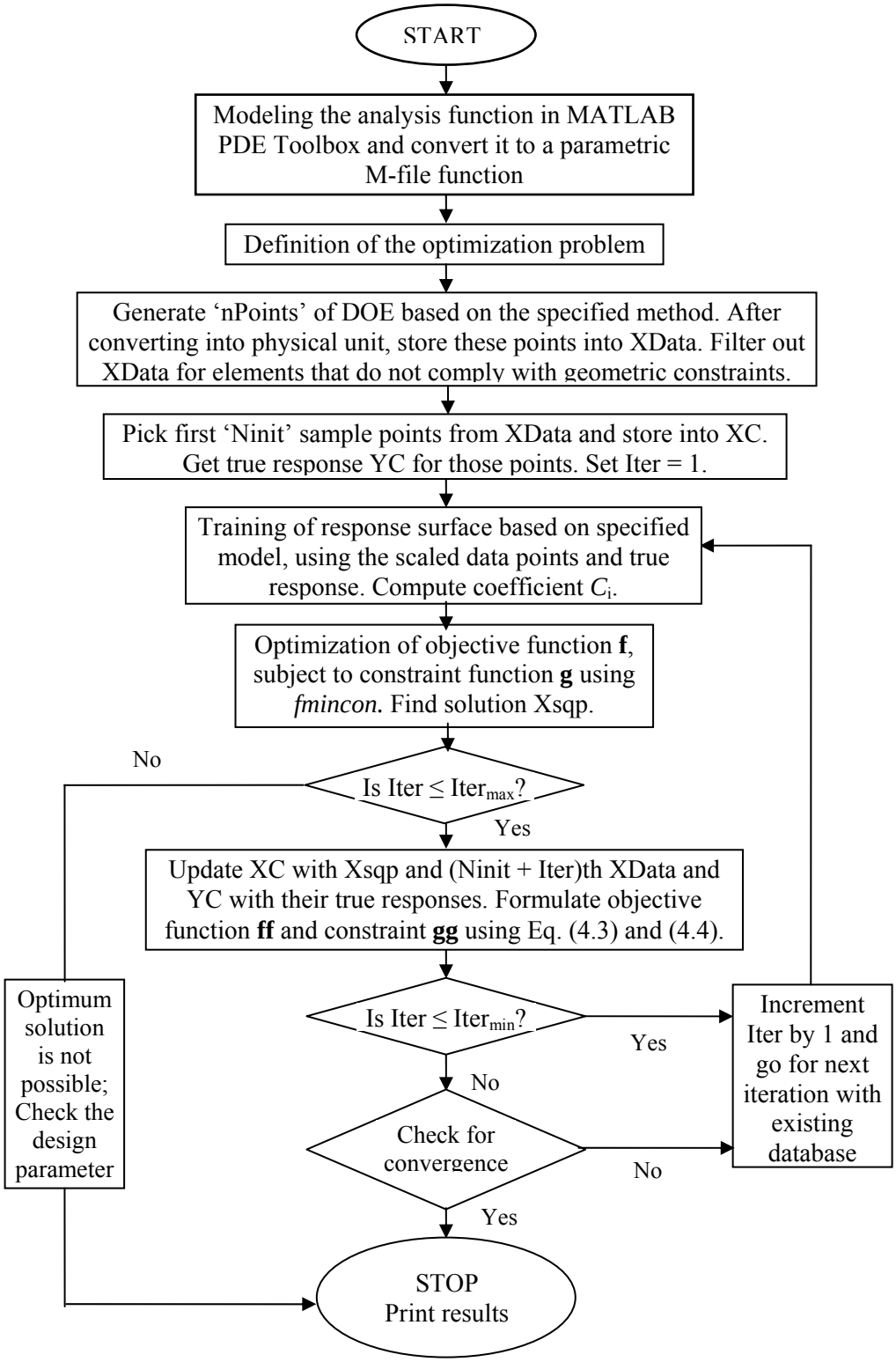

Figure 4.1 Flow chart of the proposed algorithm for structural optimization

CHAPTER 5

IMPLEMENTATION OF RBF META MODELS IN DESIGN OPTIMIZATION

5.1 Introduction

In this research, various meta models have been developed and implemented successfully for ten different application problems. These problems are of different difficulty levels, ranging from two design variables to six design variables, involving weight, or shape optimization with subject to different geometric, stress or frequency constraints. The problems studied during this research are:

1. Determining the optimal location and radius of a hole for minimum weight design of a rectangular plate with one circular hole.
2. Determining the optimal location and radius of a hole for minimum weight design of a rectangular plate with two circular holes.
3. Stress minimization of a rectangular plate with three circular holes by finding the optimal locations for the holes.
4. Shape optimization of a five stepped cantilever beam.
5. Minimum weight design of a trapezoidal plate.
6. Weight minimization of a trapezoidal plate with one circular hole by finding the heights of two parallel sides and the radius of the hole.
7. Weight minimization of a trapezoidal plate with one circular hole by finding the heights of two parallel sides and the optimal location and radius of the hole.

8. Minimum weight design of a quadrangular plate.
9. Determination of the length of three sides and the radius of the hole for minimum weight design of a quadrangular plate with one circular hole.
10. Determination of the length of three sides and the location and radius of the hole for minimum weight design of a quadrangular plate with one circular hole.

The FEM models are generated using MATLAB PDE Toolbox and triangular mesh elements are used for all the cases. The RSM used are based on three different low discrepancy sequencing techniques namely, Halton, Sobol and Faure sequence using four different RBF models namely, Multiquadratic Interpolation (MQI), Multiquadratic Regularization (MQR), Gauss Interpolation (GuassI) and Gauss Regularization (GaussR). For each RBF model with a specific sequencing method, two different initial data levels (i.e. number of DOE points) are set up for ensuring sufficient DOE points for the creation of initial response surface to determine the best possible results. So, the total number of experimental combinations becomes 24 for each example. Finally, these results are compared to the results obtained by solving the same problems using the built-in MATLAB optimization function *fmincon*.

It is found that for most of the implementations, RBF based models give better results than the *fmincon* function (i.e. direct SQP solution by *fmincon*). The number of functional evaluations required (also the time) for the convergence of RSM based optimization is also significantly less than that required in case of *fmincon* function.

The detailed description of the application problems studied in this research is presented in the following sections.

5.2 Rectangular Plate with a Circular Hole – Minimum Weight Design

The first problem solved in this work is a rectangular plate with one circular hole as shown in Figure 5.1. One end of the plate is fixed and a tensile pressure load of 1000 Psi is applied along the edge of the other end.

The plate has dimensions of 30 × 20 × 1 all in inch. It is made of steel with Young's Modulus of Elasticity, $E = 29 \times 10^6$ Psi, Yield Strength, $\sigma_Y = 36 \times 10^3$ Psi, Poisson's ration, $\upsilon = 0.31$ and weight density = 0.285 lbf/inch^3.

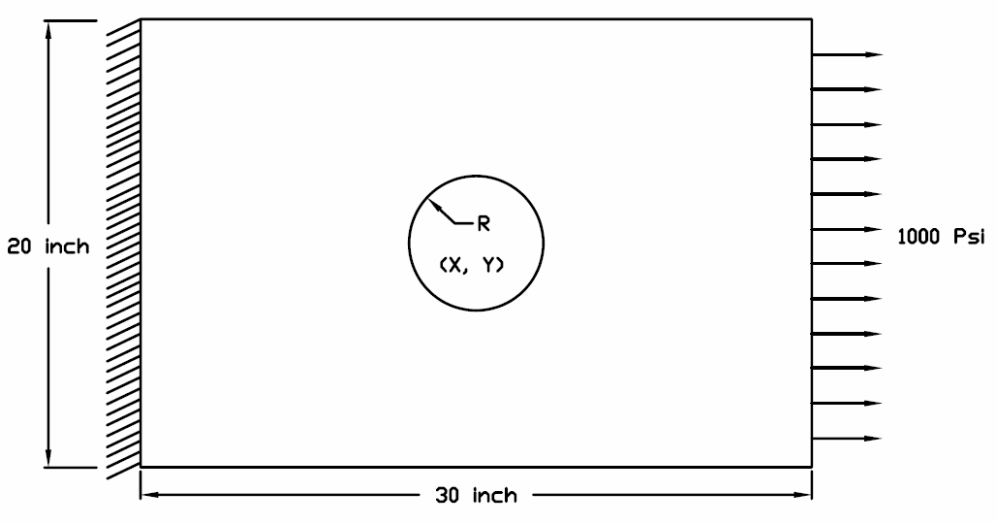

Figure 5.1 Rectangular plate with a circular hole

The objective of this analysis is to find the optimal location and radius for the hole to minimize the volume of the plate (i.e. the weight) such that the maximum von Mises stress developed in the structure would not exceed one third of the Yield strength ($\sigma_Y/3$). Thus the problem formulation is as follows:

Design variables: Location and radius of the hole [X, Y, R].

Lower bounds for the design variables are: [2 2 1] and upper bounds for the design variables are: [28 18 8].

Objective function: Minimize the volume [minimize V]

Subject to the constraints –

a. Geometric constraints (to ensure that the hole lies inside the plate):

$X - R \geq 2$, $Y - R \geq 2$, $X + R \leq 28$ and $Y + R \leq 18$.

b. Von Mises Stress constraint: Max. $\sigma_{VM} \leq 12000$ Psi.

As discussed earlier, for each combination of a specific sequencing technique and RBF model, two different numbers of initial DOE points have been used to create the response surface which makes 24 total numbers of experimental combinations. The first set consists of 10 DOE points, whereas the second set consists of 30 DOE points. All 24 simulation runs converge to give the same result with the optimal location for the center of the hole, X = 15, Y = 10 and, radius R = 8 inch. The minimum volume of the plate is 398.9381 $inch^3$ and the maximum von Mises stress with this result is 10249.1733 Psi. The simulation sets with 10 initial DOE points took 22 function evaluations and sets with 30 initial DOE points took 42 function evaluations to converge to this result. Note that the four significant results represented in this thesis are for numerical comparison. They are not to be interpreted as engineering design data.

To compare the results obtained from response surface optimization methods, the same problem was solved using MATLAB built-in optimization function *fmincon*. The randomly selected initial values for the design variables are 20, 12 and 4 inch for X, Y and R respectively. The optimal results obtained is X = 16.3562, Y= 10 and R= 8

inch. The minimum volume of the plate is 398.9381 $inch^3$ and the maximum von Mises stress with this result is 10610.7763 Psi. The optimization process took 45 function evaluations to converge to this result.

The comparative plots of variations of design variables, volume of the plate and the maximum von Mises stress with number of function evaluations are presented in Figure 5.2, Figure 5.3 and Figure 5.4. The optimal design and the von Mises stress distribution are presented in Figure 5.5 and Figure 5.6 respectively.

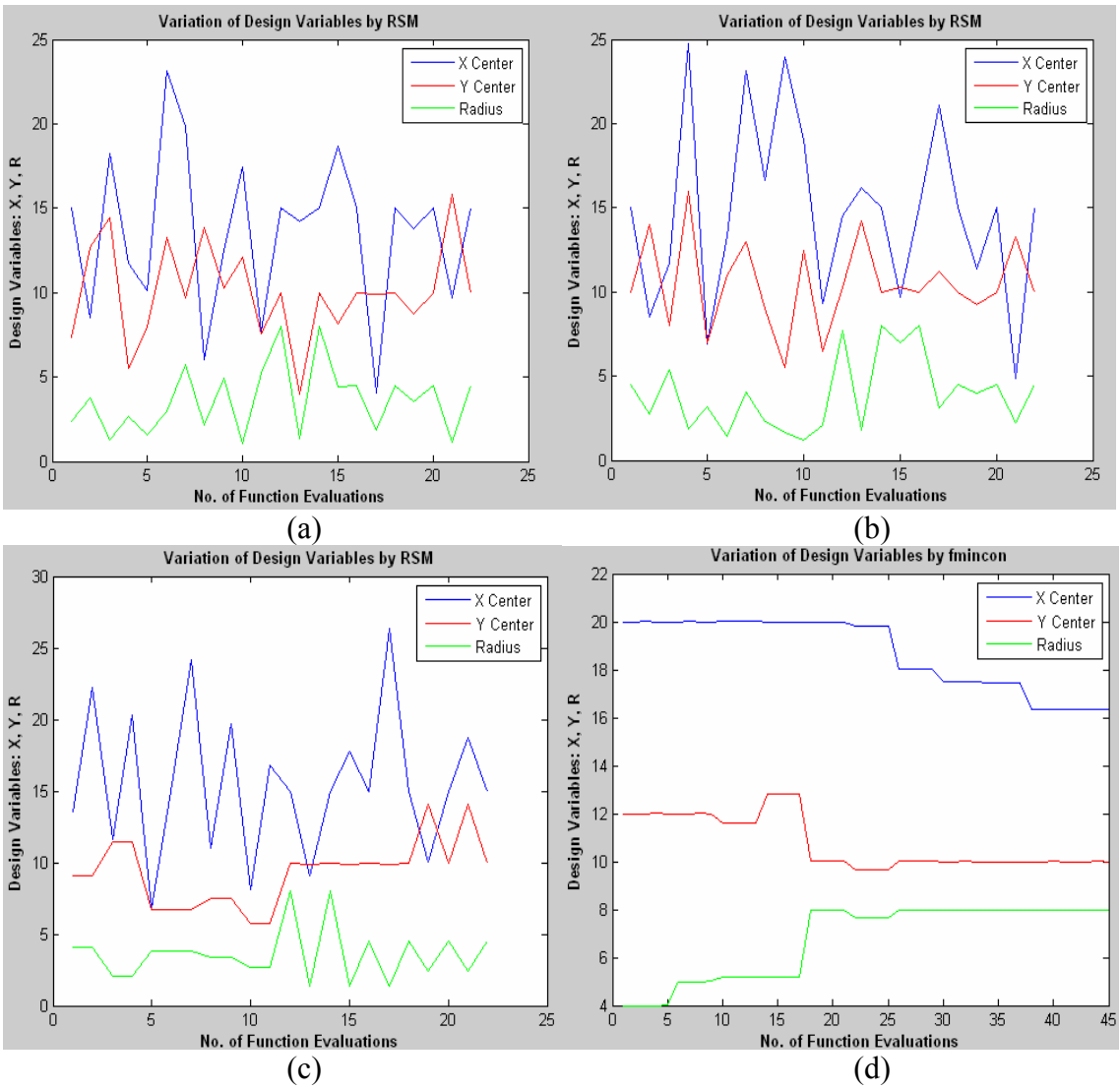

Figure 5.2 Variation of design variables for rectangular plate with a circular hole by (a) Halton sequencing with MQI model, (b) Sobol Sequencing with MQI model, (c) Faure sequencing with MQI model and (d) fmincon function

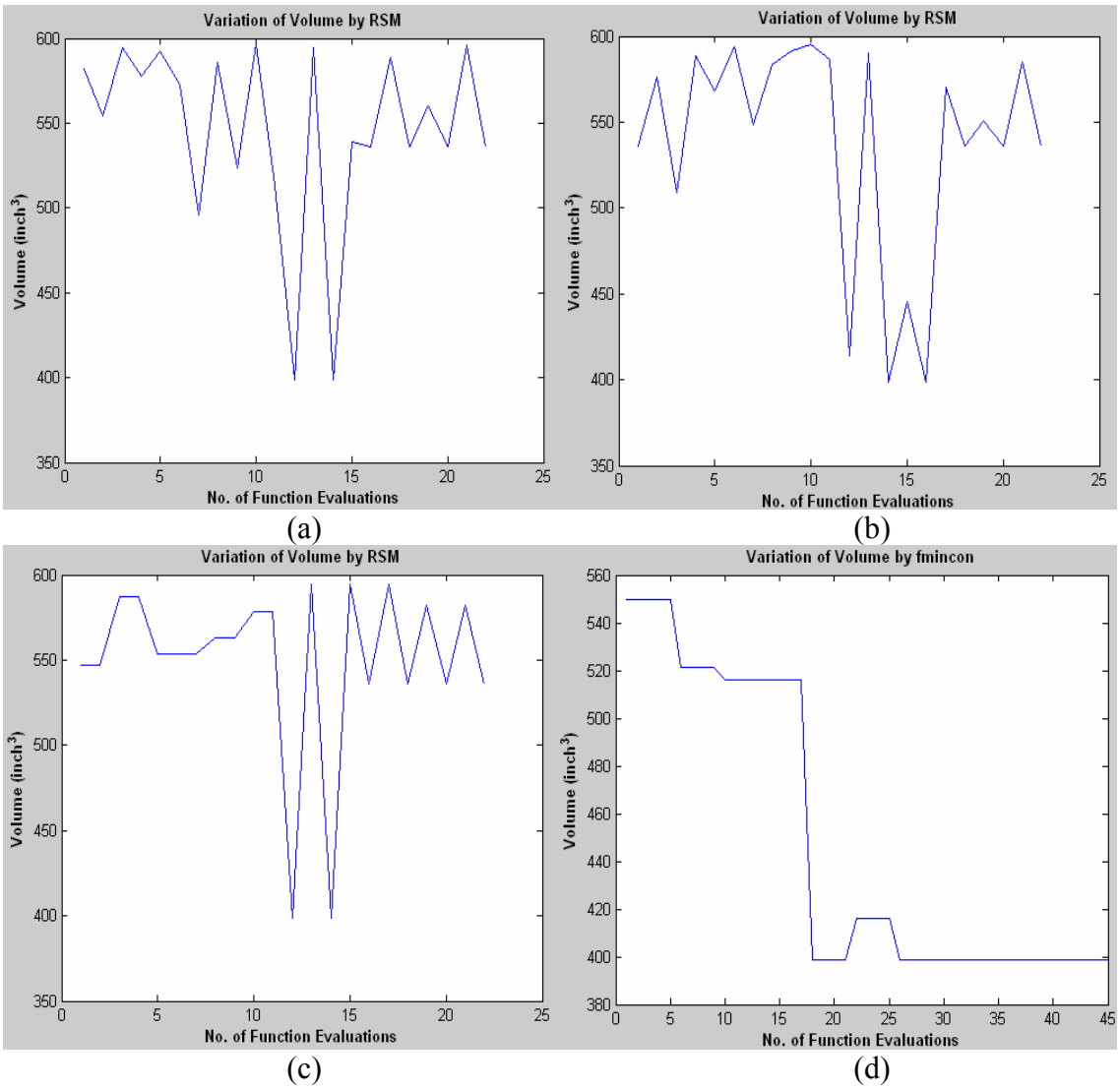

Figure 5.3 Variation of volume for rectangular plate with a circular hole by (a) Halton sequencing with MQI model (10 initial DOE), (b) Sobol Sequencing with MQI model (10 initial DOE), (c) Faure sequencing with MQI model (10 initial DOE) and (d) *fmincon* function

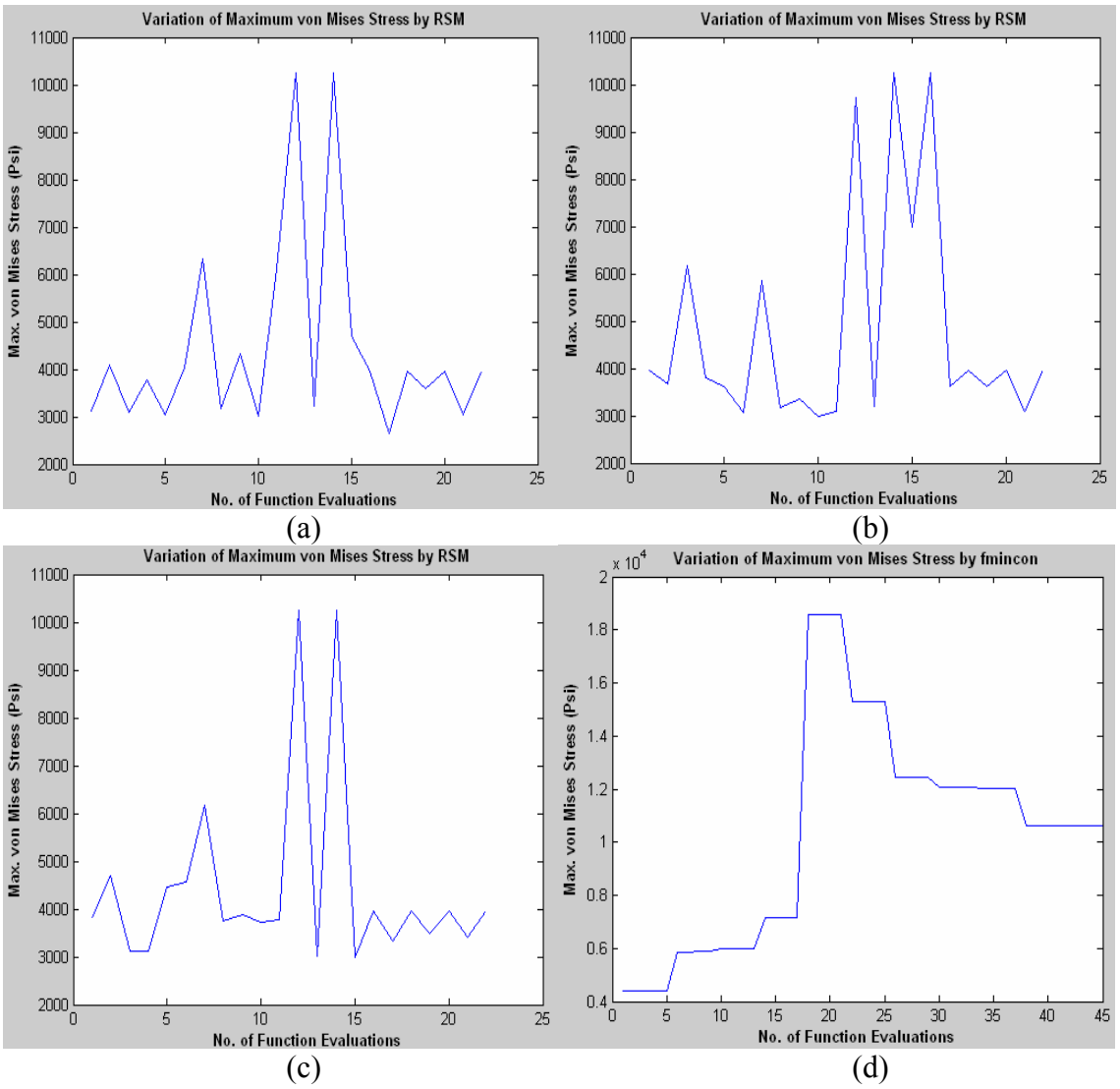

Figure 5.4 Variation of max. von Mises stress for rectangular plate with a circular hole by (a) Halton sequencing with MQI model (10 initial DOE), (b) Sobol Sequencing with MQI model (10 initial DOE), (c) Faure sequencing with MQI model (10 initial DOE) and (d) *fmincon* function

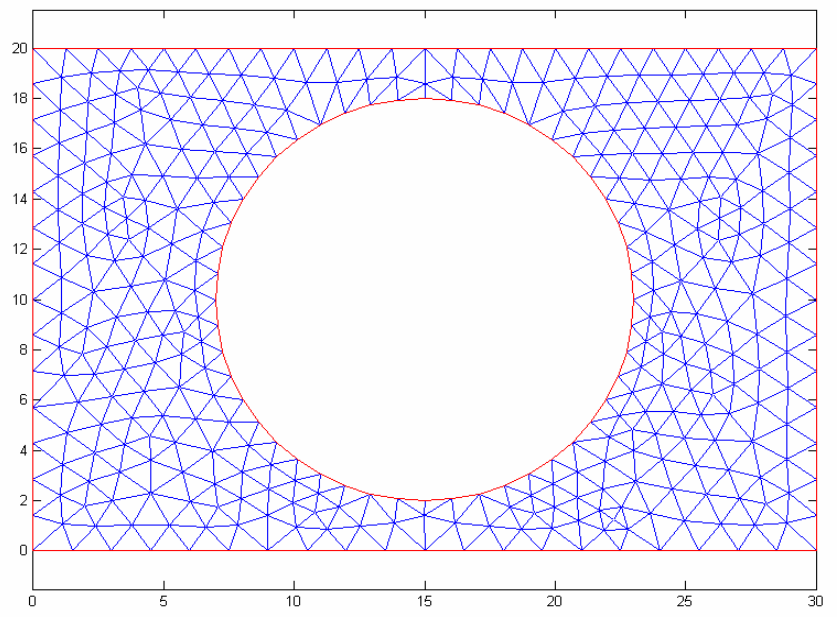

Figure 5.5 Optimum design of the rectangular plate with a circular hole

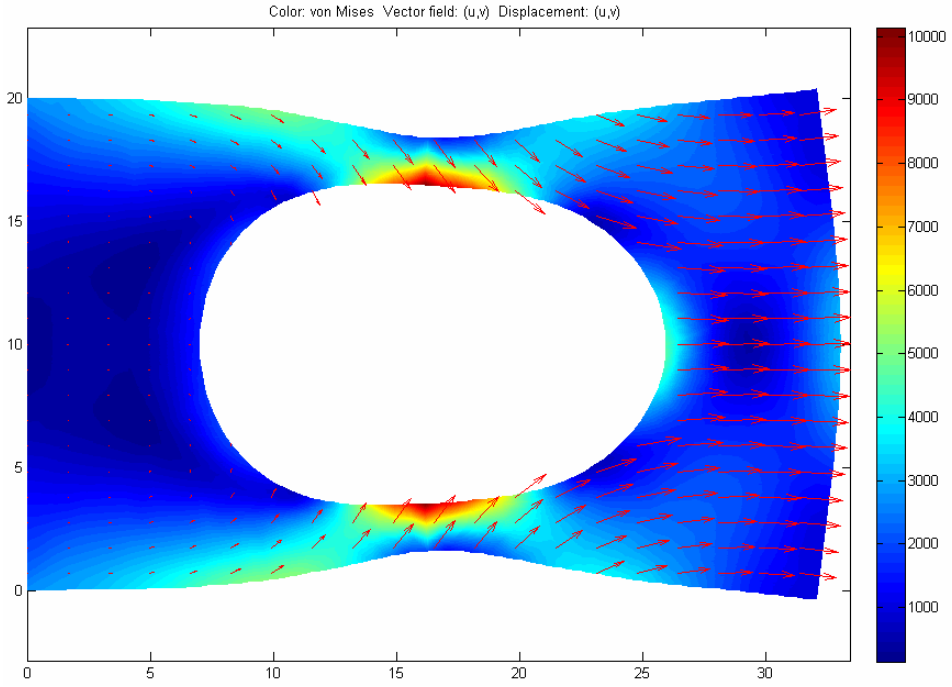

Figure 5.6 von Mises stress distribution with the optimum design for the rectangular plate with circular hole

5.3 Rectangular Plate with Two Circular Holes – Minimum Weight Design

The second problem solved is a rectangular plate with two circular holes as shown in Figure 5.7. The plate is made of steel with Young's Modulus of Elasticity, E = 29×10^6 Psi, Yield Strength, $\sigma_Y = 36 \times 10^3$ Psi, Poisson's ration, $\upsilon = 0.31$ and weight density = 0.285 lbf/inch^3.

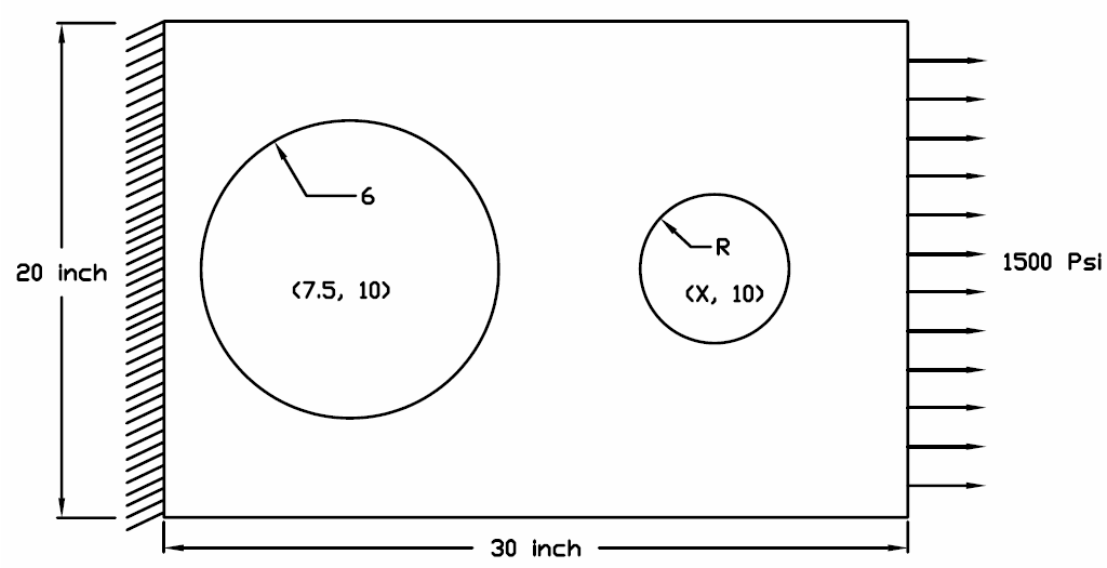

Figure 5.7 Rectangular plate with two circular holes

The plate has dimensions of 30 × 20 × 1 all in inch. Left end of the plate is fixed and a tensile pressure load of 1500 Psi is applied along the right edge. The left hole has a radius of 6 inch and it's center is fixed at 7.5 inch from the left edge and 10 inch above the bottom edge. The center of the right hole is fixed at 10 inch above the bottom edge. The location of the X center (i.e. the location of the center along the length of the plate) and the radius of the hole are to be determined such that the volume of the plate

(hence the weight) is minimized subject to von Mises stress developed does not exceed one third of the Yield strength ($\sigma_Y/3$) of steel. The problem formulation is as follows:

Design variables: Location of X coordinate of center and radius of the hole [X, R].

Lower bounds for the design variables are: [17 1] and upper bounds for the design variables are: [28 7].

Objective function: Minimize the volume [minimize V]

Subject to the constraints –

a. Geometric constraints (to ensure that the hole lies inside the plate and does not intersect the left hole):

$$X - R \geq 16,\ X + R \leq 28.$$

b. Von Mises Stress constraint: Max. $\sigma_{VM} \leq 12000$ Psi.

As in the case with the first problem, the total numbers of experimental combination here is also 24. For each combination of a specific sequencing technique and RBF model, two different numbers of initial DOE points have been used to create the response surface. The first set consists of 10 DOE points, whereas the second set consists of 30 DOE points. All 24 simulation runs converge to give the same result with the optimal location for the X center of the hole, X = 22 and radius R = 6 inch. The minimum volume of the plate is 373.8053 $inch^3$ and the maximum von Mises stress with this result is 11905.1532 Psi. The simulation sets with 10 initial DOE points took 22 function evaluations and sets with 30 initial DOE points took 42 function evaluations to converge to this result.

The same problem was solved using MATLAB built-in optimization function *fmincon* for comparing the results with response surface model. The initial values for the design variables X and R are randomly selected as 25 and 1 inch respectively. The optimal results obtained is X = 22 and R= 6 inch. The minimum volume of the plate is 373.8053 $inch^3$ and the maximum von Mises stress with this result is 11905.1532 Psi. The optimization process took 22 function evaluations to converge to this result. These results are exactly same as those obtained from response surface model.

The comparative plots of variations of design variables, volume of the plate and the maximum von Mises stress with number of function evaluations are presented in Figure 5.8, Figure 5.9 and Figure 5.10. The optimal design and the von Mises stress distribution are presented in Figure 5.11 and Figure 5.12 respectively.

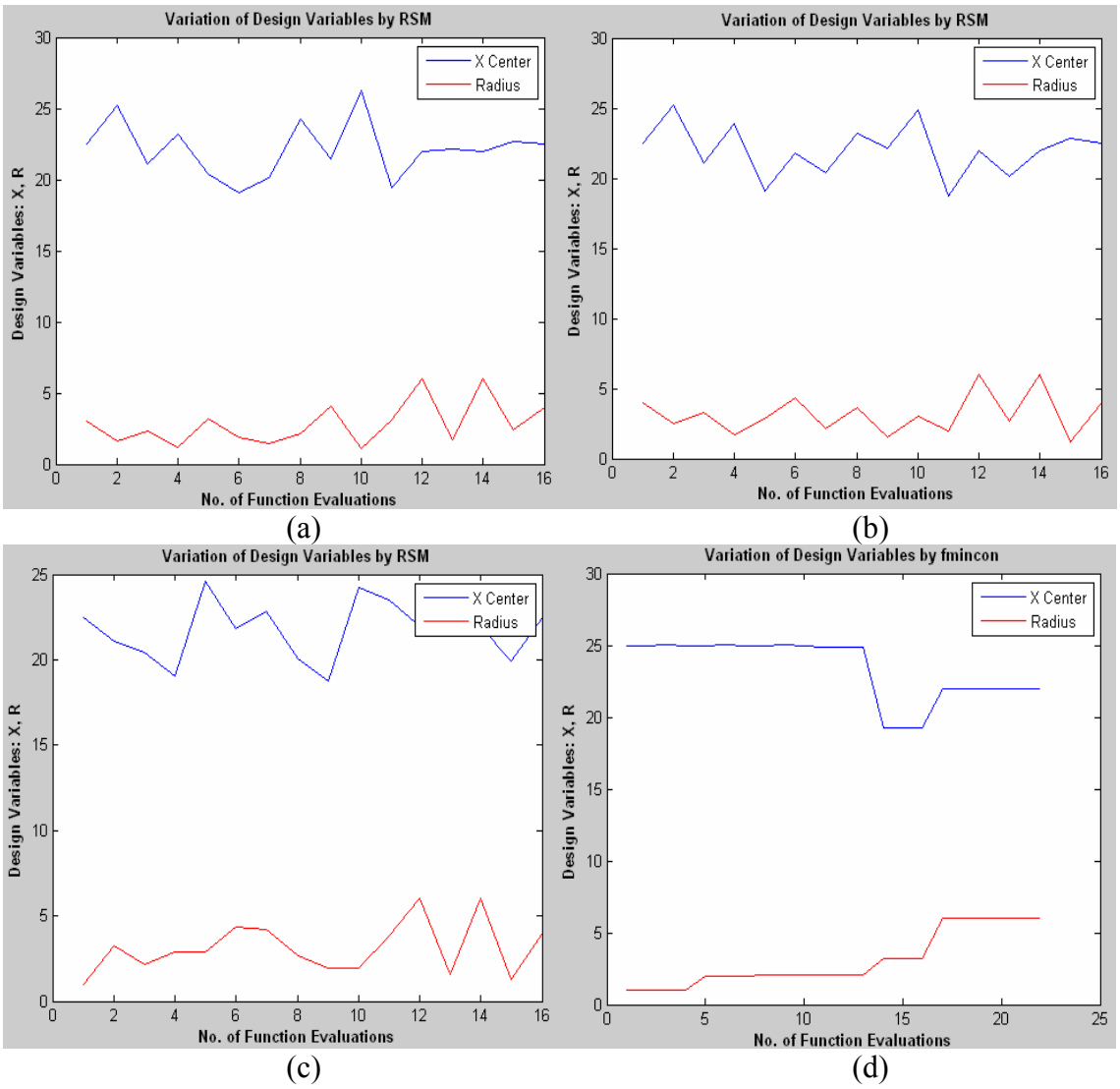

Figure 5.8 Variation of design variables for rectangular plate with two circular holes by (a) Halton sequencing with MQI model (10 initial DOE), (b) Sobol Sequencing with MQI model (10 initial DOE), (c) Faure sequencing with MQI model (10 initial DOE) and (d) *fmincon* function

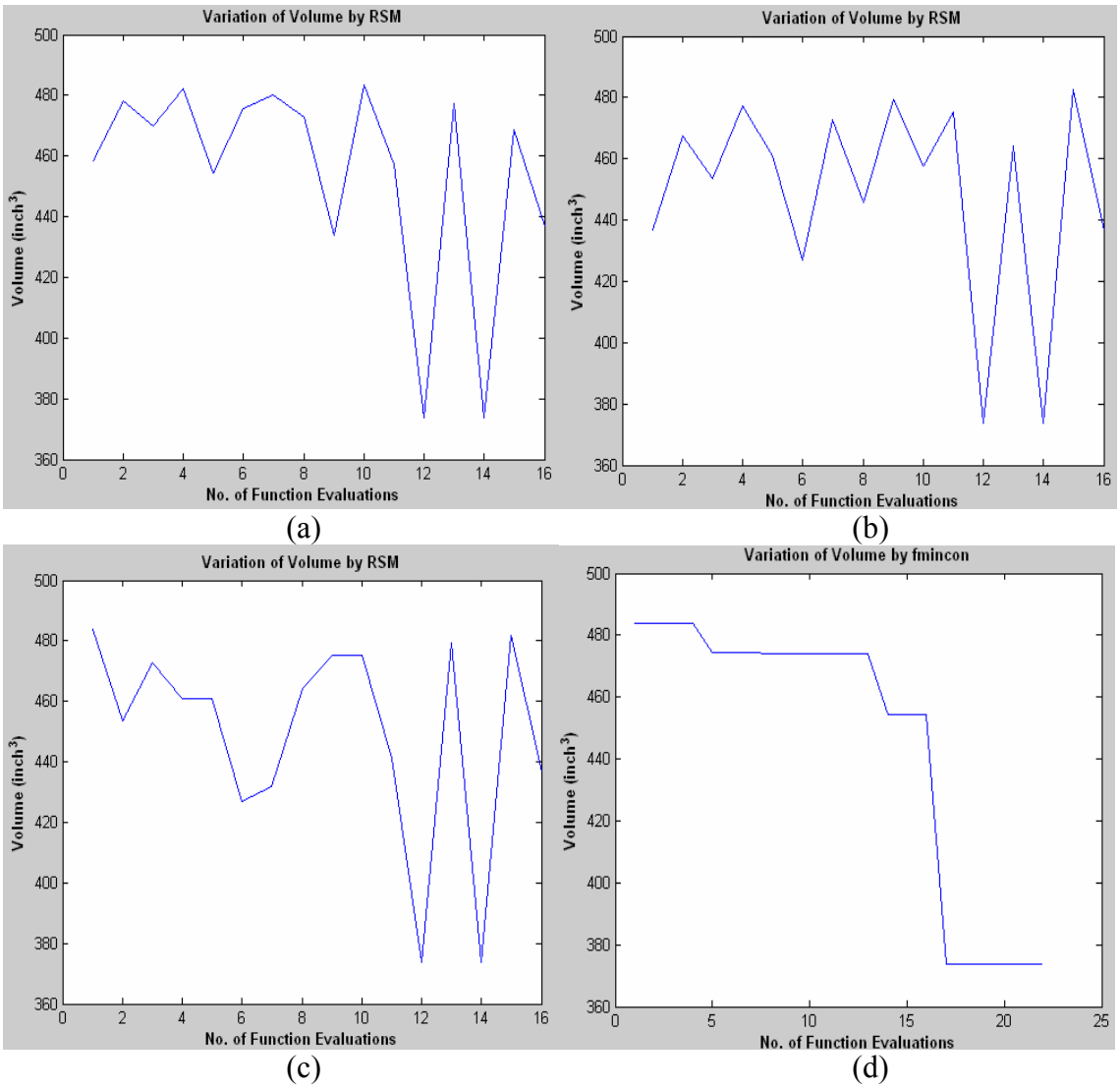

Figure 5.9 Variation of volume for rectangular plate with two circular holes by (a) Halton sequencing with MQI model (10 initial DOE), (b) Sobol Sequencing with MQI model (10 initial DOE), (c) Faure sequencing with MQI model (10 initial DOE) and (d) *fmincon* function

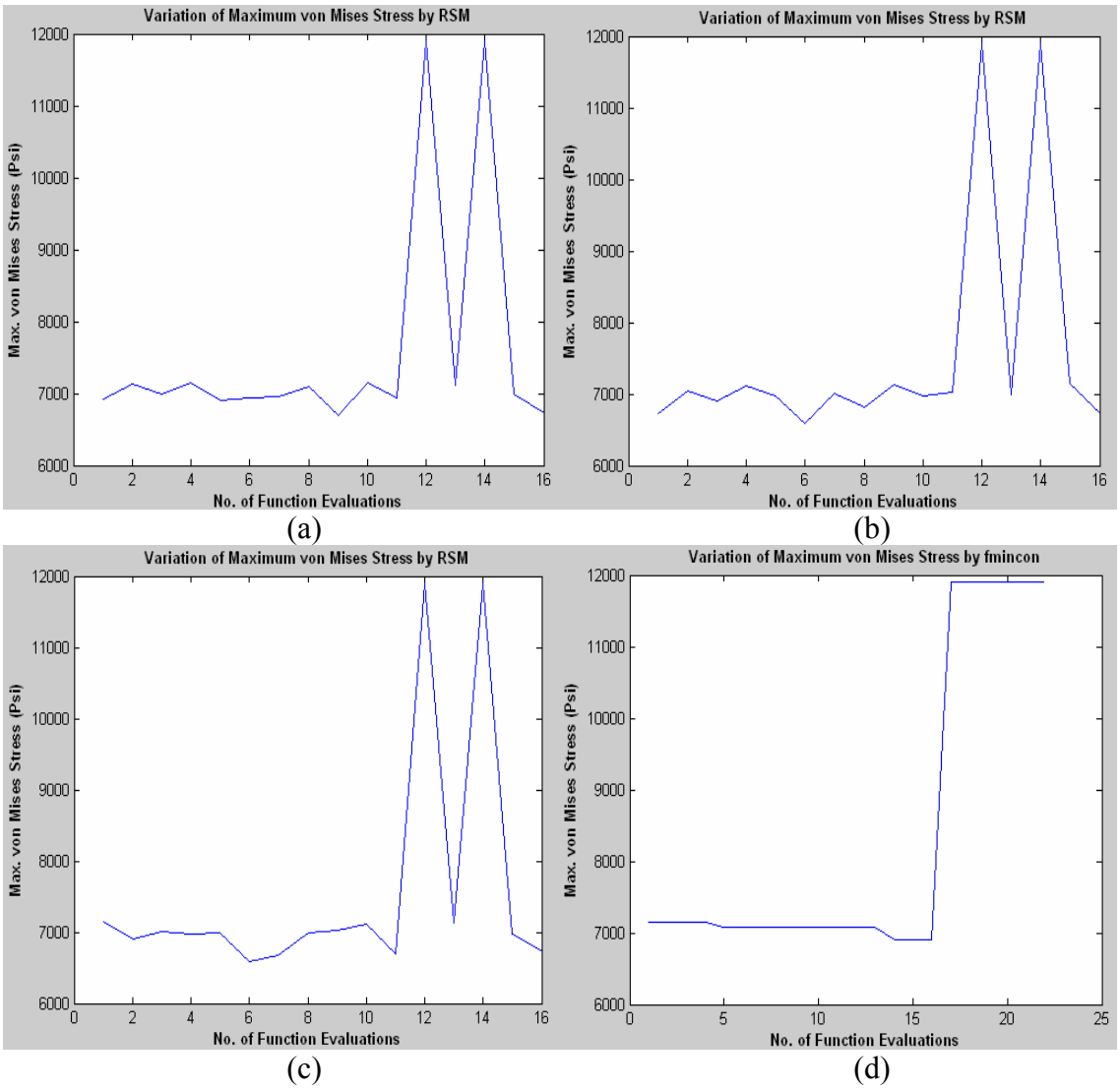

Figure 5.10 Variation of max. von Mises stress for rectangular plate with two circular holes by (a) Halton sequencing with MQI model (10 initial DOE), (b) Sobol Sequencing with MQI model (10 initial DOE), (c) Faure sequencing with MQI model (10 initial DOE) and (d) *fmincon* function

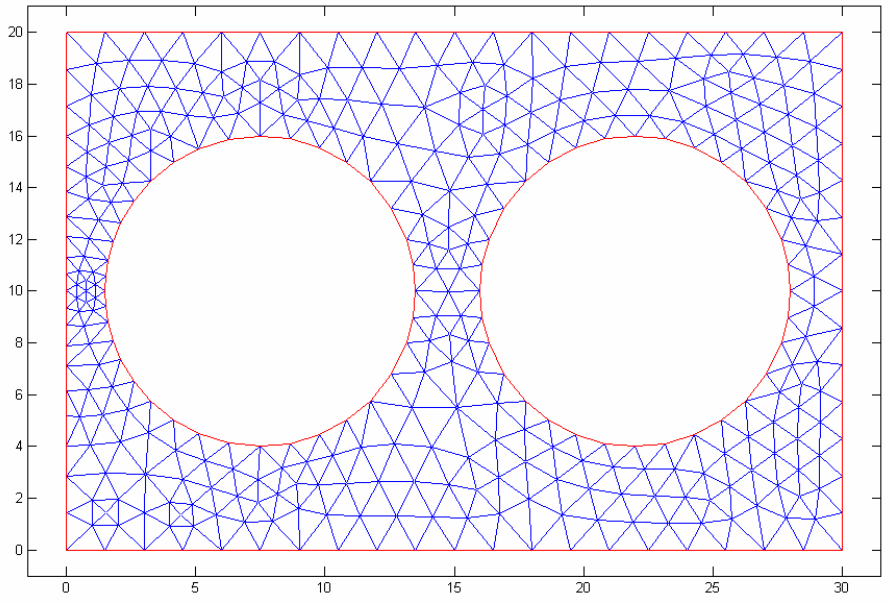

Figure 5.11 Optimum design of the rectangular plate with two circular holes

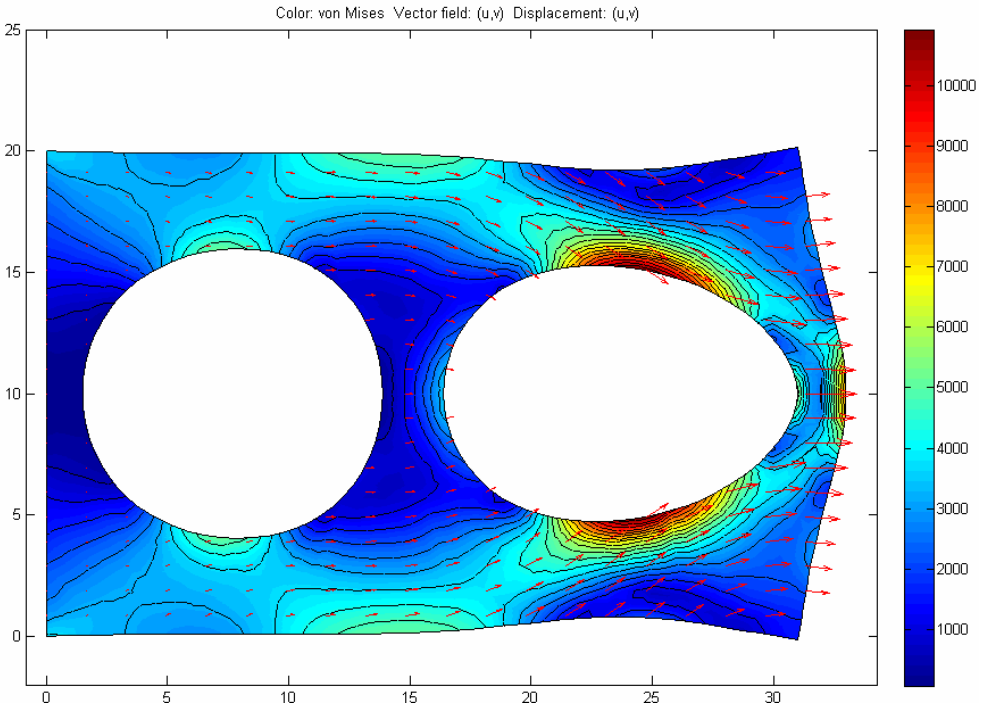

Figure 5.12 von Mises stress distribution with the optimum design for the rectangular plate with two circular holes

5.4 Rectangular Plate with Three Holes – Minimization of Maximum Stress

The third problem solved in this work is a rectangular plate with three holes, as shown in Figure 5.13. The left edge of the plate is fixed and a tensile load of 2000 Psi is applied along the right edge. The plate has dimensions of 30 × 20 × 1 all in inch. The radius of the larger hole is 3 inch and the smaller two have a radius of 1.5 inch each.

The plate is made of steel with Young's Modulus of Elasticity, $E = 29 \times 10^6$ Psi, Yield Strength, $\sigma_Y = 36 \times 10^3$ Psi, Poisson's ration, $\upsilon = 0.31$ and weight density = 0.285 lbf/inch^3.

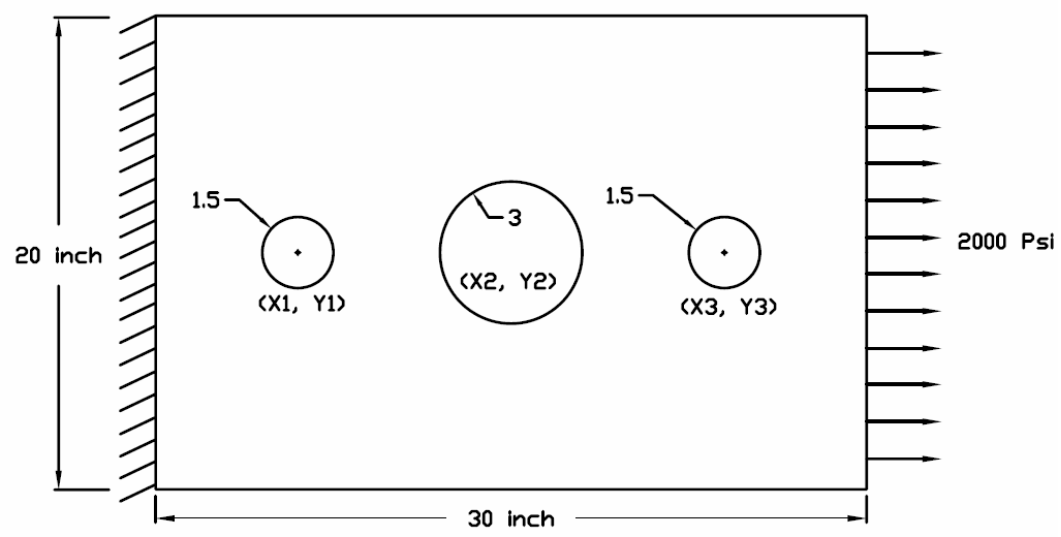

Figure 5.13 Rectangular plate with three holes

The objective of this analysis is to find the optimum locations for the holes so that the maximum von Mises stress developed in the structure would be minimum,

subjected to some specific geometric constraints. The problem formulation is as follows:

Design variable: Locations of the centers [X1, Y1, X2, Y2, X3, Y3]

Lower bounds and upper bounds of the design variables are [3.5, 7.5, 11.5, 7.5, 21.5, 7.5] and [6, 12, 16, 12, 26, 12] respectively.

Objective function: Minimize the maximum von Mises stress [minimize max. σ_{VM}].

Subject to the geometric constraints –

Distance between first and second holes should be at least 4.6 inch.

$$\text{i.e. } d_1 = \sqrt{(x_1 - x_2)^2 + (y_1 - y_2)^2} \geq 4.6$$

Distance between second and third holes should be at least 4.6 inch.

$$\text{i.e. } d_2 = \sqrt{(x_2 - x_3)^2 + (y_2 - y_3)^2} \geq 4.6$$

And distance between first and third holes should be at least 3.1 inch.

$$\text{i.e. } d_3 = \sqrt{(x_1 - x_3)^2 + (y_1 - y_3)^2} \geq 3.1$$

These are to ensure that none of the holes can intersect one another.

A total of 24 experiments were carried out to find the best possible RBF model. For each combination of a specific sequencing technique and RBF model, two different numbers of initial DOE points have been used to create the response surface. The first set consists of 10 DOE points, whereas the second set consists of 30 DOE points. For Halton sequencing method, MQR RSM with 10 initial DOE points gives the best results. For this case, the optimum locations for the holes are (3.5, 10.8438), (11.5, 10.1681) and (24.6596, 10.1735) respectively with maximum von Mises stress of

6161.7255 Psi and the optimization process converges with 22 function evaluations. For Sobol sequencing technique, all the 8 experimental combinations give the same results. The optimum locations for the holes in this case are, (4.75, 9.75), (13.75, 9.75) and (23.75, 9.75) respectively with maximum von Mises stress of 6113.463 Psi. However, for this problem, Faure sequencing technique with MQI RSM and GuassR RSM with 30 initial DOE points give the best possible results. The optimum locations for the holes in this case are, (5.7449, 8.9694), (12.9694, 8.9694) and (22.9694, 8.9694) respectively with maximum von Mises stress of 6002.8299 Psi. The problem converges after 42 function evaluations.

To compare these results with MATLAB built-in function *fmincon*, experiment has been performed with randomly selected starting points for the center locations of the three holes as (5.1, 9.6), (13.5, 9.6) and, (24.5, 9.5) respectively. The optimal locations for the holes obtained are (5.7486, 10.3579), (12.9906, 10.2343) and, (24.2794, 10.3257) respectively with maximum von Mises stress of 6111.1 Psi and the optimization process converged in 506 functional evaluations. So, the best results obtained using RBF models are less than that of using *fmincon* function and *fmincon* also takes much more functional evaluations than the RBF models.

With an intention to improve the design further, the results obtained from the response surface optimization were used again as the initial design variable input for another round of *fmincon* function optimizations with the lower and upper bounds for the design variables were initial input – 0.5 and initial input + 0.5 respectively.

However the optimization processes failed to give any improvement to the previous designs.

The comparative plots of variations of design variables and the maximum von Mises stress with number of function evaluations are presented in Figure 5.14 and Figure 5.15. The optimal design and the von Mises stress distribution are presented in Figure 5.16 and Figure 5.17 respectively.

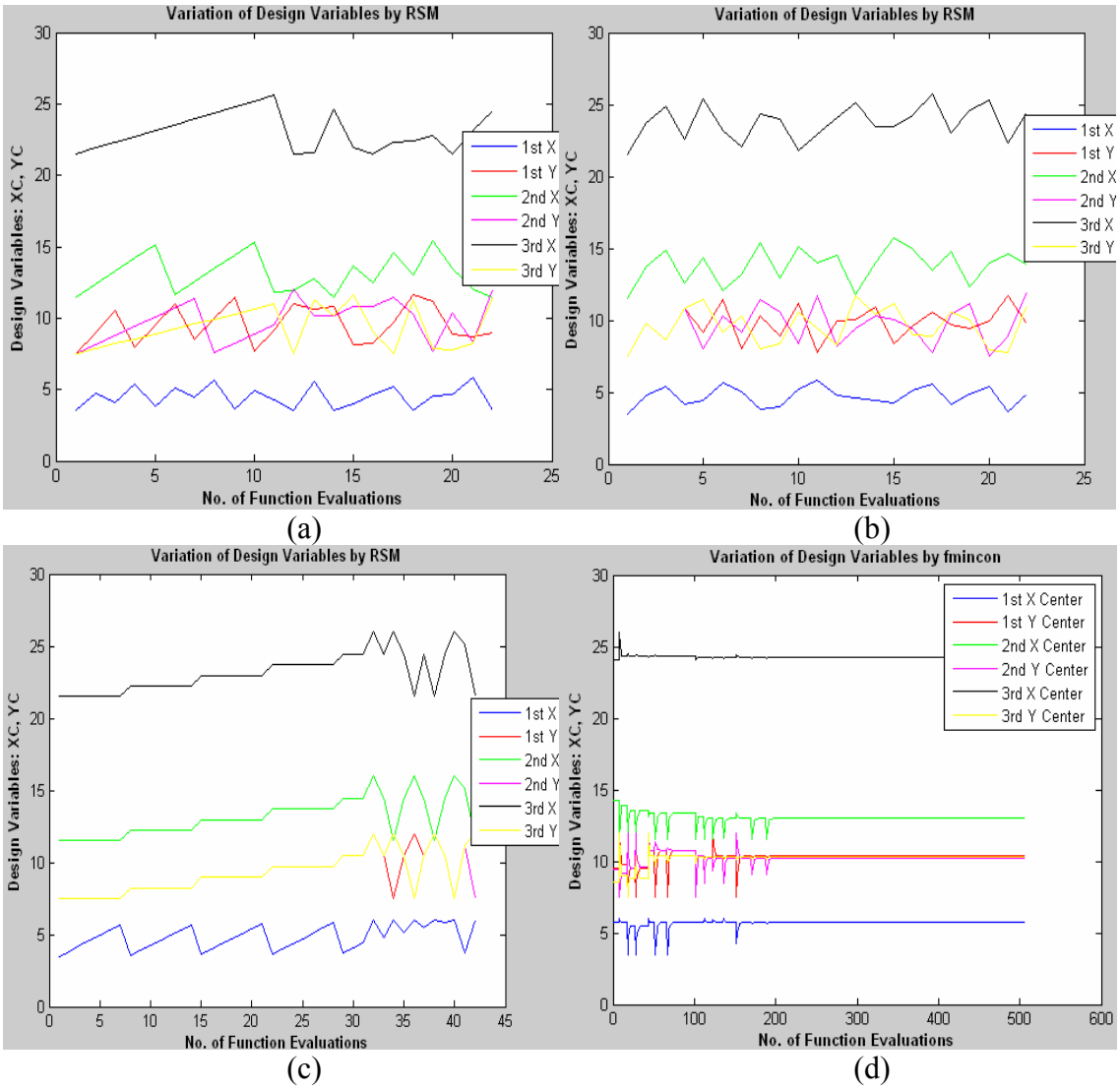

Figure 5.14 Variation of design variables for rectangular plate with three circular holes by (a) Halton sequencing with MQR model (10 initial DOE), (b) Sobol Sequencing with MQI model (10 initial DOE), (c) Faure sequencing with MQI model (30 initial DOE) and (d) *fmincon* function

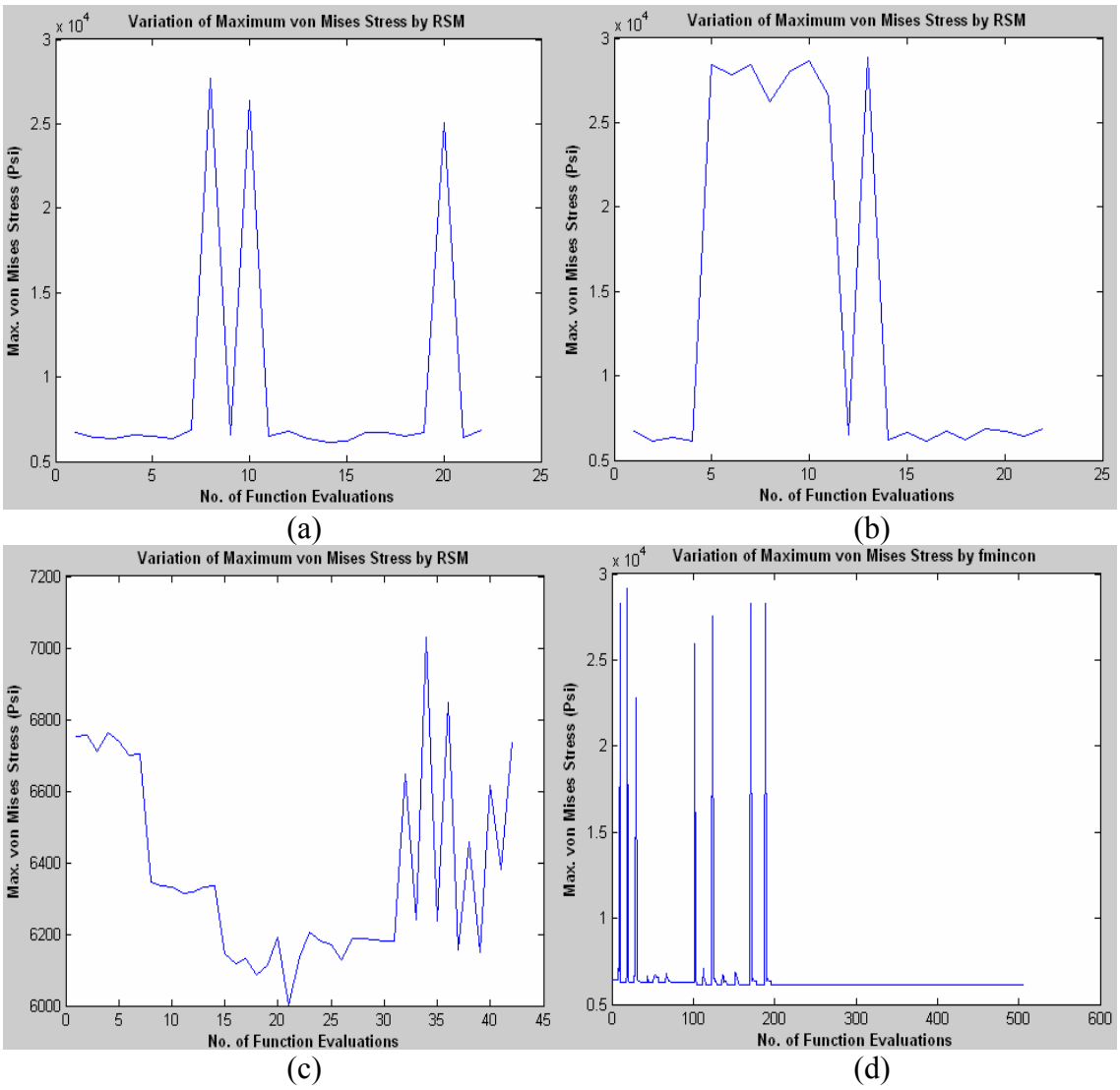

Figure 5.15 Variation of maximum von Mises stress for rectangular plate with three circular holes by (a) Halton sequencing with MQR model(10 initial DOE), (b) Sobol Sequencing with MQI model(10 initial DOE), (c) Faure sequencing with MQI model (30 initial DOE) and (d) *fmincon* function

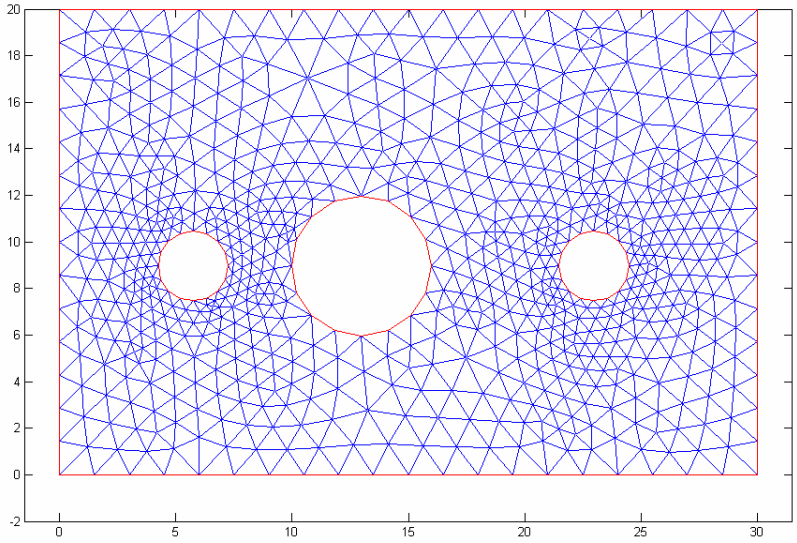

Figure 5.16 Optimum design for the rectangular plate with three circular holes

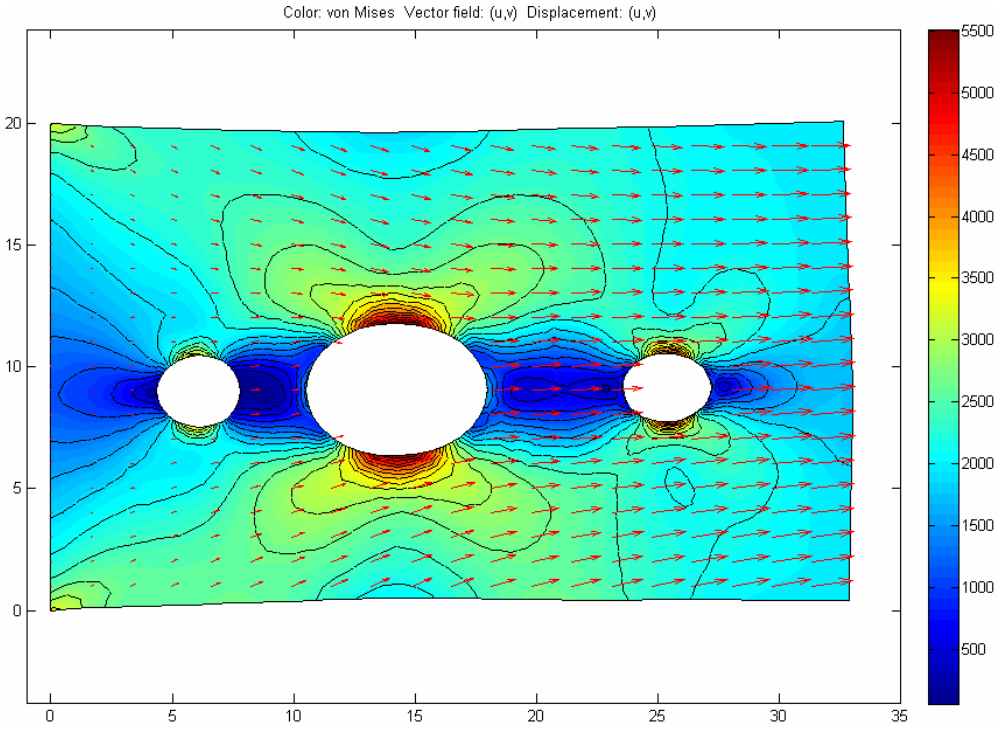

Figure 5.17 von Mises stress distribution with the optimum design for the rectangular plate with three circular holes

5.5 Five Stepped Cantilever Beam – Eigen Value Problem

The fourth problem solved is a five stepped cantilever steel beam as shown in Figure 5.17. One end of the beam is fixed and the other end is free. The beam is not subjected to any external loading. The length of each step is 24 inch. So, the total length of the beam is 120 inch.

The steel beam has a Young's modulus of 3×10^7psi, poisson's ration 0.31 and weight density 0.285 lbf/in^3.

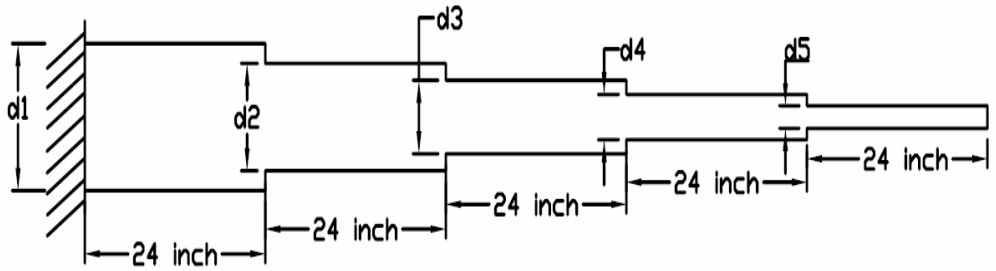

Figure 5.18 Five stepped cantilever beam

The objective of this problem is to find the optimum heights for each of the steps of the beam so that the First Natural Frequency (in-plane) is maximized subjected to the some specific geometric constraints. The problem formulation is as follows:

Design variables: Heights of each step [d1, d2, d3, d4, d5]

The lower and upper bounds for the design variables are [0.05, 0.04, 0.03, 0.02, 0.01] and [4, 3.5, 3, 2.5, 2] respectively.

Objective function: Maximize the first natural frequency [minimize – f1]

Subject to the following geometric constraints:

$$d2 - d1 \leq -0.1,\ \ d3 - d2 \leq -0.1,$$

$$d4 - d3 \leq -0.1,\ \ d5 - d4 \leq -0.1$$

These constraints have been used to ensure that the heights of the steps follow the condition: $d1 > d2 > d3 > d4 > d5$.

In order to determine the best possible RBF model, 24 experiments were performed. Similar to the previous problems, for each combination of a specific sequencing technique and RBF model, two different numbers of initial DOE points have been used to create the response surface. The first set consists of 10 DOE points, whereas the second set consists of 30 DOE points. It is found that Halton sequence with MQR RBF model for 30 initial DOE points produces the maximum first natural frequency of 14.8820 Hz. The optimum heights of the steps are d1 = 4 inch, d2 = 3.5 inch, d3 = 3 inch, d4 = 1.7998 inch and d5 = 0.18554 inch. The number of function evaluations required to converge is 42. For Sobol sequencing technique, MQI RBF model with 10 initial DOE points produces the maximum first natural frequency of 14.2947 Hz. The optimum heights of the steps are d1 = 3.5463 inch, d2 = 3.3018 inch, d3 = 3 inch, d4 = 0.96445 inch and d5 = 0.30561 inch. The problem converged with 22 function evaluations. For Faure sequencing technique, MQI RBF model with 30 initial DOE points produces the maximum first natural frequency of 14.2015 Hz. The optimum heights of the steps are d1 = 3.6667 inch, d2 = 3.5 inch, d3 = 2.4127 inch, d4 = 1.5735 inch and d5 = 0.38783 inch. The problem converged with 42 function evaluations.

In order to compare these results, the same problem is solved using MATLAB built-in function *fmincon* with a randomly selected initial values for the design variables as d1= 4 inch, d2=3.5 inch, d3=3 inch, d4 = 2.5 inch, and d5 = 2 inch. The maximum first natural frequency is found to be 13.1653 Hz. The optimum heights are d1 = 4 inch, d2 = 3.2719 inch, d3 = 2.136 inch, d4 = 1.2891 inch and d5 = 0.61245 inch. The total number of function evaluations was 1005 for this case.

With an intention to improve the design further, the following hybrid approach is tested. Starting from the best results obtained from the response surface optimization as the initial design variable inputs for another round of *fmincon* function optimization. The lower and upper bounds for the design variables were initial input – 0.005 and initial input + 0.005 respectively. Halton sequencing with MQR RSM model with 30 initial DOE produces the best results. The optimization process took 1005 function evaluations to give an improved design of d1 = 4.005 inch, d2 = 3.505 inch, d3 = 3.005 inch, d4 = 1.8048 inch and d5 =0.19054 inch with maximum first natural frequency of 14.9598 Hz. This optimal design and the first mode shape for this design are presented in Figure 5.20 and Figure 5.21 respectively. The result shows that the first natural frequency increases from 14.8820 Hz (RSM result) to 14.9598 Hz. This improvement is achieved with 1005 additional finite element solutions.

The comparative plots of variations of design variables and the maximum first natural frequency with number of function evaluations are presented in Figure 5.18 and Figure 5.19 respectively.

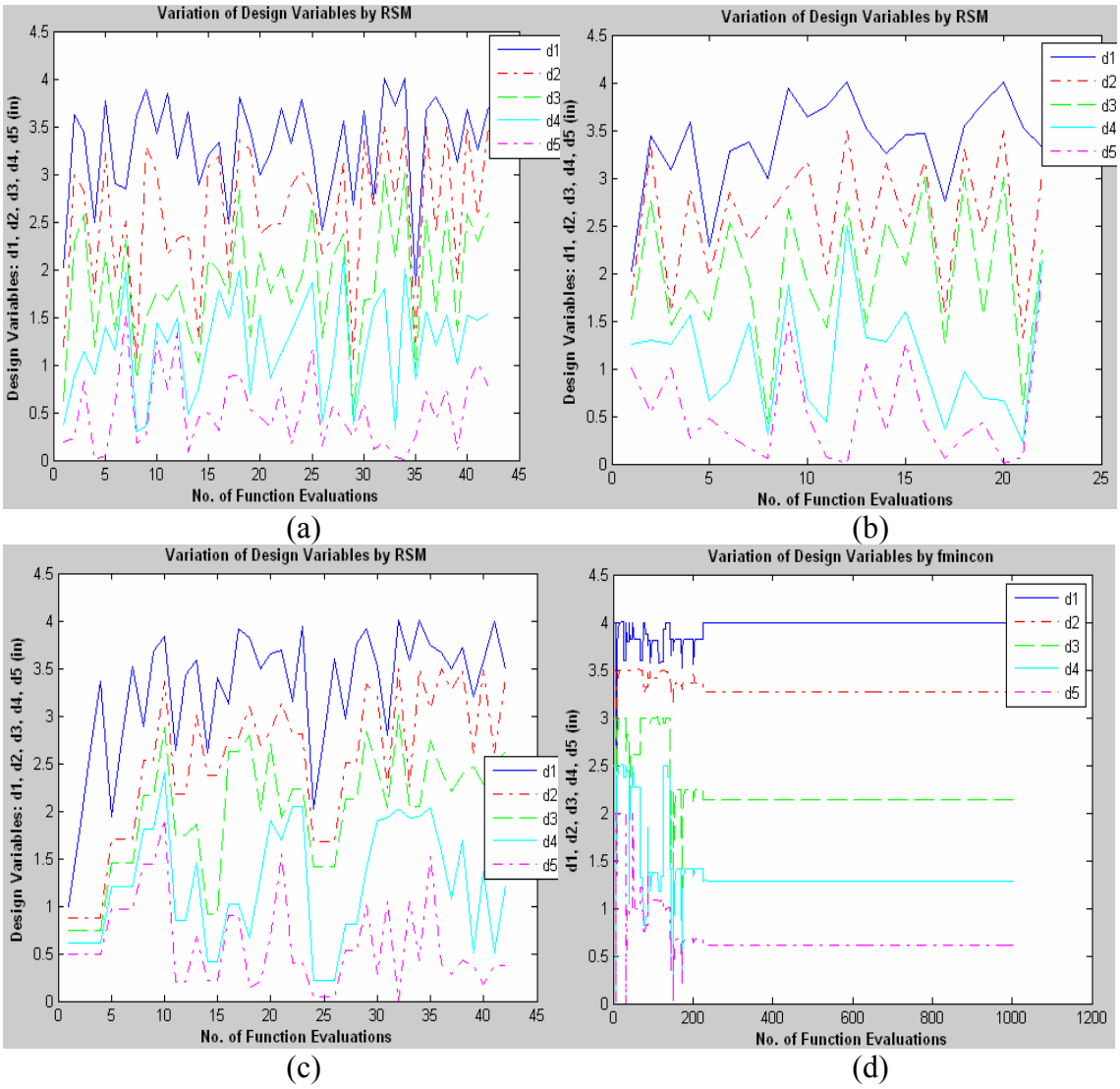

Figure 5.19 Variation of design variables for five stepped cantilever beam by (a) Halton sequencing with MQR model (30 initial DOE), (b) Sobol Sequencing with MQI model (10 initial DOE), (c) Faure sequencing with MQI model (30 initial DOE) and (d) *fmincon* function

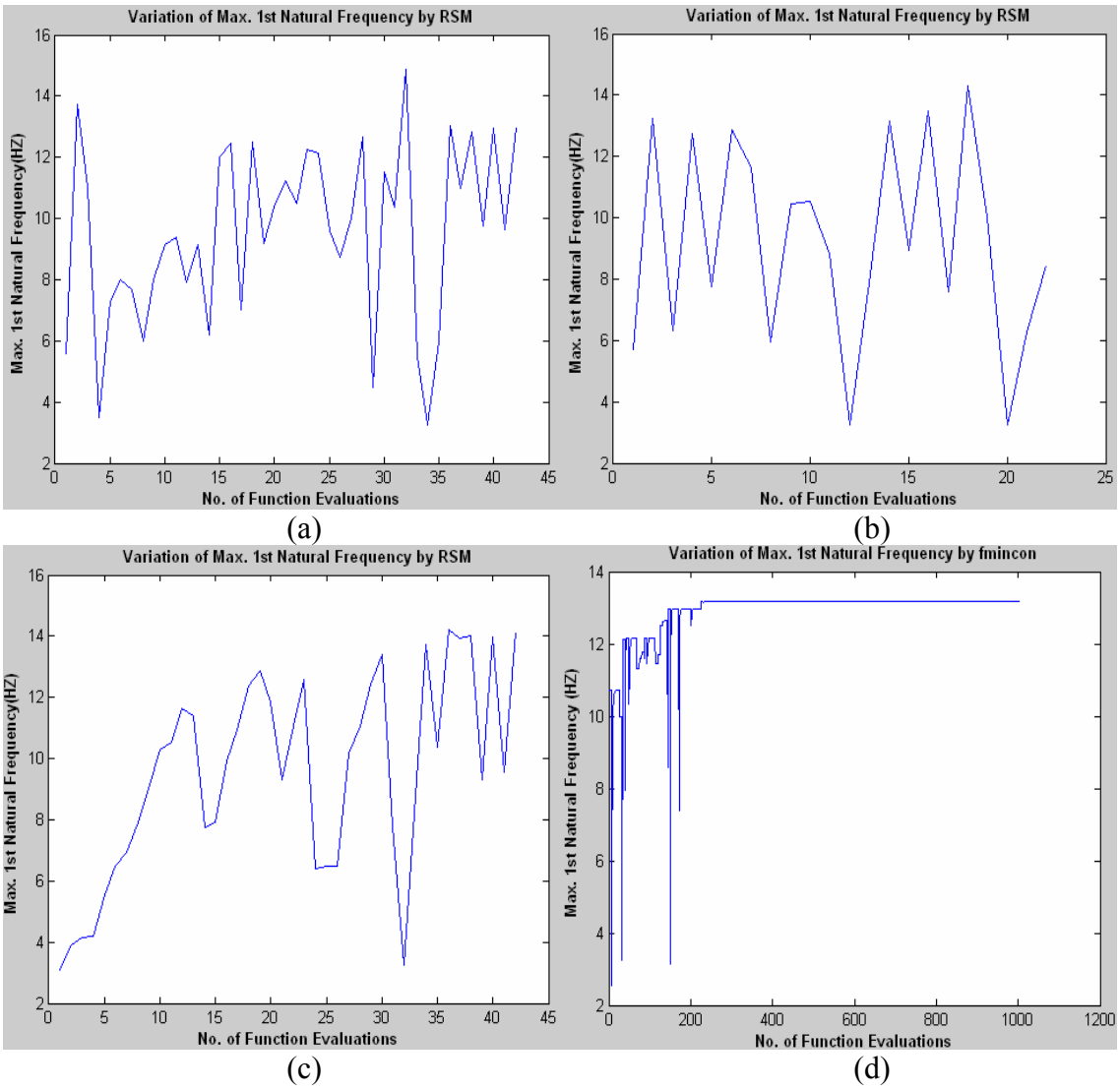

Figure 5.20 Variation of maximum first natural frequency for five stepped cantilever beam by (a) Halton sequencing with MQR model (30 initial DOE), (b) Sobol Sequencing with MQI model (10 initial DOE), (c) Faure sequencing with MQI model (30 initial DOE) and (d) *fmincon* function

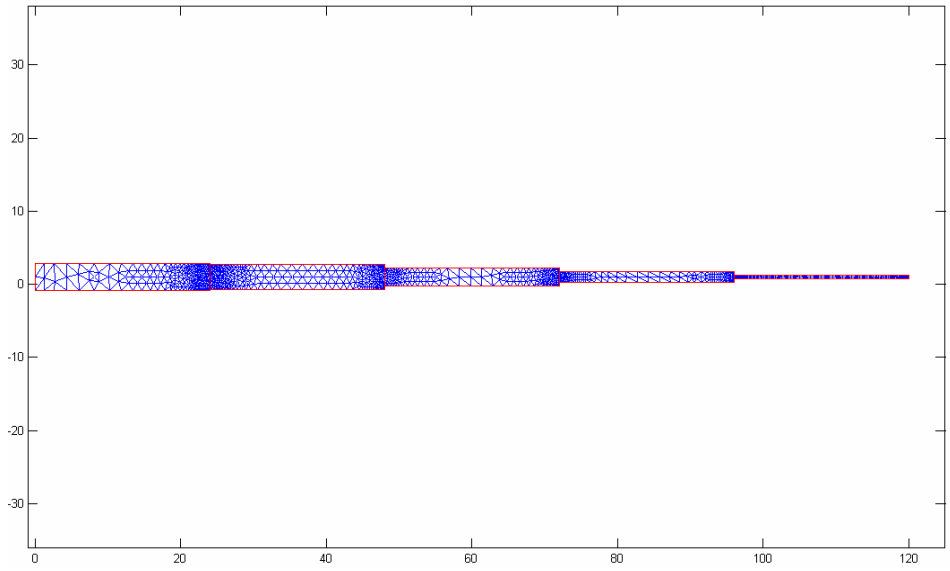

Figure 5.21 Optimum design for the five stepped cantilever beam

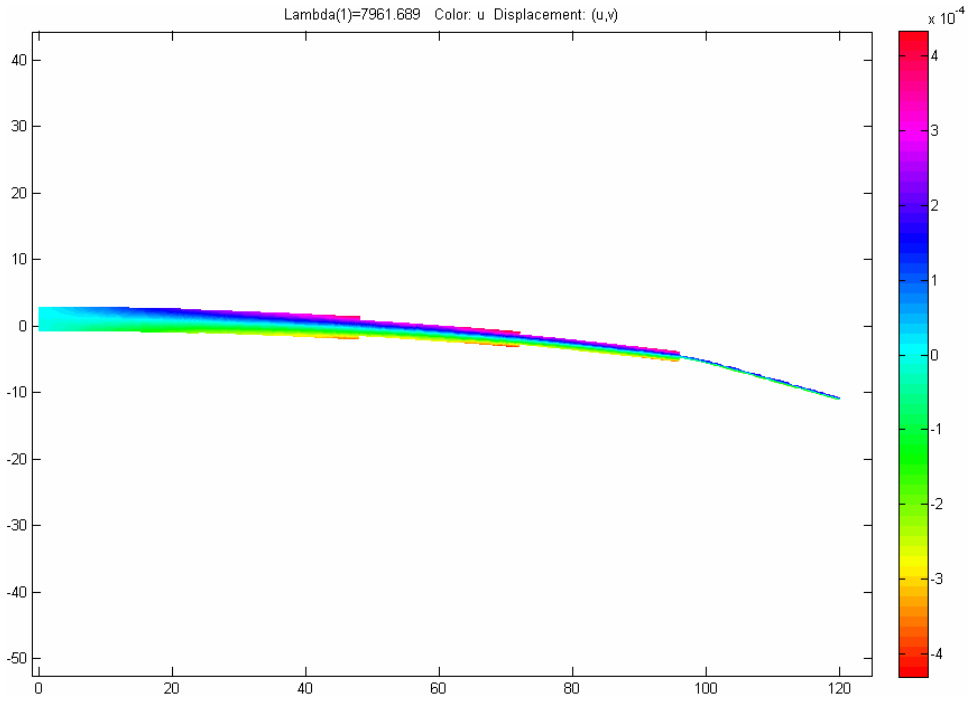

Figure 5.22 First mode shape for the optimal design of five stepped cantilever beam

5.6 Trapezoidal Plate – Minimum Weight Design

The fifth problem solved in this work is a trapezoidal plate as shown in Figure 5.22. Left edge of the plate is fixed and an outward pressure load of 2000 Psi is applied along the top edge.

The length of the plate is 30 inch and the thickness is 1 inch. The plate is made of aluminum with Young's Modulus of Elasticity, $E = 1 \times 10^7$ Psi, Yield Strength, σ_Y = 60000 Psi, Poisson's ration, $\upsilon = 0.33$ and weight density = 0.1 lbf/inch^3.

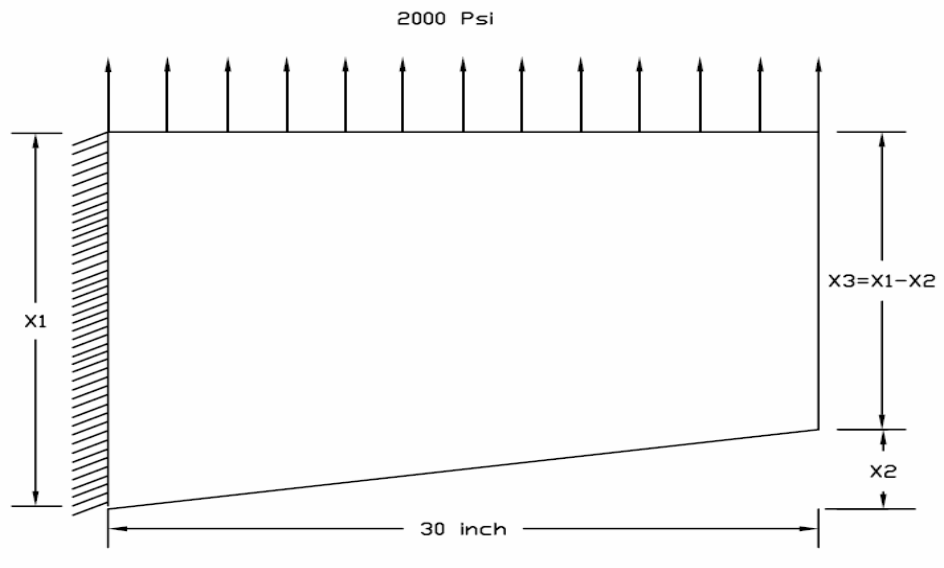

Figure 5.23 Trapezoidal Plate

The objective of this problem is to find the optimal heights of the two parallel edges of the trapezoid which would minimize the volume (hence the weight) of the plate such that the maximum von Mises stress developed in the structure would not exceed 40000 Psi (σ_Y/1.5). The problem formulation is as follows:

Design variable: [X1, X2]

Lower and upper bounds for the design variables are [15, 2] and [25, 12] respectively.

Objective function: Minimize the volume [minimize V]

Subject to von Mises stress constraints - Max. $\sigma_{VM} \leq 40000$ Psi.

A total of 24 experiments were performed in order to determine the best possible RBF model. As usual, for each combination of a specific sequencing technique and RBF model, two different numbers of initial DOE points have been used to create the response surface. The first set consists of 10 DOE points, whereas the second set consists of 30 DOE points. For Halton sequence, GuassI RBF with 30 initial DOE points produces the best minimum volume for the plate. In this case, the optimal design has a volume of 273.5808 $inch^3$ and the optimal values for the design variables are X1 = 15 inch and X2 = 12 inch. The maximum von Mises stress for this design is 40002.1676 Psi. The optimization process requires 42 function evaluations for convergence. For Sobol sequence, MQR RBF with 10 initial DOE points produces the best results with a volume of 274.7537 $inch^3$. The optimal values for the design variables are X1 = 15.1585 inch and X2 = 12 inch. The maximum von Mises stress for this design is 39995.5541 Psi. The optimization process converges after 22 function evaluations. For Faure sequence, MQI RSM with 10 initial DOE points produces the best results with a volume of 273.3937 $inch^3$. The optimal values for the design variables are X1 = 15.1131 inch and X2 = 12 inch. The maximum von Mises stress for this design is 40026.3866 Psi. The optimization process converges after 22 function evaluations.

For optimization using *fmincon* function, the same problem produces a volume of 277.542 $inch^3$ for a randomly selected initial design variables, X1 = 16 and X2 = 3. The optimum design variables are X1 = 15 inch and X2 = 11.4972 inch. Corresponding maximum von Mises stress for this case is 40000 Psi. The total number of function evaluations is 22 for this case. The comparative plots of variations of design variables, volume of the plate and the maximum von Mises stress with number of function evaluations are presented in Figure 5.23, Figure 5.24 and Figure 5.25 respectively.

To improve the design further, the best results achieved from the response surface optimizations were used again as the initial design variables input for another round of *fmincon* function optimizations. The lower and upper bounds for the design variables were initial input – 0.5 and initial input + 0.5 respectively. This time, Faure sequence with MQI RSM and 10 initial DOE points gives the best results. The optimization process took 19 function evaluations to give an improved design of X1 = 15.2624 inch and X2 = 12.5 inch with a volume of 270.3715 $inch^3$. The corresponding maximum von Mises stress is 40000 Psi. The optimal design and the von Mises stress distribution for this design are presented in Figure 5.26 and Figure 5.27 respectively.

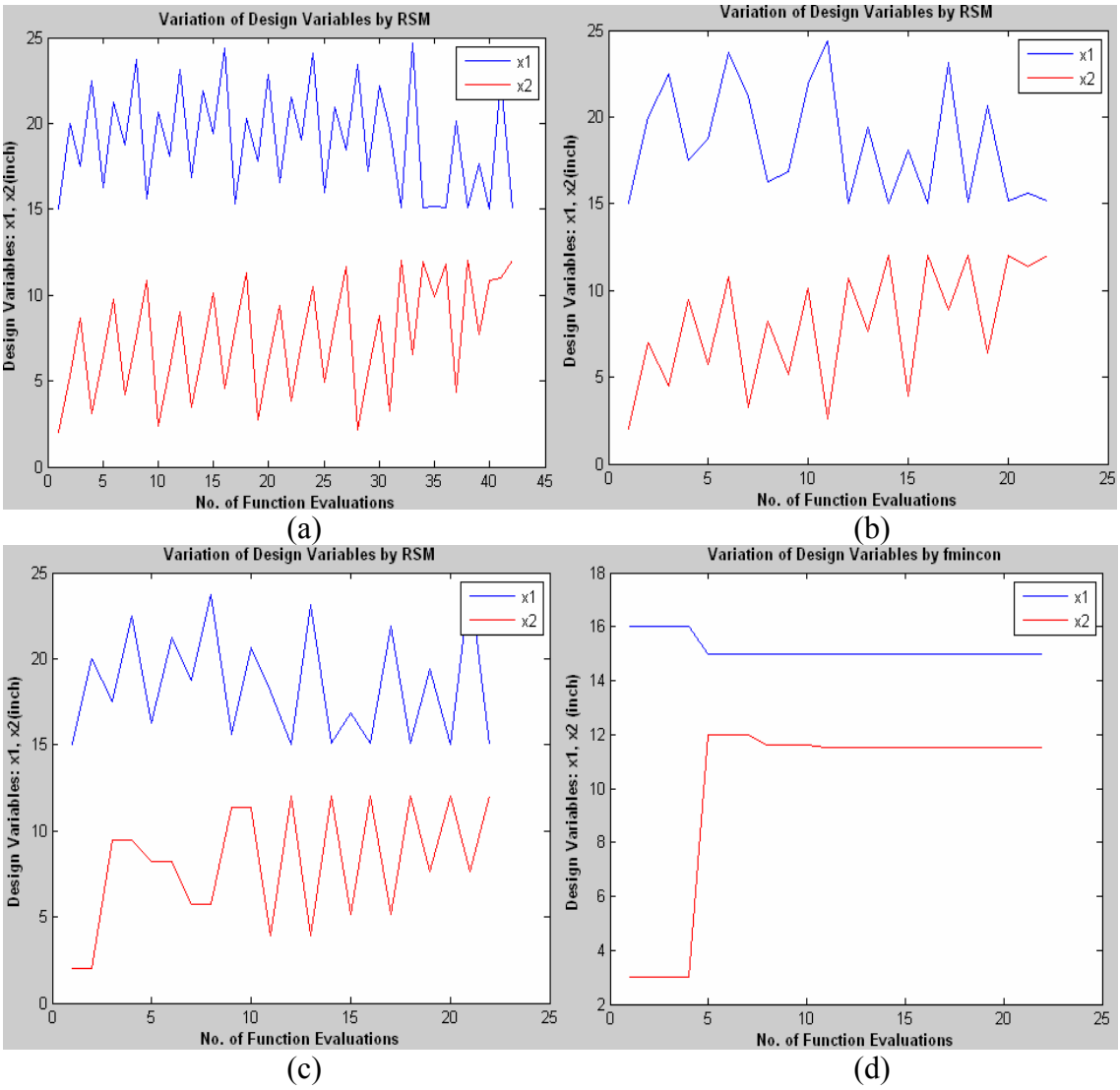

Figure 5.24 Variation of design variables for trapezoidal plate by (a) Halton sequencing with GaussI model (30 initial DOE), (b) Sobol Sequencing with MQR model (10 initial DOE), (c) Faure sequencing with MQI model (10 initial DOE) and (d) *fmincon* function

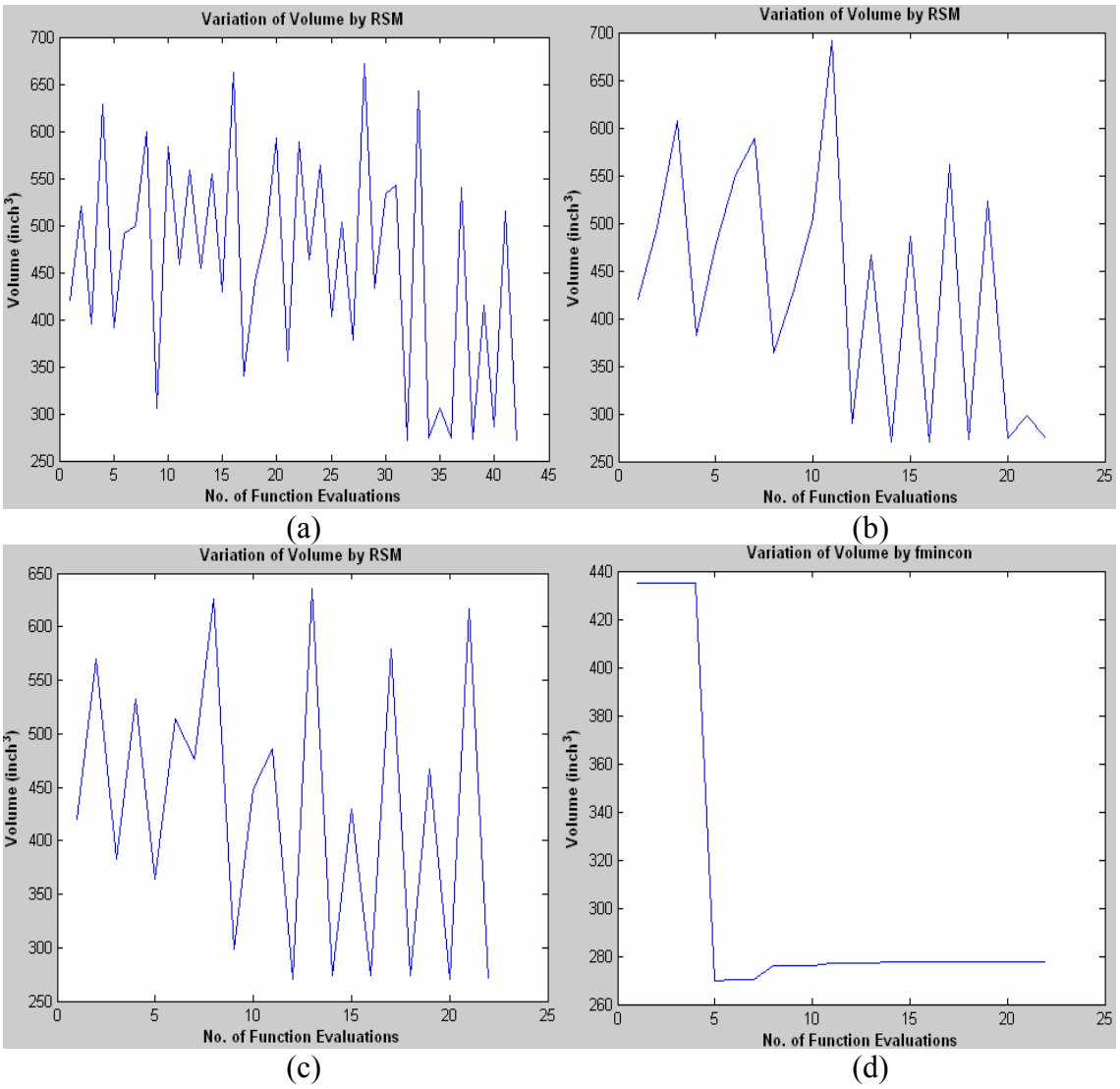

Figure 5.25 Variation of volume for trapezoidal plate by (a) Halton sequencing with GaussI model (30 initial DOE), (b) Sobol Sequencing with MQR model (10 initial DOE), (c) Faure sequencing with MQI model (10 initial DOE) and (d) *fmincon* function

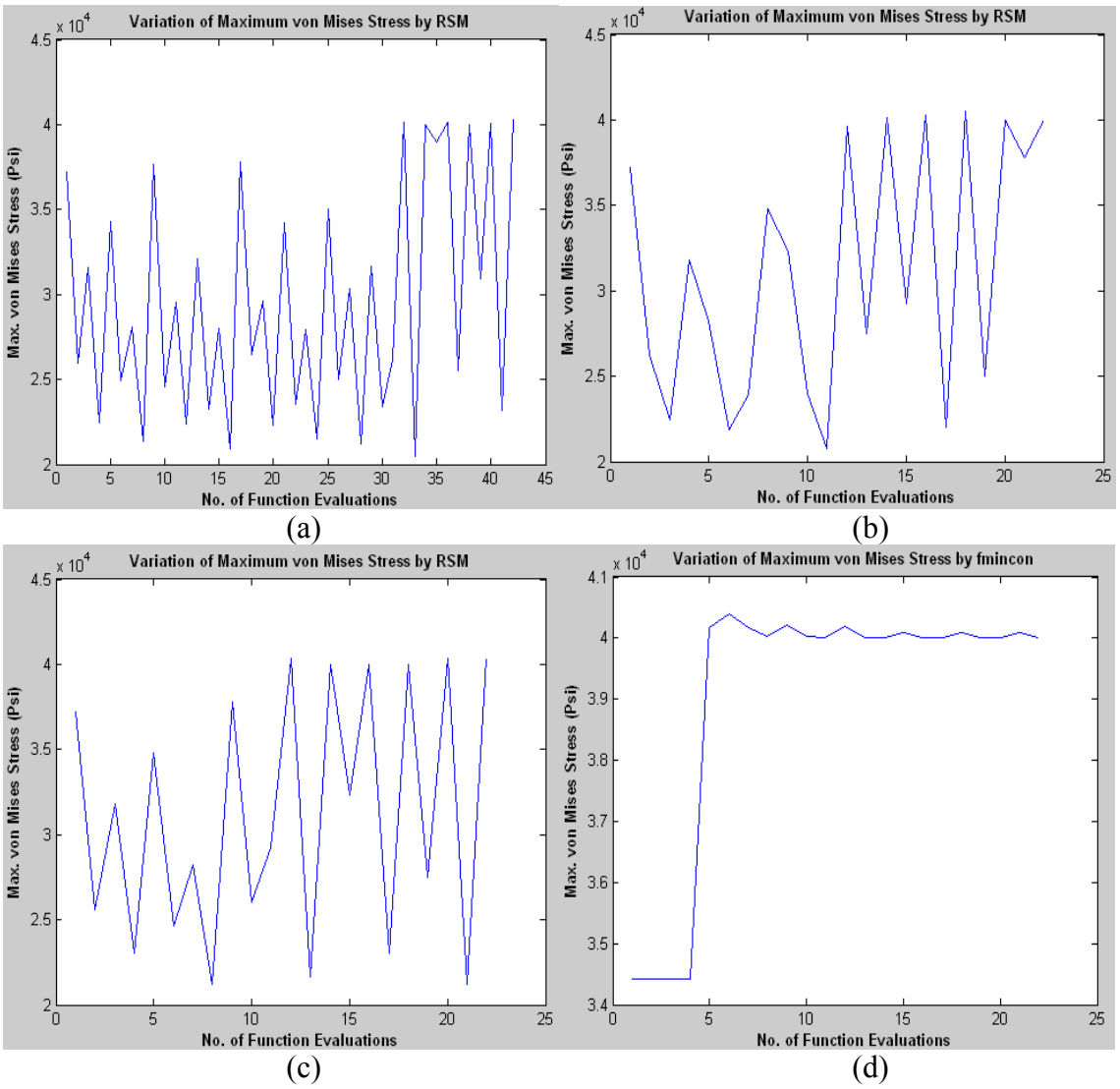

Figure 5.26 Variation of maximum von Mises stress for trapezoidal plate by (a) Halton sequencing with GaussI model (30 initial DOE), (b) Sobol Sequencing with MQR model (10 initial DOE), (c) Faure sequencing with MQI model (10 initial DOE) and (d) *fmincon* function

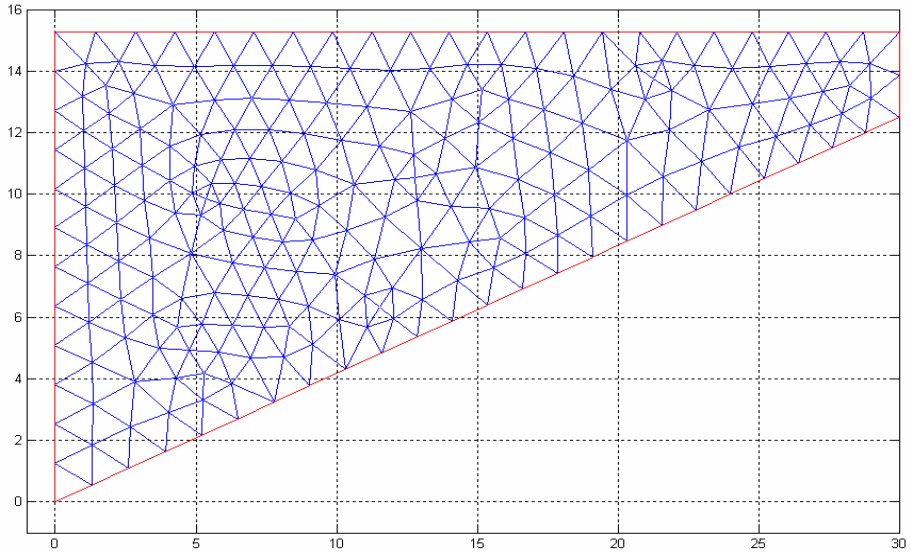

Figure 5.27 Optimal design for trapezoidal plate

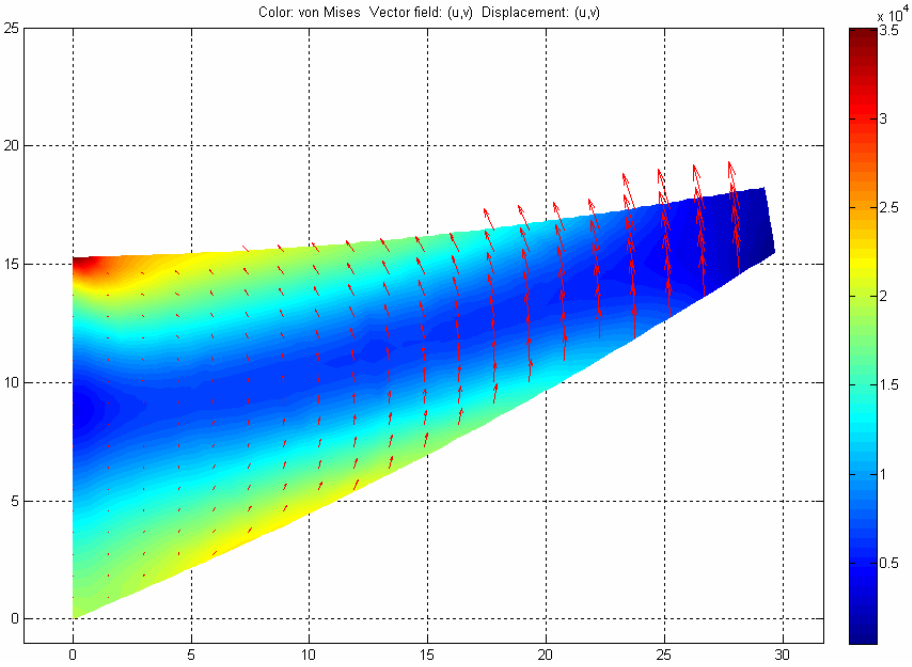

Figure 5.28 Maximum von Mises stress distribution for the optimal design of the trapezoidal plate

5.7 Trapezoidal Plate with a Circular Hole Fixed at Center – Minimum Weight Design

The sixth problem solved in this work is a trapezoidal plate with a circular hole. The center of the hole is fixed in such a way that it is always at the middle of the plate's length and it's Y center coordinate is parameterized so that it is always at the middle of the height of the plate with respect to the right parallel edge of the trapezoid as shown in Figure 5.28. The length of the plate is 30 inch and the thickness is 1 inch. The coordinates of the center of the hole can be expressed as (Xc, Yc) ≡ (15, $X2 + \frac{X1 - X2}{2}$).

Left edge of the plate is fixed and an outward pressure load of 2000 Psi is applied along the top edge.

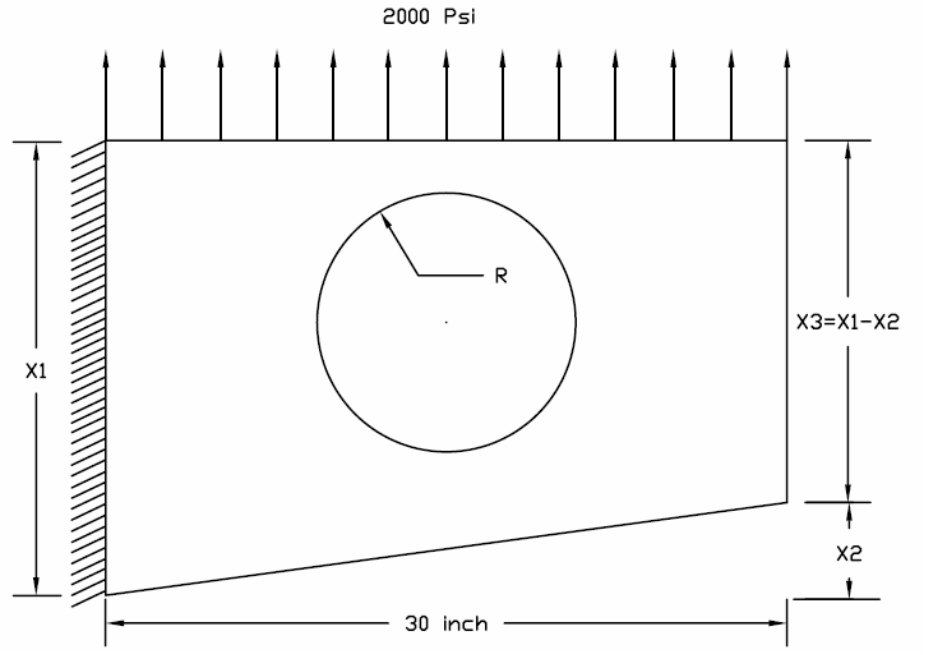

Figure 5.29 Trapezoidal plate with a circular hole fixed at center

The plate is made of aluminum with Young's Modulus of Elasticity, $E = 1 \times 10^7$ Psi, Yield Strength, $\sigma_Y = 60000$ Psi, Poisson's ration, $\upsilon = 0.33$ and weight density = 0.1 lbf/inch^3.

The objective of this problem is to find the optimal heights of the two parallel edges of the trapezoid and the radius of the hole which would minimize the volume (hence the weight) of the plate such that the maximum von Mises stress developed in the structure would not exceed 40000 Psi ($\sigma_Y/1.5$). The problem formulation is as follows:

Design variable: [X1, X2, R]

Lower and upper bounds for the design variables are, [20, 2, 4] and [25, 6, 8] respectively.

Objective function: Minimize the volume [minimize V]

Subject to –

a. Geometric constraints (to ensure that the hole lies inside the plate):

$$X1 - X2 \geq 2R + 0.5$$

b. von Mises stress constraint: Max. $\sigma_{VM} \leq 40000$ Psi.

As in the case of the previous problems, a total of 24 experiments were performed in order to determine the best possible RBF model. For each combination of a specific sequencing technique and RBF model, two different numbers of initial DOE points have been used to create the response surface. The first set consists of 10 DOE points, whereas the second set consists of 30 DOE points. For Halton sequence, GuassI RBF with 30 initial DOE points produces the best minimum volume for the plate. In

this case, the optimal design has a volume of 406.4515 $inch^3$ and the optimal values for the design variables are X1 = 20 inch, X2 = 4.07035 inch and R = 6.49414 inch. The maximum von Mises stress for this design is 40001.2771 Psi. The optimization process requires 42 function evaluations for convergence. For Sobol sequence, MQI RBF with 30 initial DOE points produces the best results with a volume of 407.5787 $inch^3$. The optimal values for the design variables are X1 = 20 inch, X2 = 3.92083 inch and R = 3.92083 inch. The maximum von Mises stress for this design is 39437.2554 Psi. The optimization process converges after 42 function evaluations. For Faure sequence, MQR RSM with 10 initial DOE points produces the best results with a volume of 408.2261 $inch^3$. The optimal values for the design variables are X1 = 20 inch, X2 = 3.77638 inch, and R = 6.5584 inch. The maximum von Mises stress for this design is 39337.1115 Psi. The optimization process converges after 22 function evaluations.

For *fmincon* function, the same problem produces an optimal volume of 408.8521 $inch^3$ for a randomly selected initial design variables, X1 = 20, X2 = 5, and R = 4. The optimum design variables are X1 = 20 inch, X2 = 3.0553 inch, and R = 6.8012 inch. Corresponding maximum von Mises stress for this case is 39999.9996 Psi. The total number of function evaluations is 114 for this case. The comparative plots of variations of design variables, volume of the plate and the maximum von Mises stress with number of function evaluations are presented in Figure 5.29, Figure 5.30 and Figure 5.31 respectively.

The best results achieved from the response surface optimizations were used again as the initial design variables input for another round of *fmincon* function

optimizations. The lower and upper bounds for the design variables were initial input – 0.5 and initial input + 0.5 respectively. This time, Faure sequence with MQR RSM and 10 initial DOE points produces the best results. The optimization process took 54 function evaluations to produce an improved design of X1 = 19.5 inch, X2 = 4.2096 inch, and R = 6.2058 inch with a volume of 400.8658 $inch^3$. The maximum von Mises stress is 39999.7094 Psi.

The optimal design and the von Mises stress distribution for this design are presented in Figure 5.32 and Figure 5.33 respectively.

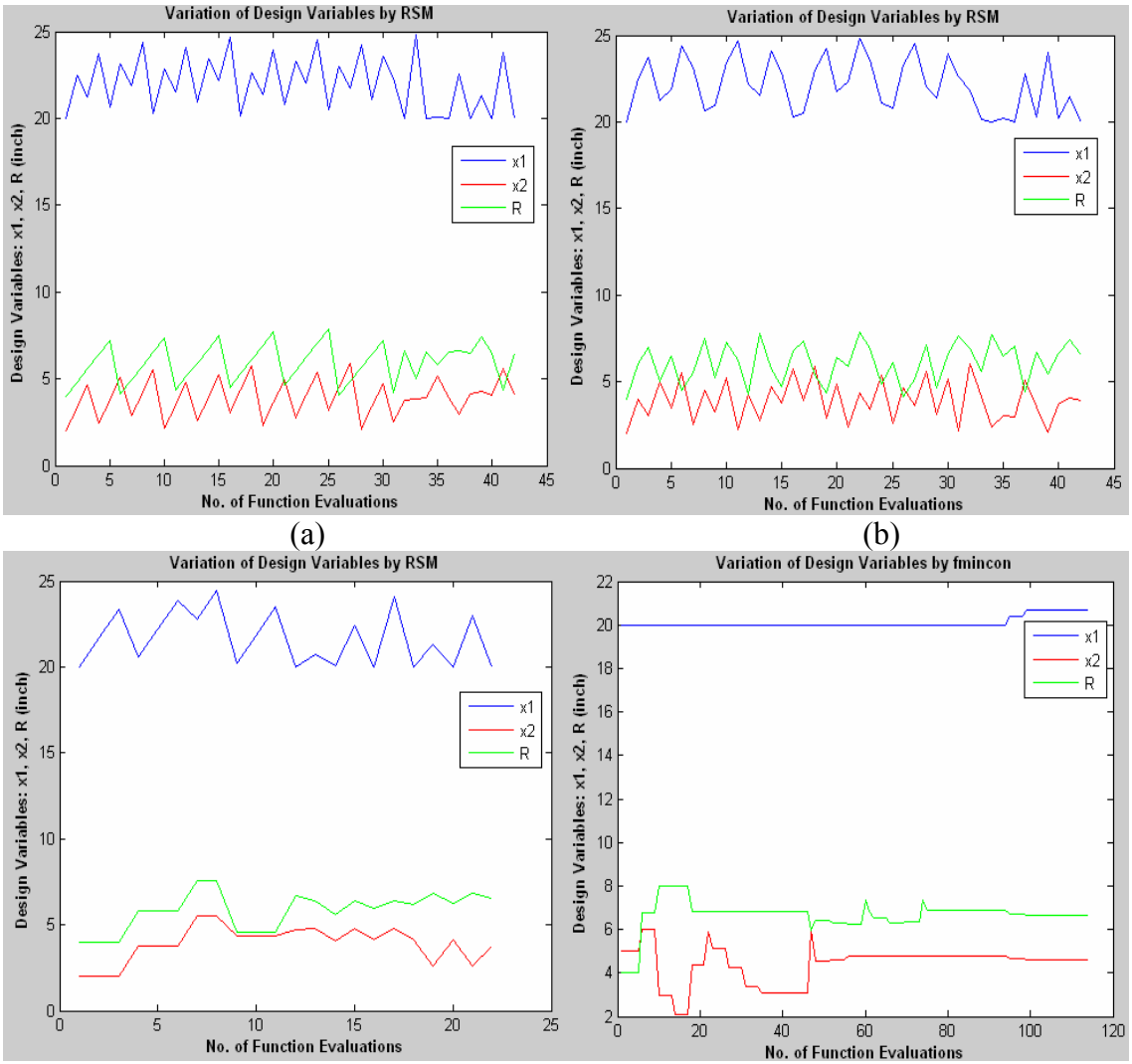

Figure 5.30 Variation of design variables for trapezoidal plate with a circular hole fixed at center by (a) Halton sequencing with GaussI model (30 initial DOE), (b) Sobol Sequencing with MQI model (30 initial DOE), (c) Faure sequencing with MQR model (10 initial DOE) and (d) *fmincon* function

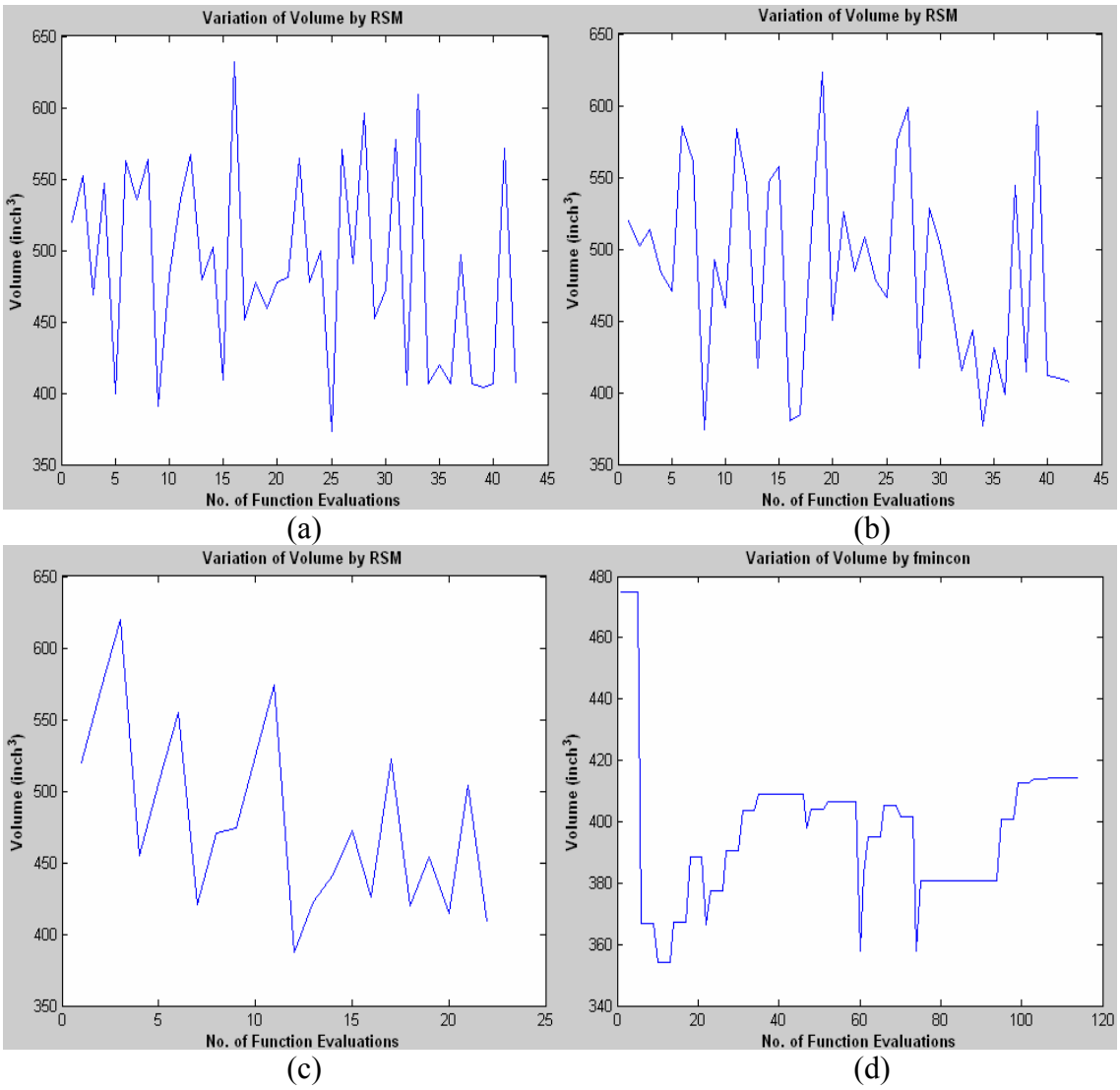

Figure 5.31 Variation of volumes for trapezoidal plate with a circular hole fixed at center by (a) Halton sequencing with GaussI model (30 initial DOE), (b) Sobol Sequencing with MQI model (30 initial DOE), (c) Faure sequencing with MQR model (10 initial DOE) and (d) *fmincon* function

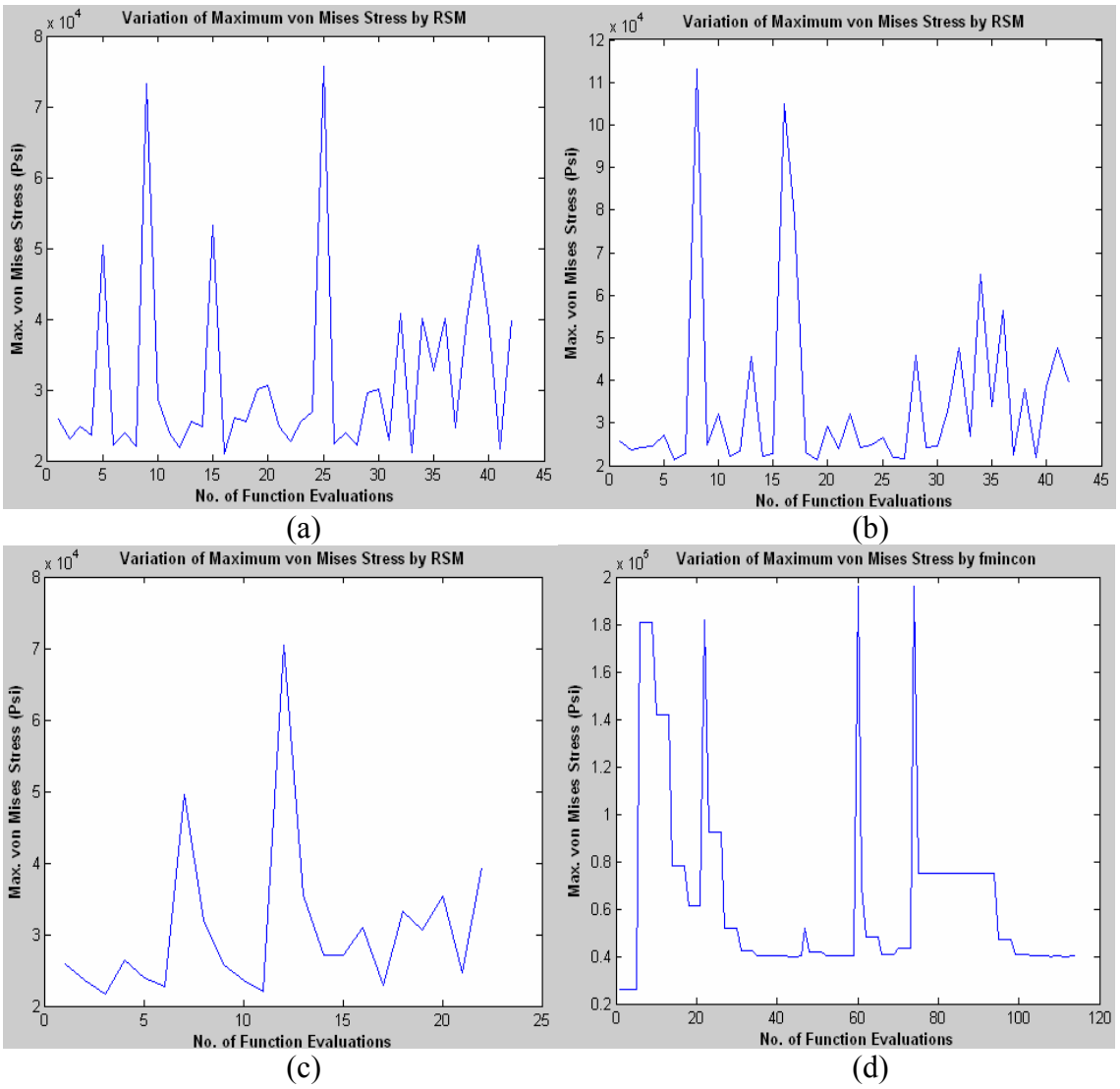

Figure 5.32 Variation of maximum von Mises stress for trapezoidal plate with a circular hole fixed at center by (a) Halton sequencing with GaussI model (30 initial DOE), (b) Sobol Sequencing with MQI model (30 initial DOE), (c) Faure sequencing with MQR model (10 initial DOE) and (d) *fmincon* function

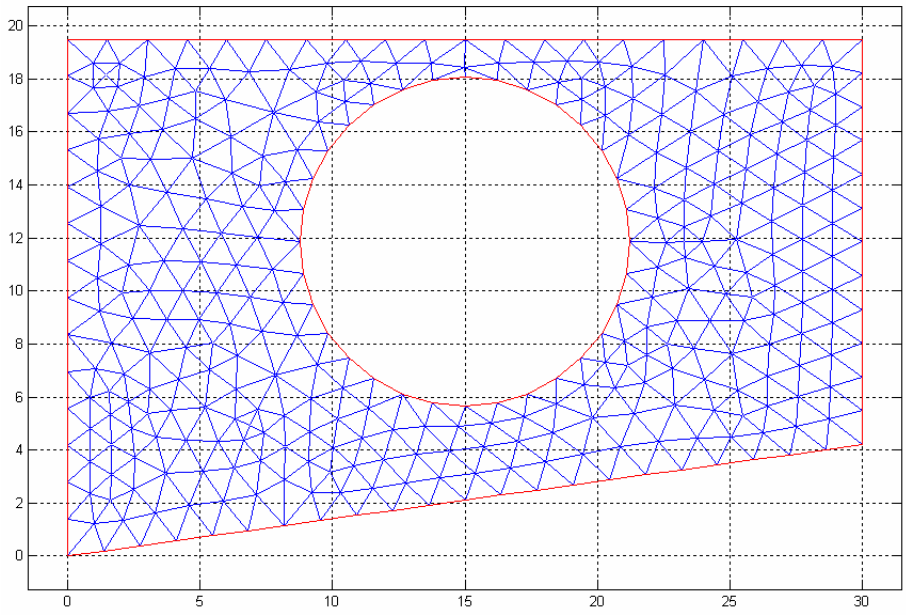

Figure 5.33 Optimal design for trapezoidal plate with circular hole fixed at center

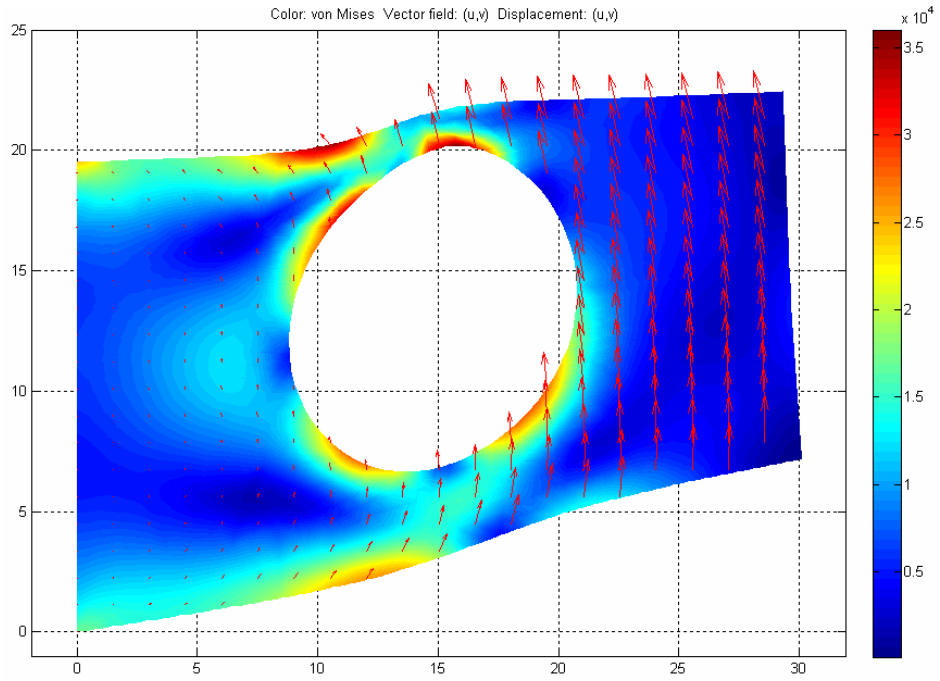

Figure 5.34 von Mises stress distribution for optimal design of trapezoidal plate with circular hole fixed at center

5.8 Trapezoidal Plate with a Circular Hole with Unspecified Center Location – Minimum Weight Design

The seventh problem solved in this work is a trapezoidal plate with a circular hole as shown in Figure 5.34. The location of the center is not specified in this problem. It can be anywhere inside the plate provided some constraints are satisfied. Left edge of the plate is fixed and an outward pressure load of 2000 Psi is applied along the top edge. The length of the plate is 30 inch and the thickness is 1 inch.

The plate is made of aluminum with Young's Modulus of Elasticity, $E = 1 \times 10^7$ Psi, Yield Strength, $\sigma_Y = 60000$ Psi, Poisson's ration, $\upsilon = 0.33$ and weight density = 0.1 lbf/inch^3.

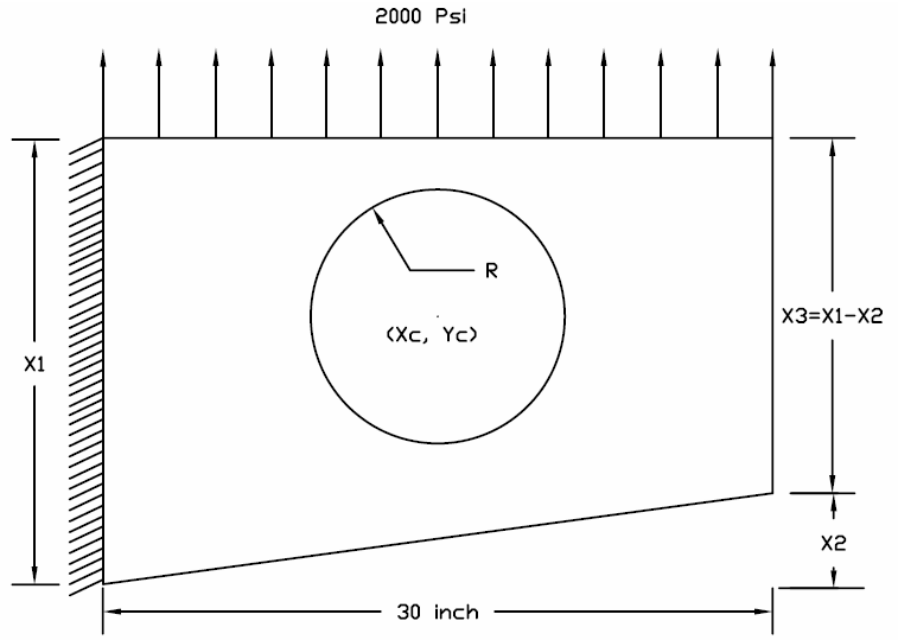

Figure 5.35 Trapezoidal plate with a circular hole with unspecified center location

The objective of this problem is to find the optimal heights of the two parallel edges of the trapezoid and the center location and radius of the hole which would minimize the volume (hence the weight) of the plate such that the maximum von Mises stress developed in the structure would not exceed 40000 Psi ($\sigma_Y/1.5$). The problem formulation is as follows:

Design variable: [X1, X2, Xc, Yc, R]

Lower and upper bounds for the design variables are, [15 4 10 5 2] and [20 6 15 15 4] respectively.

Objective function: Minimize the volume [minimize V]

Subject to –

(a) Geometric constraints (to ensure that the hole lies inside the plate):

$$Xc - R \geq 1, \;\; Xc + R \leq 29,$$

$$Yc + R \leq X1 - 1, \;\; d \geq R + 1$$

Where, d is the shortest distance of the circular hole center from the bottom edge of the plate and is given by, $d = \frac{30.Yc}{\sqrt{900 + X2^2}} - \frac{X2.Xc}{\sqrt{900 + X2^2}}$

(b) von Mises stress constraint: Max. $\sigma_{VM} \leq 40000$ Psi.

A total of 24 experiments were performed in order to determine the best possible RBF model. For each combination of a specific sequencing technique and RBF model, two different numbers of initial DOE points have been used to create the response surface. The first set consists of 10 DOE points, whereas the second set consists of 30 DOE points. For Halton sequence, MQI RBF with 10 initial DOE points produces the

best minimum volume for the plate. In this case, the optimal design has a volume of 317.9507 $inch^3$ and the optimal values for the design variables are X1 = 15 inch, X2 = 5.4523 inch, Xc = 12.1476, Yc = 8.7293 and R = 6.49414 inch. The maximum von Mises stress for this design is 39287.611 Psi. The optimization process requires 22 function evaluations for convergence. For Sobol sequence, MQR RBF with 30 initial DOE points produces the best results with a volume of 316.8925 $inch^3$. The optimal values for the design variables are X1 = 15 inch, X2 = 5.8611 inch, Xc = 12.4855, Yc = 8.8735 and R = 3.92083 inch. The maximum von Mises stress for this design is 38974.2337 Psi. The optimization process converges after 42 function evaluations. For Faure sequence, MQI RSM with 30 initial DOE points produces the best results with a volume of 321.7413 $inch^3$. The optimal values for the design variables are X1 = 15 inch, X2 = 5.6703 inch, Xc = 13.764, Yc = 9.1954 and R = 3.7084 inch. The maximum von Mises stress for this design is 39337.1115 Psi. The optimization process converges after 42 function evaluations.

For *fmincon* function, the same problem produces an optimal volume of 316.7711 $inch^3$ for a randomly selected initial design variables, X1 = 20, X2 = 5, Xc = 12, Yc = 8 and R = 1. The optimum design variables are X1 = 15 inch, X2 = 5.5309 inch, Xc = 11.9201, Yc = 8.7028 and R = 4 inch. Corresponding maximum von Mises stress for this case is 40000 Psi. The total number of function evaluations is 285 for this case. The comparative plots of variations of design variables, volume of the plate and the maximum von Mises stress with number of function evaluations are presented in Figure 5.35, Figure 5.36 and Figure 5.37 respectively.

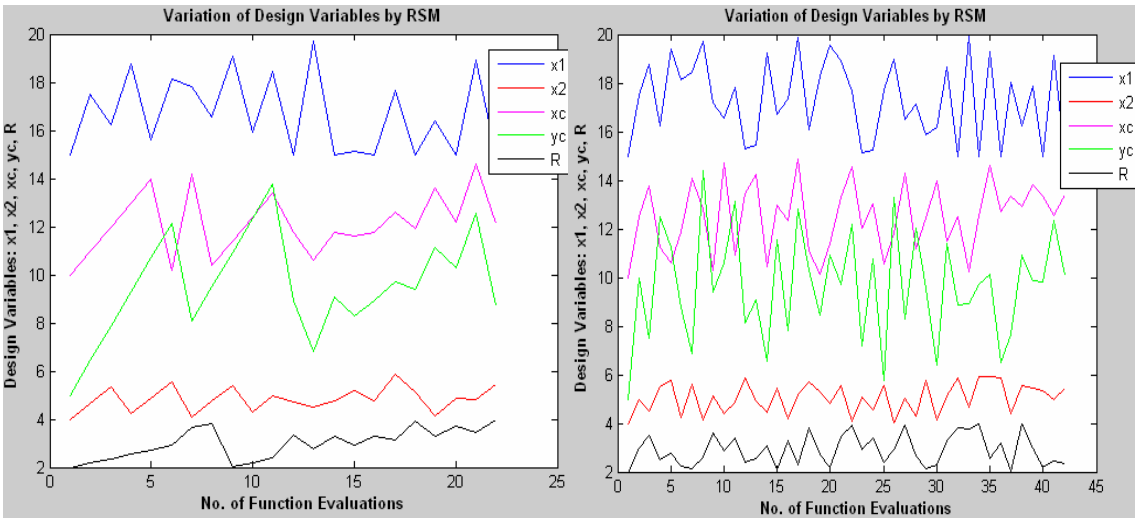

(a)

(b)

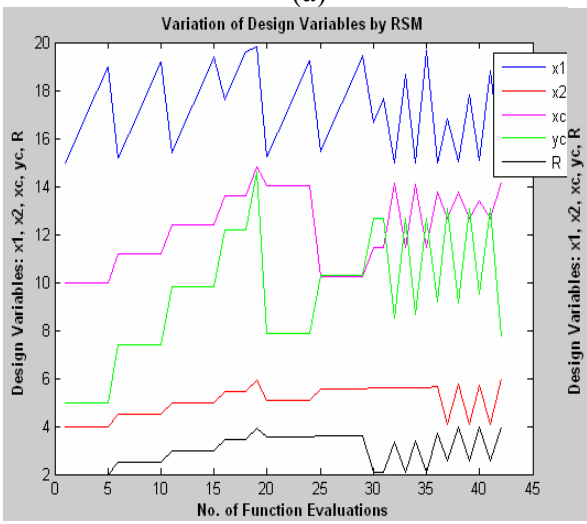

(c)

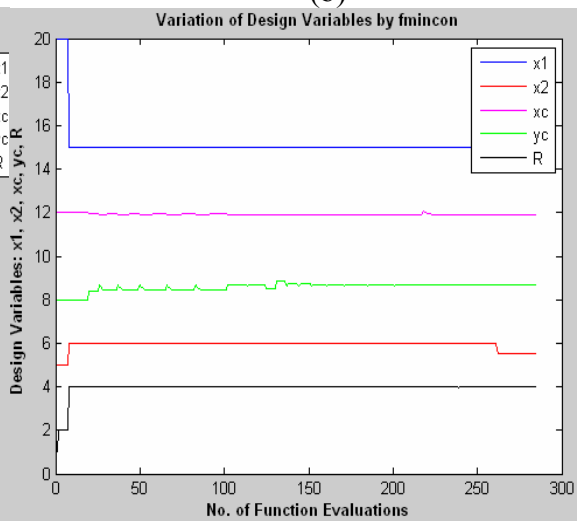

(d)

Figure 5.36 Variation of design variables for trapezoidal plate with a circular hole with unspecified center location by (a) Halton sequencing with MQI model (10 initial DOE), (b) Sobol Sequencing with MQR model (30 initial DOE), (c) Faure sequencing with MQI model (30 initial DOE) and (d) *fmincon* function

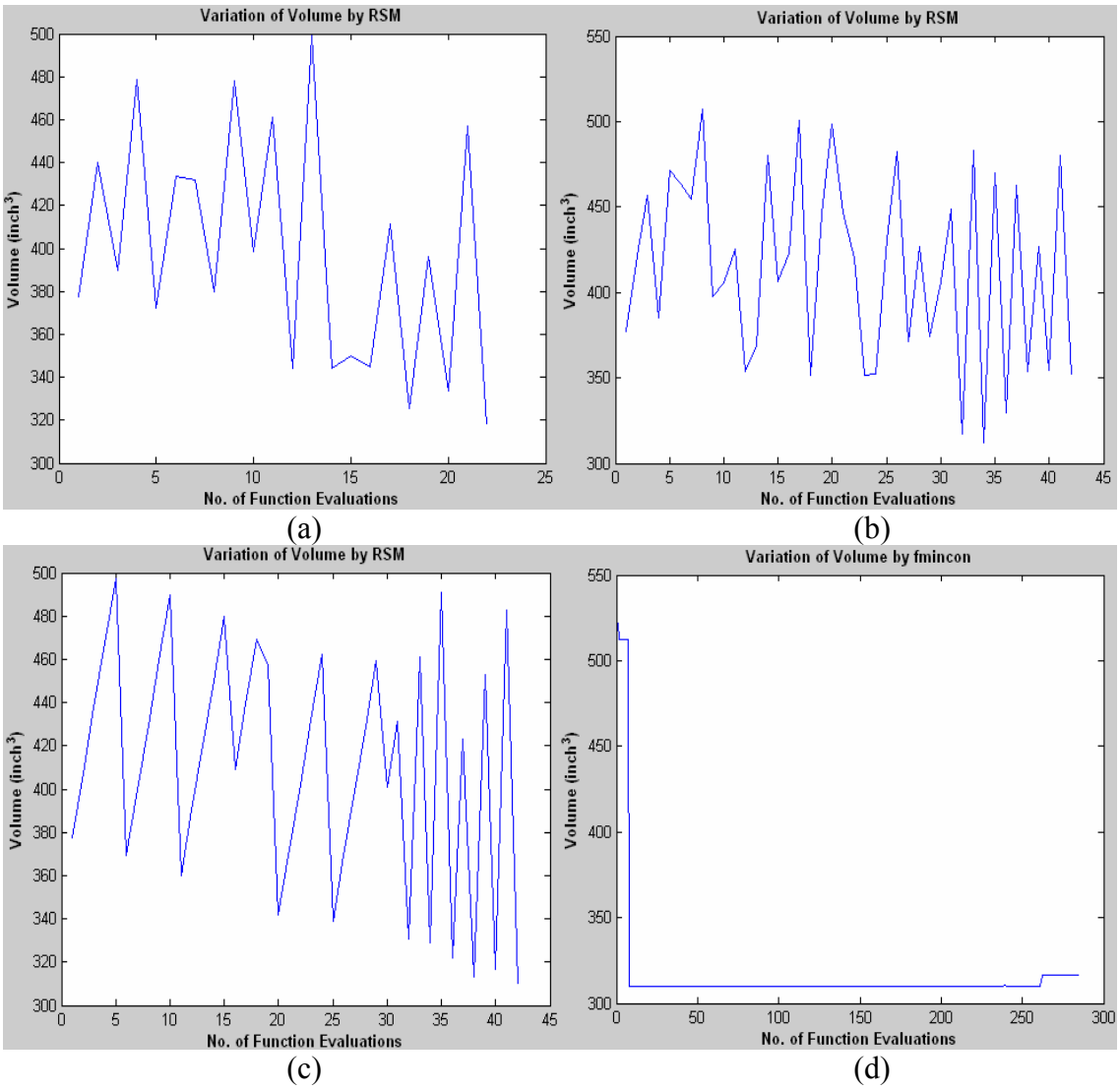

Figure 5.37 Variation of volume for trapezoidal plate with a circular hole with unspecified center location by (a) Halton sequencing with MQI model (10 initial DOE), (b) Sobol Sequencing with MQR model (30 initial DOE), (c) Faure sequencing with MQI model (30 initial DOE) and (d) *fmincon* function

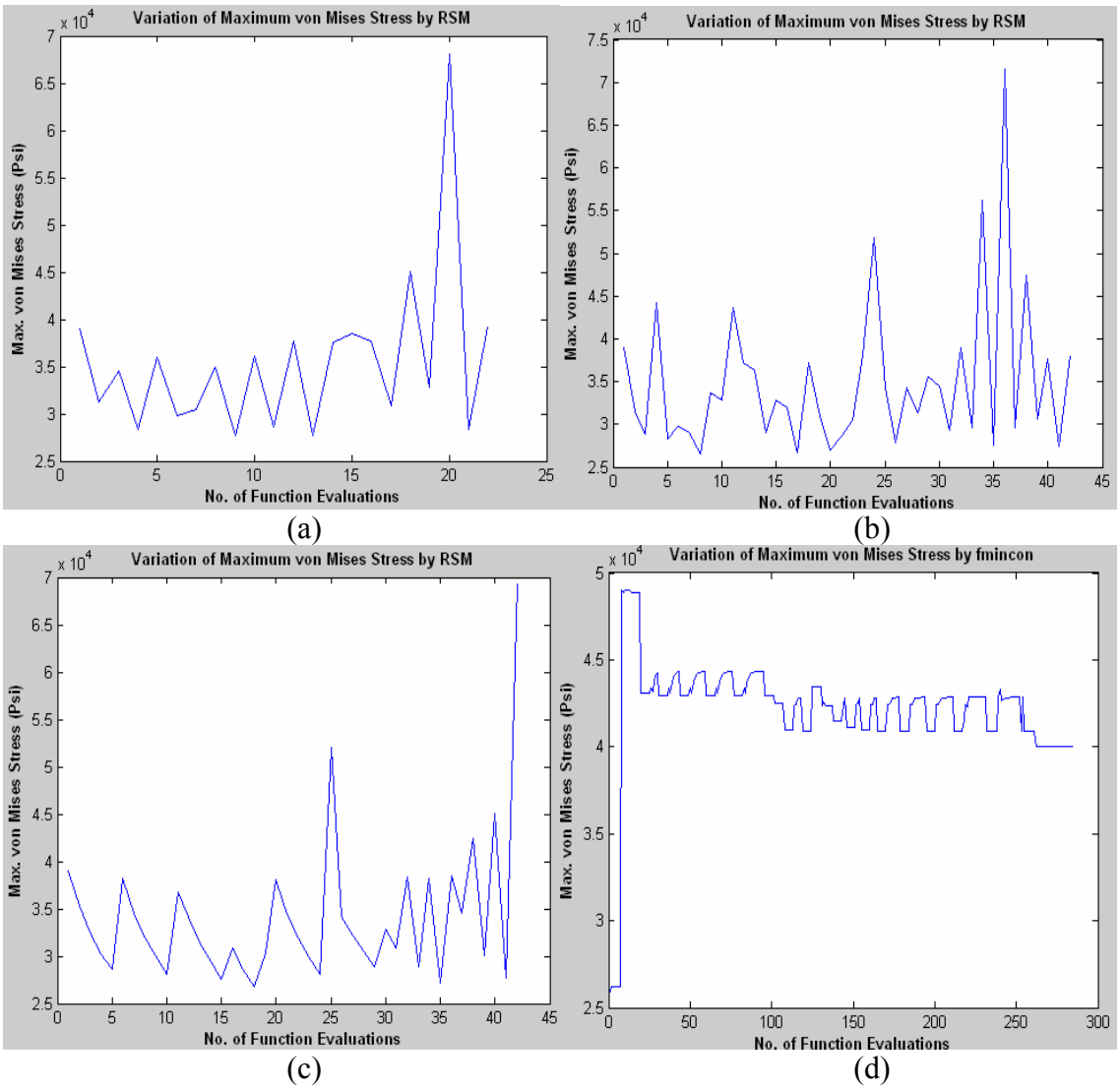

Figure 5.38 Variation of maximum von Mises stress for trapezoidal plate with a circular hole with unspecified center location by (a) Halton sequencing with MQI model (10 initial DOE), (b) Sobol Sequencing with MQR model (30 initial DOE), (c) Faure sequencing with MQI model (30 initial DOE) and (d) *fmincon* function

To improve the design further, the best results obtained from the response surface optimizations were used again as the initial design variables input for another round of *fmincon* function optimizations. The lower and upper bounds for the design

variables were initial input – 0.5 and initial input + 0.5 respectively. This time, Faure sequence with MQI RSM and 30 initial DOE points produces the best minimum volume of 300.2922 inch^3. The optimal values for the design variables are X1 = 14.5667 inch, X2 = 6.1703 inch, Xc = 14.264, Yc = 8.6954 and R = 3.749 inch. The corresponding maximum von Mises stress is 40000.0004 Psi. The optimization process took 326 function evaluations to converge. The optimal design and the von Mises stress distribution for this design are presented in Figure 5.38 and Figure 5.39 respectively.

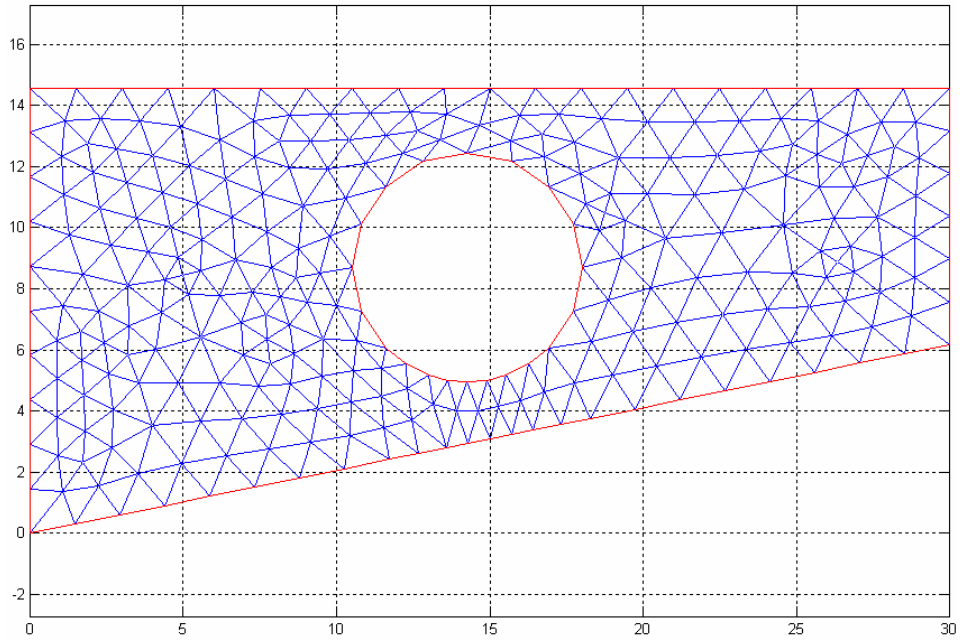

Figure 5.39 Optimal design for Trapezoidal plate with a circular hole with unspecified center location

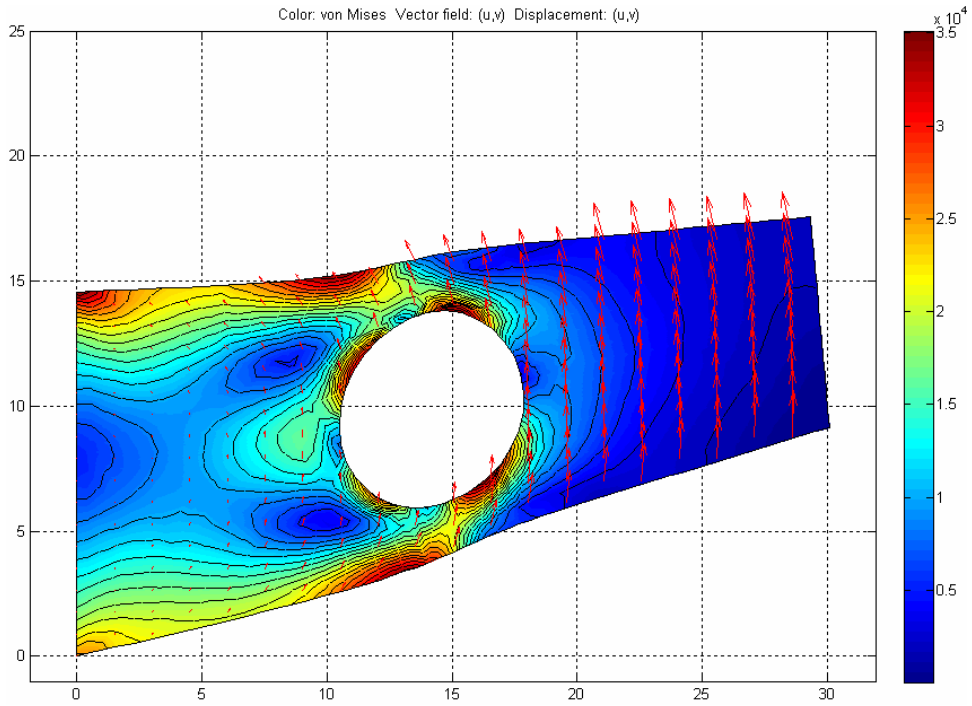

Figure 5.40 von Mises stress distribution for optimal design of Trapezoidal plate with a circular hole with unspecified center location

5.9 Quadrangular Plate – Minimum Weight Design

The eighth problem solved in this work is a quadrangular plate as shown in Figure 5.40. Left edge of the plate is fixed and an outward pressure load of 2000 Psi is applied along the top edge. The length of the top edge of the plate is 30 inch and the thickness is 1 inch.

The plate is made of aluminum with Young's Modulus of Elasticity, $E = 1 \times 10^7$ Psi, Yield Strength, $\sigma_Y = 60000$ Psi, Poisson's ration, $\upsilon = 0.33$ and weight density = 0.1 lbf/inch^3.

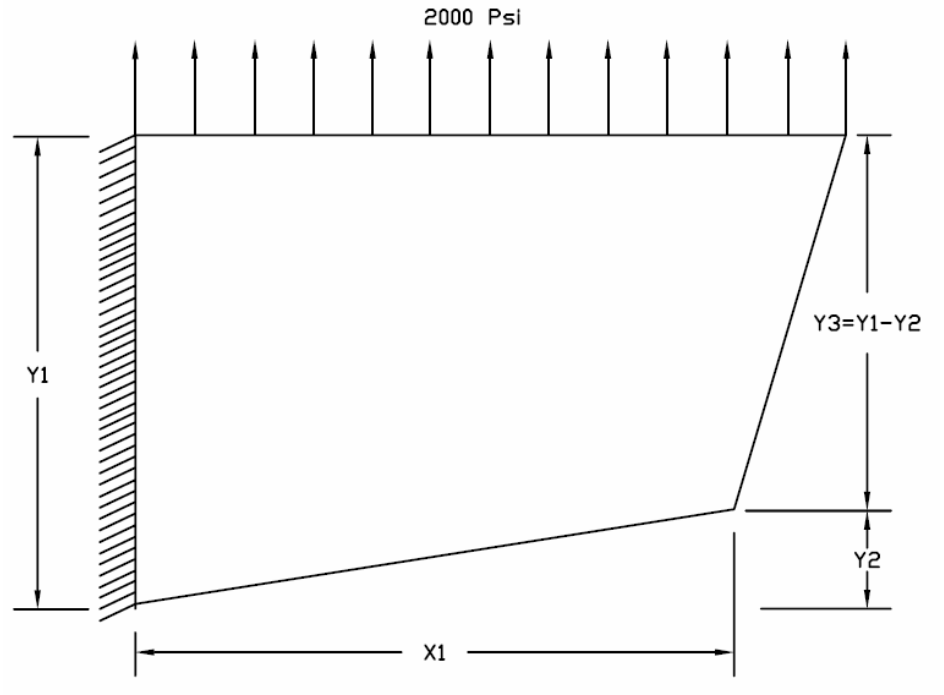

Figure 5.41 Quadrangular Plate

The objective of this problem is to find the optimal lengths of left, bottom and right edges of the plate which would minimize the volume (hence the weight) of the plate such that the maximum von Mises stress developed in the structure would not exceed 40000 Psi ($\sigma_Y/1.5$). The problem formulation is as follows:

Design variable: [X1, Y1,Y2]

Lower and upper bounds for the design variables are [1, 15, 2] and [30, 25, 12] respectively.

Objective function: Minimize the volume [minimize V]

Subject to von Mises stress constraints - Max. $\sigma_{VM} \leq 40000$ Psi.

In order to determine the best possible RBF model, a total of 24 experiments were performed. As usual, for each combination of a specific sequencing technique and RBF model, two different numbers of initial DOE points have been used to create the response surface. The first set consists of 10 DOE points, whereas the second set consists of 30 DOE points. For Halton sequence, MQI RBF with 30 initial DOE points produces the best minimum volume for the plate. In this case, the optimal design has a volume of 223.4073 $inch^3$ and the optimal values for the design variables are X1 = 6.82849 inch, Y1 = 17.5496 inch and Y2 = 6.65034 inch. The maximum von Mises stress for this design is 39644.1667 Psi. The optimization process requires 42 function evaluations for convergence. For Sobol sequence, GuassR RBF with 10 initial DOE points produces the best results with a volume of 224.7151 $inch^3$. The optimal values for the design variables are X1 = 11.5725 inch, Y1 = 16.4421 inch and Y2 = 7.80359 inch. The maximum von Mises stress for this design is 38792.1443 Psi. The optimization process converges after 22 function evaluations. For Faure sequence, GuassI RSM with 30 initial DOE points produces the best results with a volume of 226.1603 $inch^3$. The optimal values for the design variables are X1 = 5.70846 inch, Y1 = 18.1356 inch and Y2 = 6.50911 inch. The maximum von Mises stress for this design is 39956.8313 Psi. The optimization process converges after 42 function evaluations.

For optimization using *fmincon* function, the same problem produces a volume of 243.1761 $inch^3$ for a randomly selected initial design variables, X1 = 8, Y1 = 15 and Y2 = 10. The optimum values for the design variables are X1 = 10.9939 inch, Y1 = 15 inch and Y2 = 4.2852 inch. Corresponding maximum von Mises stress for this case is

40000 Psi. The total number of function evaluations is 68 for this case. The comparative plots of variations of design variables, volume of the plate and the maximum von Mises stress with number of function evaluations are presented in Figure 5.41, Figure 5.42 and Figure 5.43 respectively.

To improve the design further, the best results achieved from the response surface optimizations were used again as the initial design variables input for another round of *fmincon* function optimizations. The lower and upper bounds for the design variables were initial input – 0.5 and initial input + 0.5 respectively. This time, Sobol sequence with GuassR RSM and 10 initial DOE points gives the best results. The optimization process took 77 function evaluations to give an improved design of X1 = 11.3227 inch, Y1 = 16.2596 inch and Y2 = 7.99861 inch with a volume of 215.9669 $inch^3$. The corresponding maximum von Mises stress is 39999.9973 Psi. The optimal design and the von Mises stress distribution for this design are presented in Figure 5.44 and Figure 5.45 respectively.

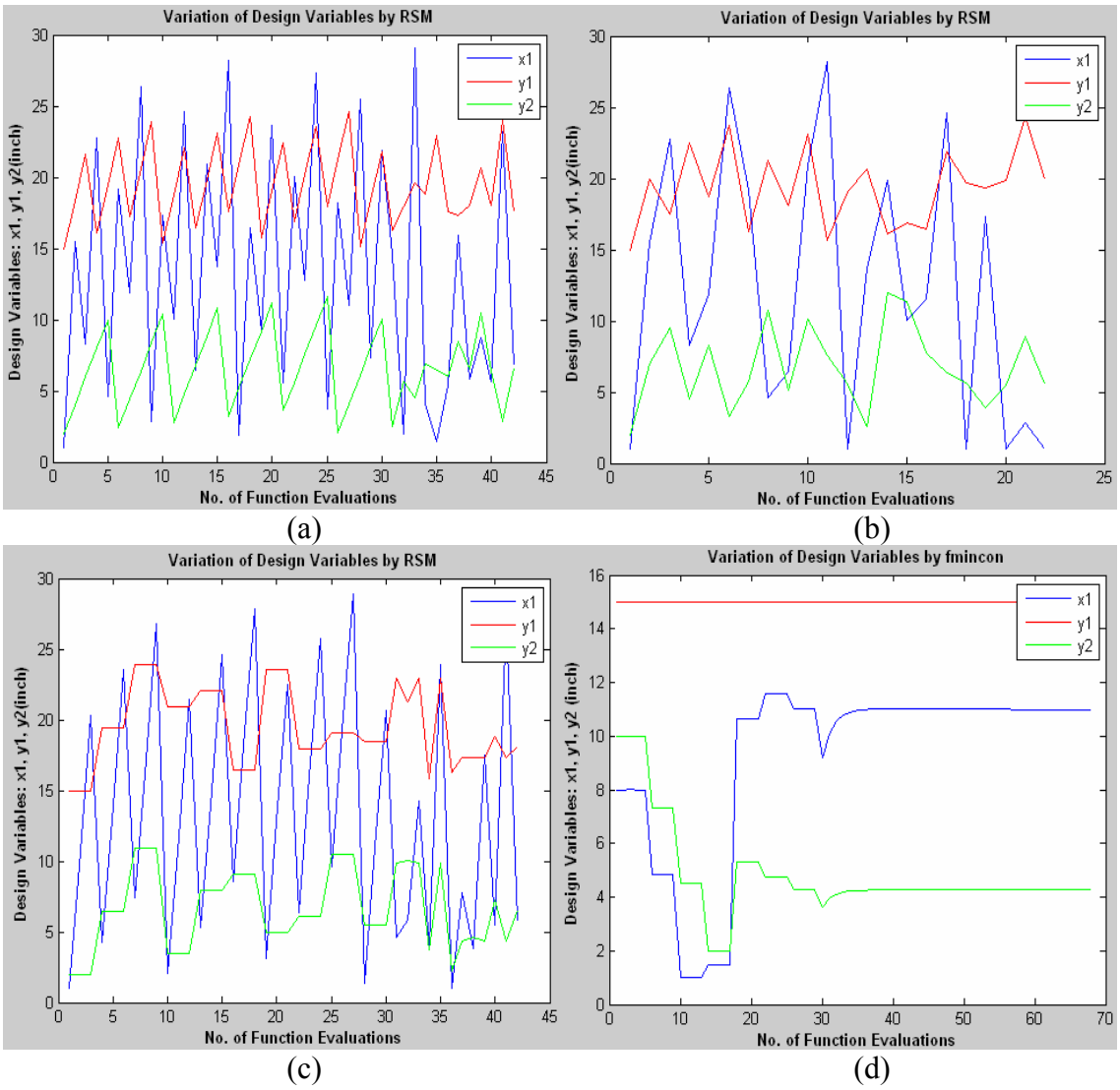

Figure 5.42 Variation of design variables for quadrangular plate by (a) Halton sequence with MQI model (30 initial DOE), (b) Sobol Sequence with GuassR model (10 initial DOE), (c) Faure sequence with GaussI model (30 initial DOE) and (d) *fmincon* function

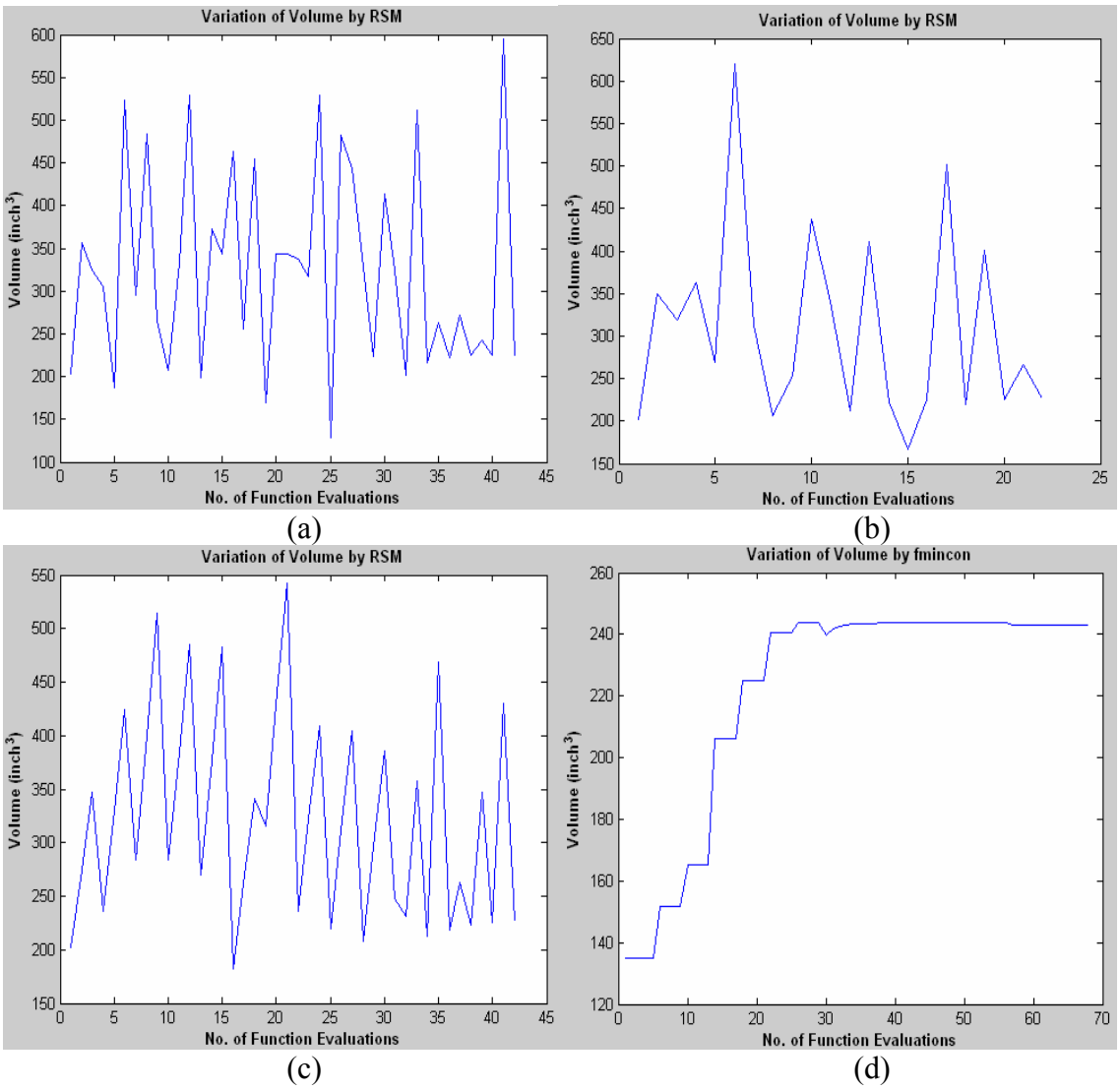

Figure 5.43 Variation of volume for quadrangular plate by (a) Halton sequence with MQI model (30 initial DOE), (b) Sobol Sequence with GuassR model (10 initial DOE), (c) Faure sequence with GaussI model (30 initial DOE) and (d) *fmincon* function

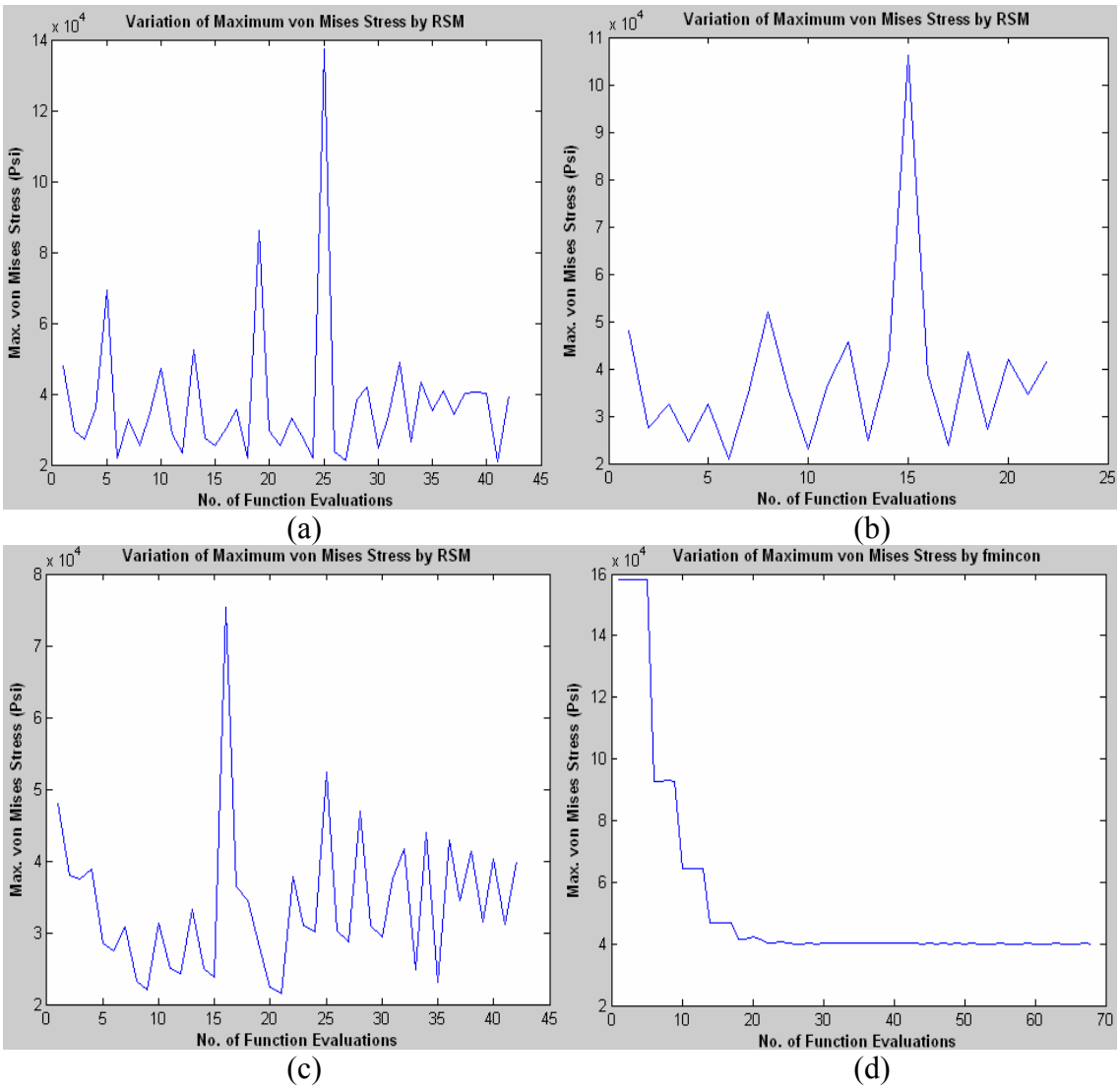

Figure 5.44 Variation of maximum von Mises stress for quadrangular plate by (a) Halton sequence with MQI model (30 initial DOE), (b) Sobol Sequence with GuassR model (10 initial DOE), (c) Faure sequence with GaussI model (30 initial DOE) and (d) *fmincon* function

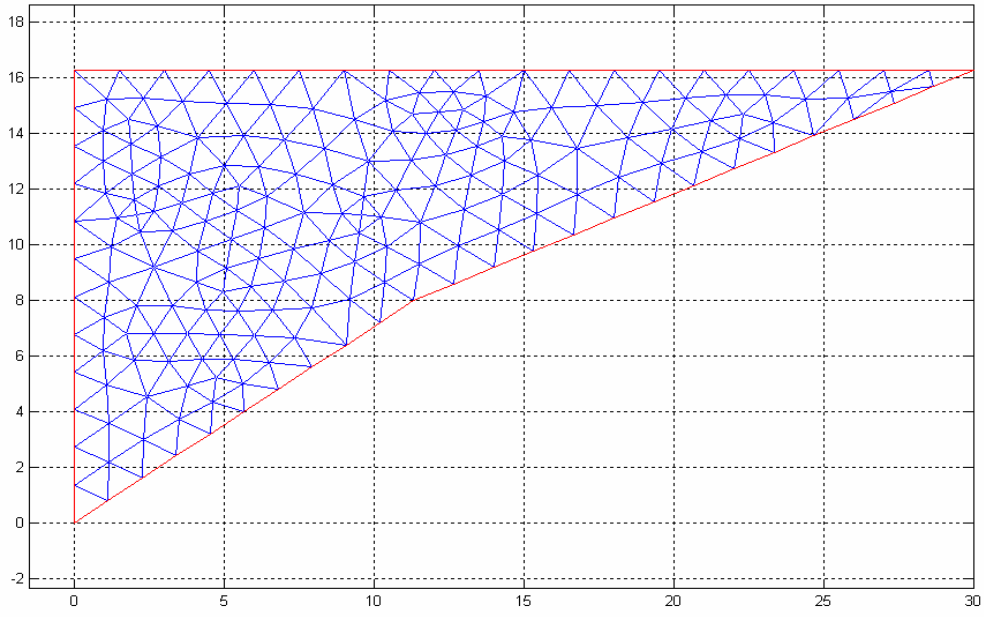

Figure 5.45 Optimal design for quadrangular plate

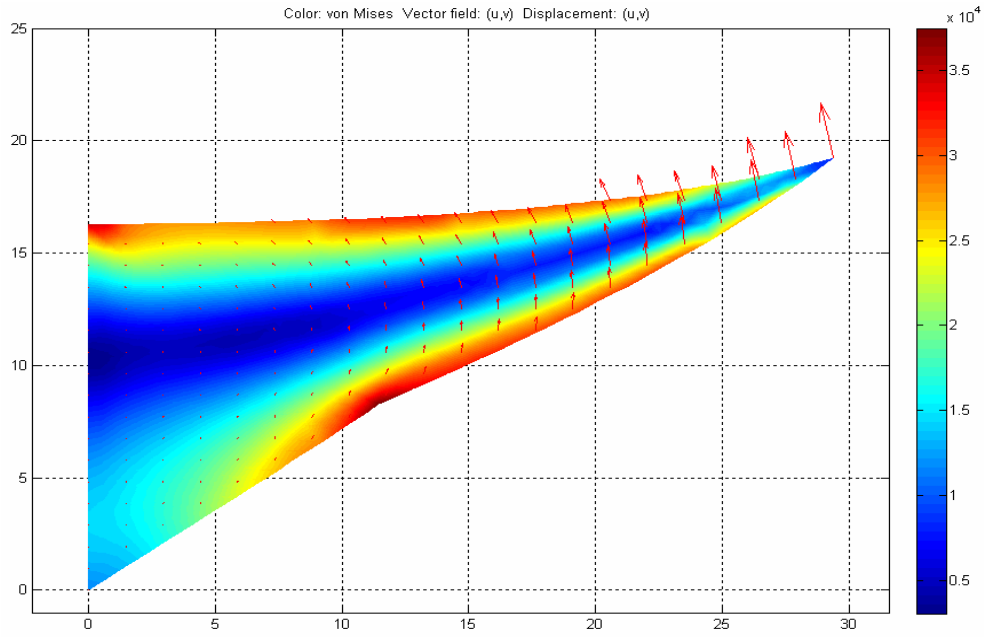

Figure 5.46 von Mises stress distribution for optimal design of quadrangular plate

5.10 Quadrangular Plate with a Circular Hole Fixed at Center – Minimum Weight Design

The ninth problem solved in this work is a quadrangular plate with a circular hole. The X center and Y center coordinates of the hole is parameterized in such a way that they are always at the middle with respect to the bottom and right edge of the plate respectively as shown in Figure 5.46. The length of the top edge of the plate is 30 inch and the thickness is 1 inch. The coordinates of the center of the hole can be expressed as $(Xc, Yc) \equiv (\frac{X1}{2},\ Y2 + \frac{Y1 - Y2}{2})$. Left edge of the plate is fixed and an outward pressure load of 2000 Psi is applied along the top edge.

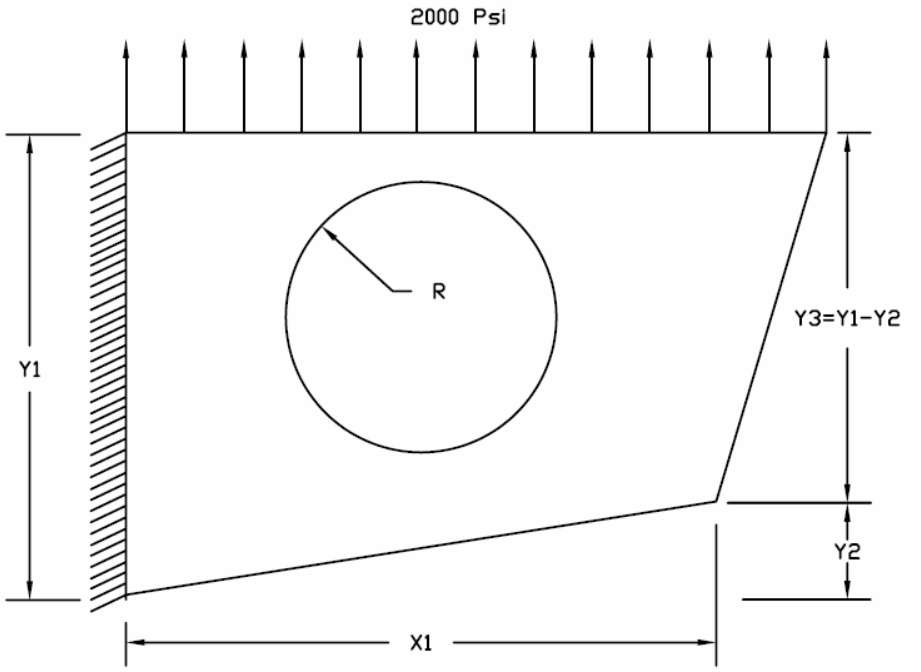

Figure 5.47 Quadrangular plate with a circular hole fixed at center

The plate is made of aluminum with Young's Modulus of Elasticity, $E = 1 \times 10^7$ Psi, Yield Strength, $\sigma_Y = 60000$ Psi, Poisson's ration, $\upsilon = 0.33$ and weight density = 0.1 lbf/inch^3.

The objective of this problem is to find the optimal lengths of left, bottom and right edges of the plate and the radius of the hole that would minimize the volume (hence the weight) of the plate such that the maximum von Mises stress developed in the structure would not exceed 40000 Psi ($\sigma_Y/1.5$). The problem formulation is as follows:

Design variable: [X1, Y1, Y2, R]

Lower and upper bounds for the design variables are, [1 15 2 1] and [30 25 12 6] respectively.

Objective function: Minimize the volume [minimize V]

Subject to –

(a) Geometric constraints (to ensure that the hole lies inside the plate):

$$X1 \geq 2R + 0.5,$$

$$Y1 - Y2 \geq 2R + 0.5$$

(b) von Mises stress constraint: Max. $\sigma_{VM} \leq 40000$ Psi.

A total of 24 experiments were performed in order to determine the best possible RBF model. For each combination of a specific sequencing technique and RBF model, two different numbers of initial DOE points have been used to create the response surface. The first set consists of 20 DOE points, whereas the second set consists of 40 DOE points. For Halton sequence, MQI RBF with 40 initial DOE points produces the

best minimum volume for the plate. In this case, the optimal design has a volume of 224.8266 $inch^3$ and the optimal values for the design variables are X1 = 13.4857 inch, Y1 = 16.6559 inch, Y2 = 8.9453 inch and R = 1 inch. The maximum von Mises stress for this design is 39606.8779 Psi. The optimization process requires 52 function evaluations for convergence. For Sobol sequence, MQI RBF with 20 initial DOE points produces the best results with a volume of 228.6264 $inch^3$. The optimal values for the design variables are X1 = 13.8423 inch, Y1 = 16.3937 inch, Y2 = 8.245 inch and R = 1.4997 inch. The maximum von Mises stress for this design is 38839.6399 Psi. The optimization process converges after 32 function evaluations. For Faure sequence, MQI RSM with 40 initial DOE points produces the best results with a volume of 224.8802 $inch^3$. The optimal values for the design variables are X1 = 11.9813 inch, Y1 = 17.5315 inch, Y2 = 9.3317 inch, and R = 1inch. The maximum von Mises stress for this design is 39286.392 Psi. The optimization process converges after 52 function evaluations.

For *fmincon* function, the same problem produces an optimal volume of 239.3363 $inch^3$ for a randomly selected initial design variables, X1 = 15, Y1 = 16, Y2 = 5, and R = 4. The optimum design variables are X1 = 4.3861 inch, Y1 = 19.1949 inch, Y2 = 5.7788 inch, and R = 1.1284 inch. Corresponding maximum von Mises stress for this case is 39993.0713 Psi. The total number of function evaluations is 153 for this case. The comparative plots of variations of design variables, volume of the plate and the maximum von Mises stress with number of function evaluations are presented in Figure 5.47, Figure 5.48 and Figure 5.49 respectively.

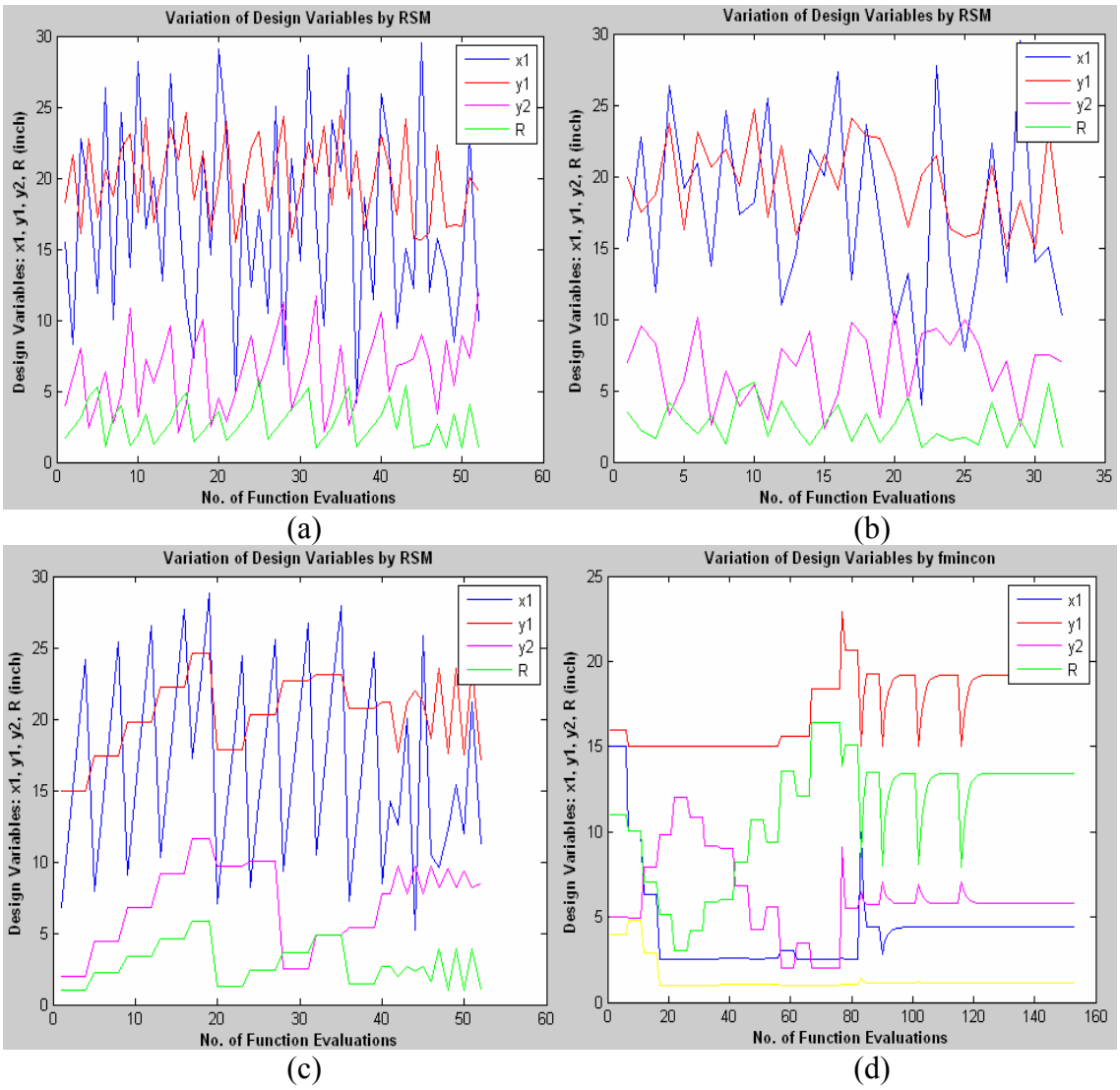

Figure 5.48 Variation of design variables for quadrangular plate with a circular hole fixed at center by (a) Halton sequence with MQI model (40 initial DOE), (b) Sobol Sequence with MQI model (20 initial DOE), (c) Faure sequence with MQI model (40 initial DOE) and (d) *fmincon* function

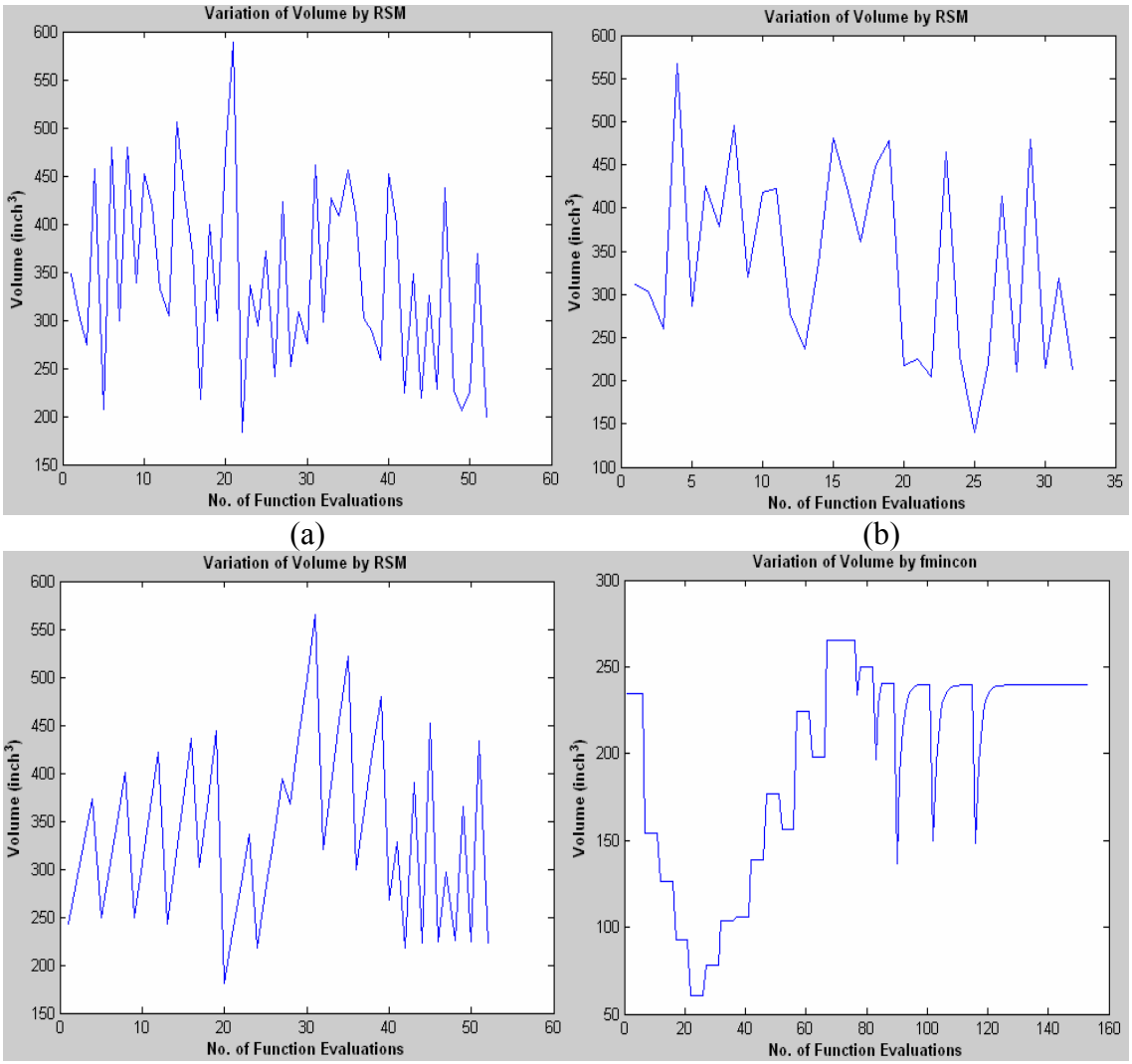

Figure 5.49 Variation of volume for quadrangular plate with a circular hole fixed at center by (a) Halton sequence with MQI model (40 initial DOE), (b) Sobol Sequence with MQI model (20 initial DOE), (c) Faure sequence with MQI model (40 initial DOE) and (d) *fmincon* function

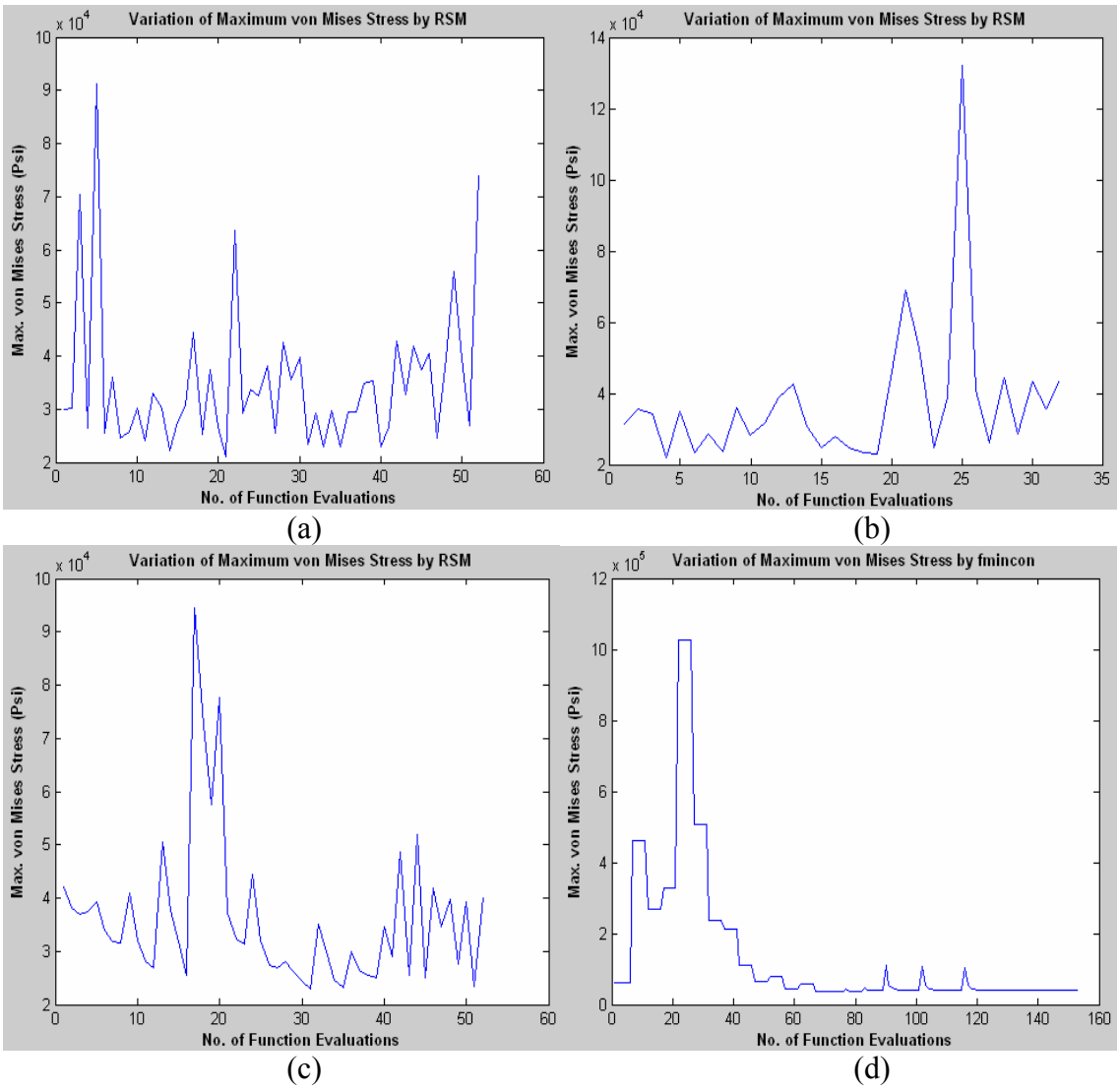

Figure 5.50 Variation of maximum von Mises stress for quadrangular plate with a circular hole fixed at center by (a) Halton sequence with MQI model (40 initial DOE), (b) Sobol Sequence with MQI model (20 initial DOE), (c) Faure sequence with MQI model (40 initial DOE) and (d) *fmincon* function

The best results obtained from the response surface optimizations were used again as the initial design variables input for another round of *fmincon* function optimizations. The lower and upper bounds for the design variables were initial input – 0.5 and initial input + 0.5 respectively. This time, Sobol sequence with MQI RSM and 20 initial DOE points produces the best results. The optimization process took 298 function evaluations to produce an improved design of X1 = 13.3423 inch, Y1 = 16.5516 inch, Y2 = 8.651 inch, and R = 1.5305 inch with a volume of 221.5685 inch^3. The maximum von Mises stress is 39954.1884 Psi. The optimal design and the von Mises stress distribution for this design are presented in Figure 5.50 and Figure 5.51 respectively.

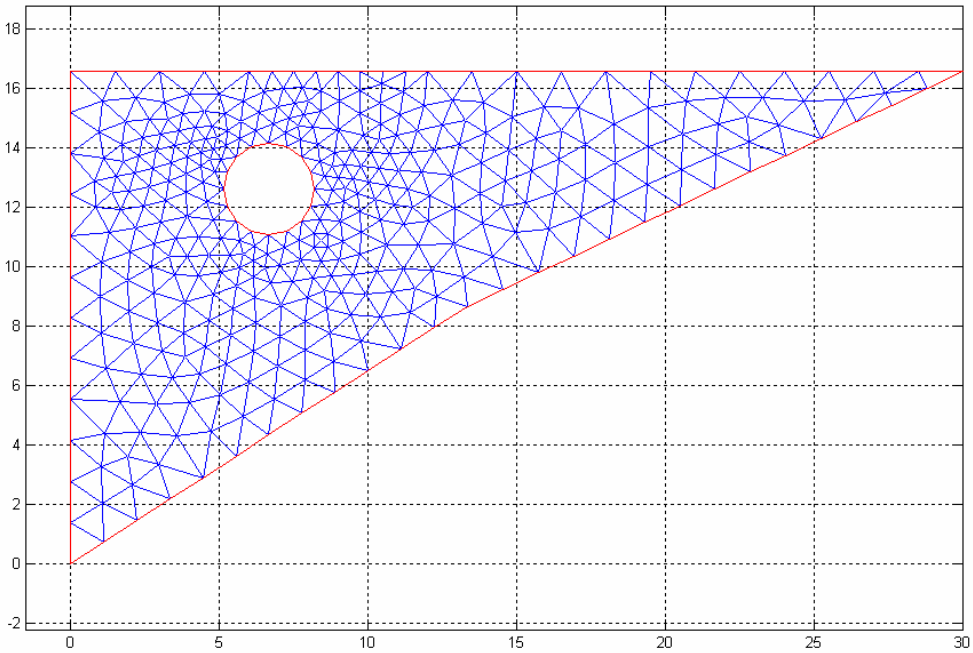

Figure 5.51 Optimal design for quadrangular plate with a circular hole fixed at center

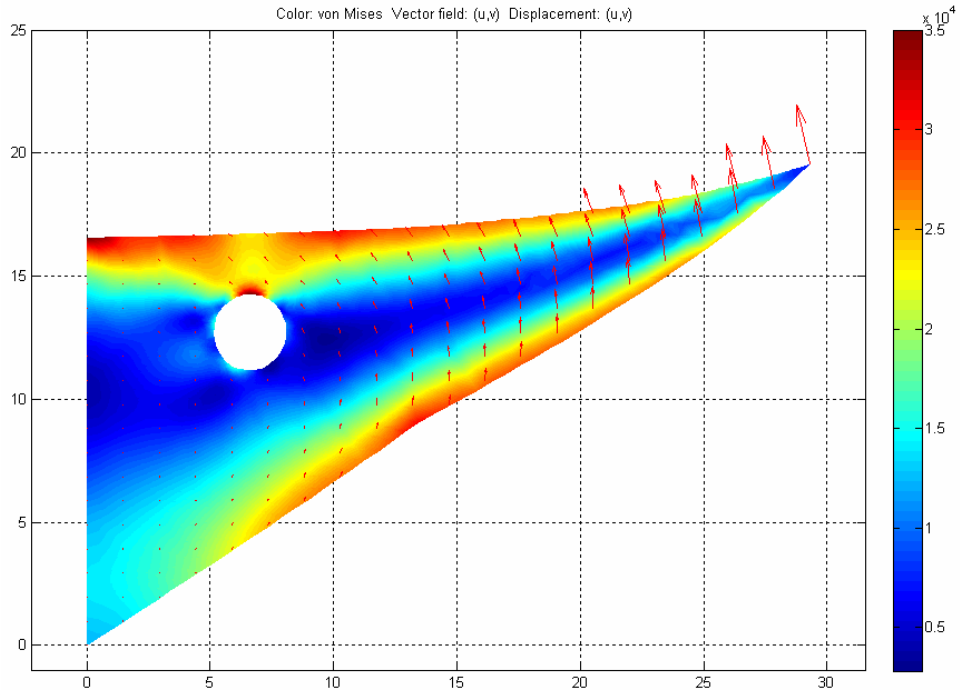

Figure 5.52 von Mises stress distribution for optimal design of quadrangular plate with a circular hole fixed at center

5.11 Quadrangular Plate with a Circular Hole with Unspecified Center Location – Minimum Weight Design

The last problem solved in this work is a quadrangular plate with a circular hole as shown in Figure 5.52. The location of the center is not specified in this problem. It can be anywhere inside the plate provided some constraints are satisfied. Left edge of the plate is fixed and an outward pressure load of 2000 Psi is applied along the top edge. The length of the top edge of the plate is 30 inch and the thickness is 1 inch.

The plate is made of aluminum with Young's Modulus of Elasticity, $E = 1 \times 10^7$ Psi, Yield Strength, $\sigma_Y = 60000$ Psi, Poisson's ration, $\upsilon = 0.33$ and weight density = 0.1 lbf/inch^3.

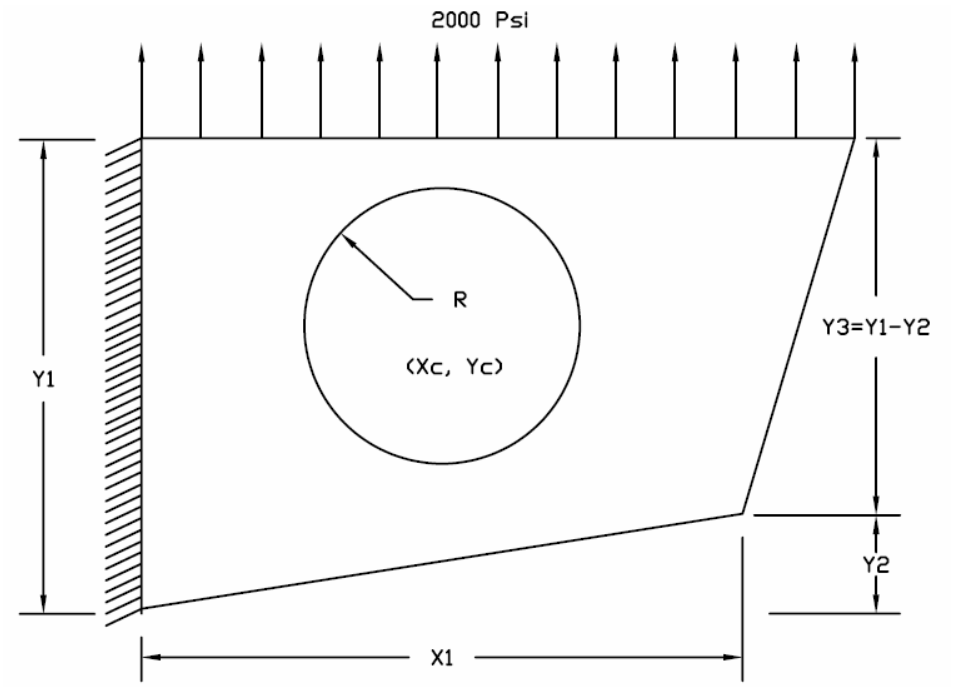

Figure 5.53 Quadrangular plate with a circular hole with unspecified center location

The objective of this problem is to find the optimal lengths of left, bottom and right edges of the plate and the center location and radius of the hole which would minimize the volume (hence the weight) of the plate such that the maximum von Mises stress developed in the structure would not exceed 40000 Psi ($\sigma_Y/1.5$). The problem formulation is as follows:

Design variable: [X1, Y1, Y2, Xc, Yc, R]

Lower and upper bounds for the design variables are, [12, 15, 2, 5, 10, 3] and [20, 20, 6, 15, 15, 5] respectively.

Objective function: Minimize the volume [minimize V]

Subject to –

(a) Geometric constraints (to ensure that the hole lies inside the plate):

$$Xc - R \geq 1, \quad Yc + R \leq Y1 - 1,$$

$$d1 \geq R + 1, \quad d2 \geq R + 1$$

Where, d1 is the shortest distance of the circular hole center from the bottom edge of the plate and is given by, $d1 = \frac{X1.Yc}{\sqrt{X1^2 + Y2^2}} - \frac{Y2.Xc}{\sqrt{X1^2 + Y2^2}}$

And d2 is the shortest distance of the circular hole center form the right edge of the plate and is given by, $d2 = \frac{(30 - X1).(Yc - Y2)}{\sqrt{(30 - X1)^2 + (Y1 - Y2)^2}} - \frac{(Y1 - Y2).(Xc - X1)}{\sqrt{(30 - X1)^2 + (Y1 - Y2)^2}}$

(b) von Mises stress constraint: Max. $\sigma_{VM} \leq 40000$ Psi.

A total of 24 experiments were performed in order to determine the best possible RBF model. For each combination of a specific sequencing technique and RBF model, two different numbers of initial DOE points have been used to create the response surface. The first set consists of 20 DOE points, whereas the second set consists of 40 DOE points. For Halton sequence, MQI RBF with 40 initial DOE points produces the best minimum volume for the plate. In this case, the optimal design has a volume of 221.5929 $inch^3$ and the optimal values for the design variables are X1 = 12.8833 inch, Y1 = 15.8807 inch, Y2 = 6 inch, Xc = 8.7544, Yc = 10 and R = 3.0338 inch. The maximum von Mises stress for this design is 39917.5646 Psi. The optimization process requires 52 function evaluations for convergence. For Sobol sequence, MQI RBF with 40 initial DOE points produces the best results with a volume of 222.8673 $inch^3$. The optimal values for the design variables are X1 = 12.5134 inch, Y1 = 15.0112 inch, Y2 =

4.5298 inch, Xc = 10.2276, Yc = 10 and R = 3 inch. The maximum von Mises stress for this design is 39789.6959 Psi. The optimization process converges after 52 function evaluations. For Faure sequence, all the RSM with 40 initial DOE points produces the same best results with a volume of 258.3025 $inch^3$. The optimal values for the design variables are X1 = 15.4519 inch, Y1 = 15.9329 inch, Y2 = 4.0525 inch, Xc = 13.3965, Yc = 10.1166 and R = 3.6997 inch. The maximum von Mises stress for this design is 37150.8379 Psi. The optimization process converges after 52 function evaluations.

For *fmincon* function, the same problem produces an optimal volume of 215.9873 $inch^3$ for a randomly selected initial design variables, X1 = 15, Y1 = 20, Y2 = 5, Xc = 12, Yc = 8 and R = 1. The optimum design variables are X1 = 12 inch, Y1 = 15.9662 inch, Y2 = 6 inch, Xc = 9.5188, Yc = 10.8025 and R = 3.054 inch. Corresponding maximum von Mises stress for this case is 39999.9326 Psi. The total number of function evaluations is 516 for this case. The comparative plots of variations of design variables, volume of the plate and the maximum von Mises stress with number of function evaluations are presented in Figure 5.53, Figure 5.54 and Figure 5.55 respectively.

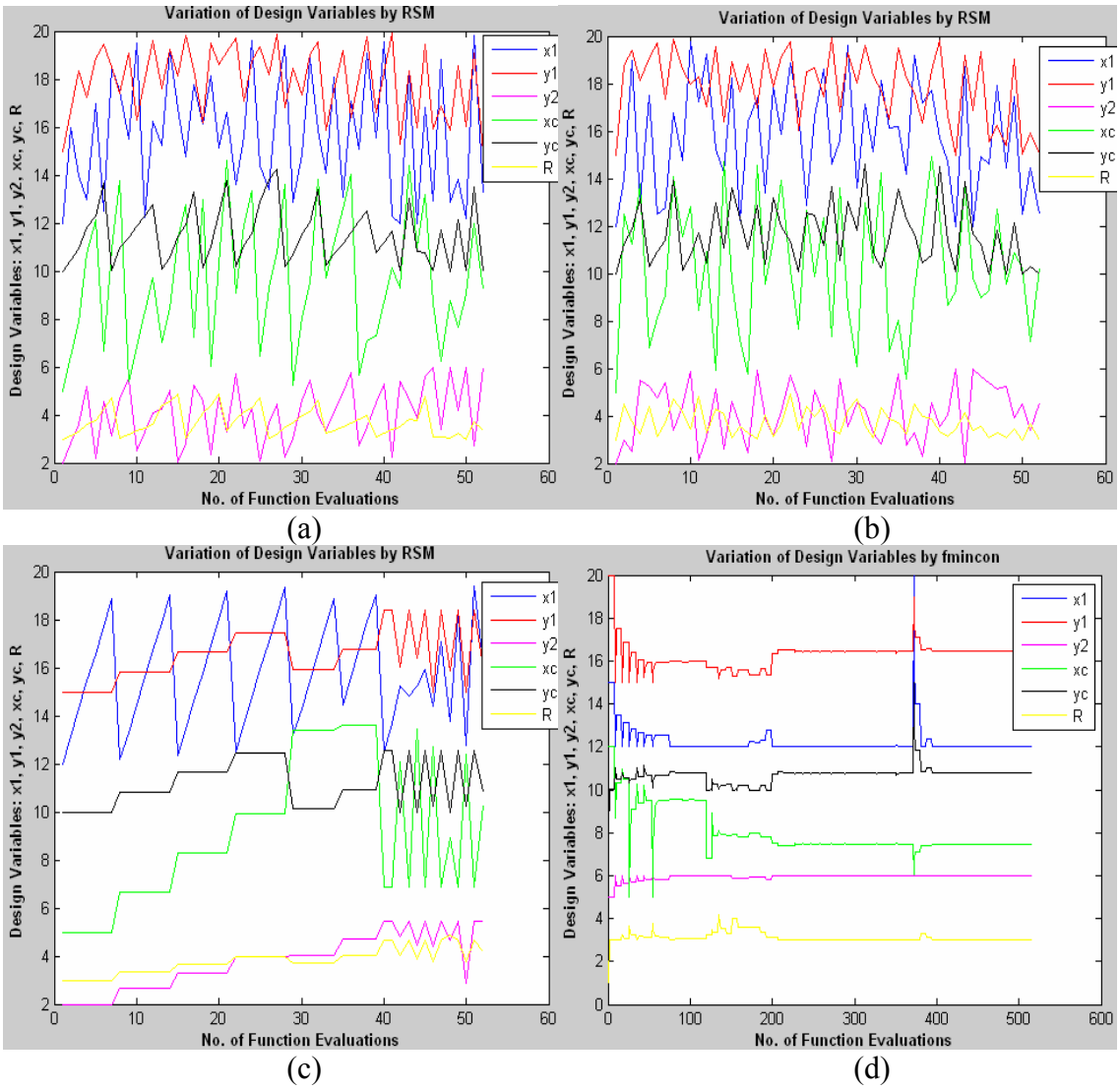

Figure 5.54 Variation of design variables for quadrangular plate with a circular hole with unspecified center location by (a) Halton sequence with MQI model (40 initial DOE), (b) Sobol Sequence with MQI model (40 initial DOE), (c) Faure sequence with MQI model (40 initial DOE) and (d) *fmincon* function

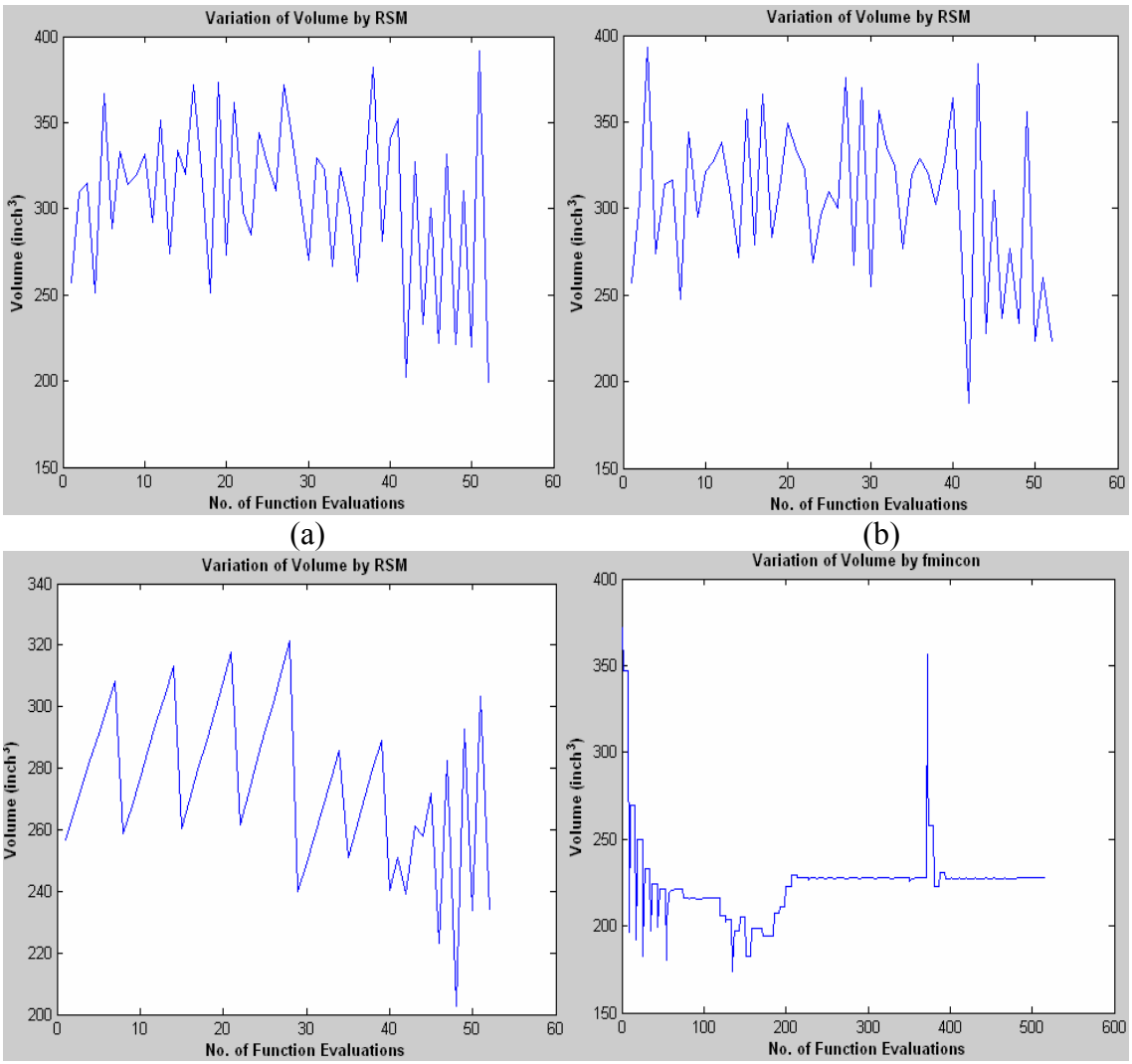

Figure 5.55 Variation of volume for quadrangular plate with a circular hole with unspecified center location by (a) Halton sequence with MQI model (40 initial DOE), (b) Sobol Sequence with MQI model (40 initial DOE), (c) Faure sequence with MQI model (40 initial DOE) and (d) *fmincon* function

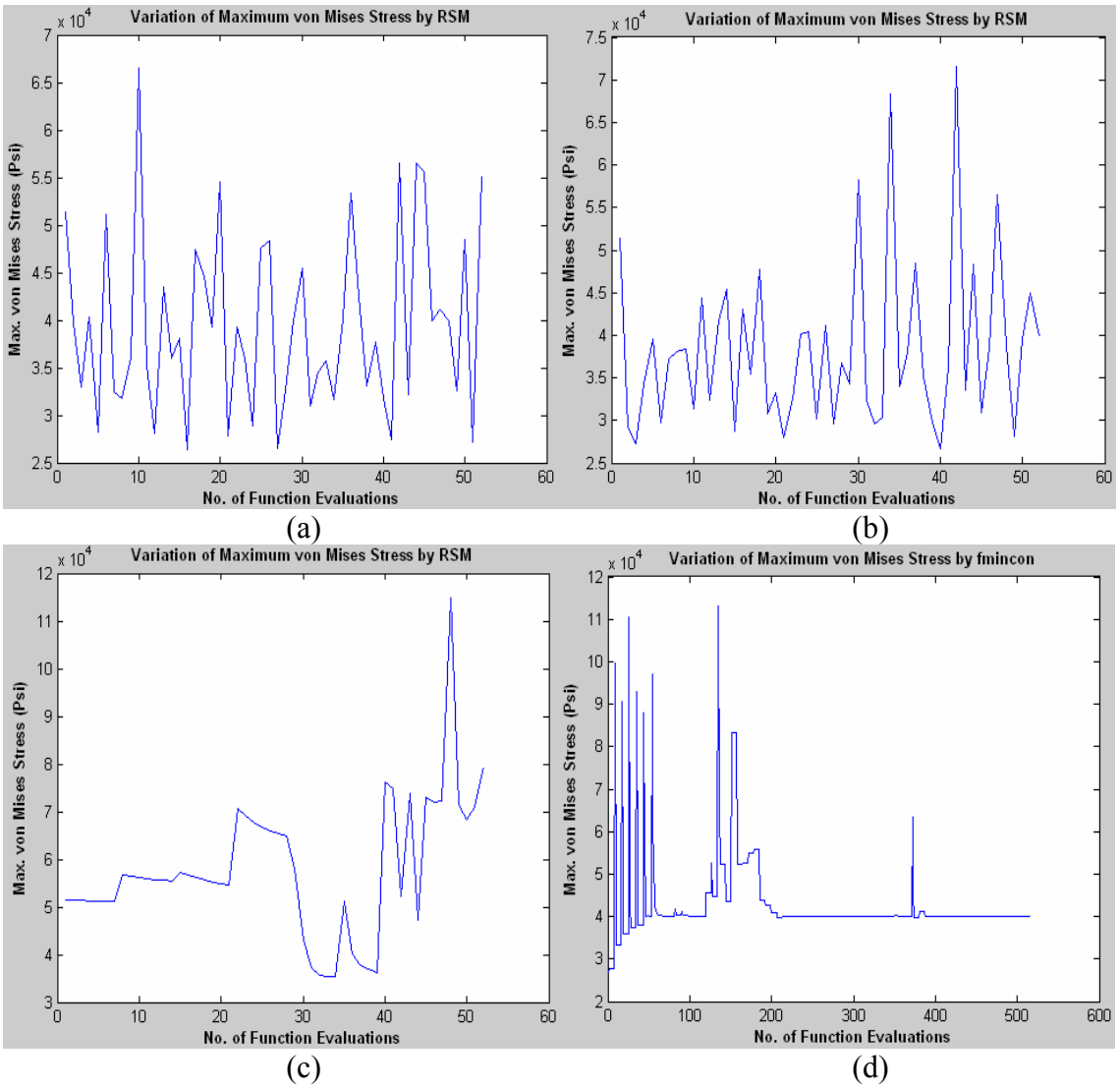

Figure 5.56 Variation of maximum von Mises stress for quadrangular plate with a circular hole with unspecified center location by (a) Halton sequence with MQI model (40 initial DOE), (b) Sobol Sequence with MQI model (40 initial DOE), (c) Faure sequence with MQI model (40 initial DOE) and (d) *fmincon* function

To improve the design further, the best results obtained from the response surface optimizations were used again as the initial design variables input for another round of *fmincon* function optimizations. The lower and upper bounds for the design

variables were initial input – 0.5 and initial input + 0.5 respectively. This time, Halton sequence with MQI RSM and 40 initial DOE points produces the best minimum volume of 210.59 inch^3. The optimal values for the design variables are X1 = 12.6983 inch, Y1 = 15.5892 inch, Y2 = 6.5 inch, Xc = 9.241, Yc = 10.4998 and R = 2.8055 inch. The corresponding maximum von Mises stress is 40000.0014 Psi. The optimization process took 260 function evaluations to converge. The optimal design and the von Mises stress distribution for this design are presented in Figure 5.56 and Figure 5.57 respectively.

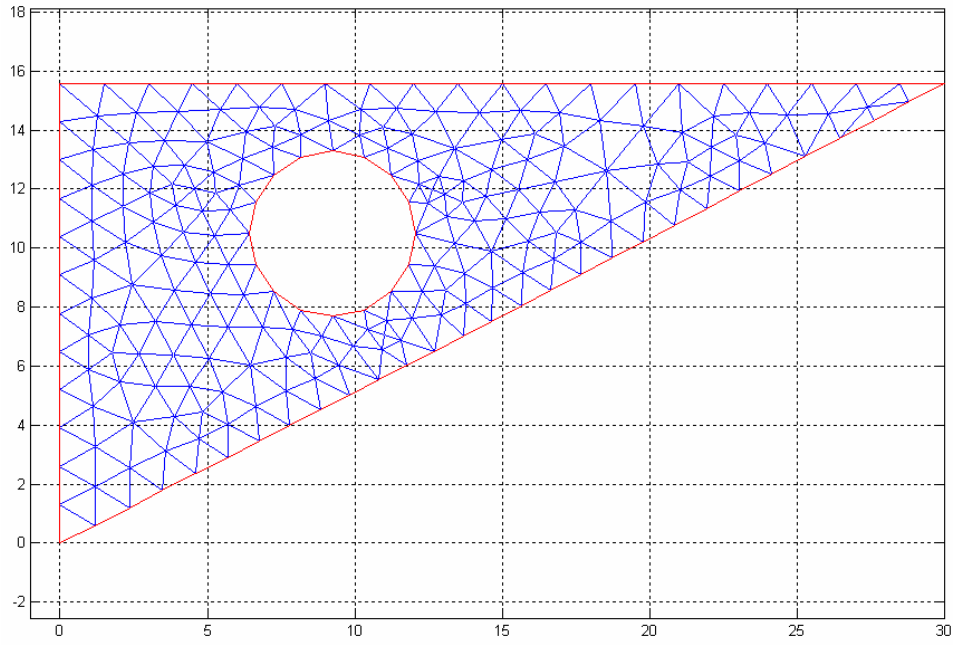

Figure 5.57 Optimal design for quadrangular plate with a circular hole with unspecified center location

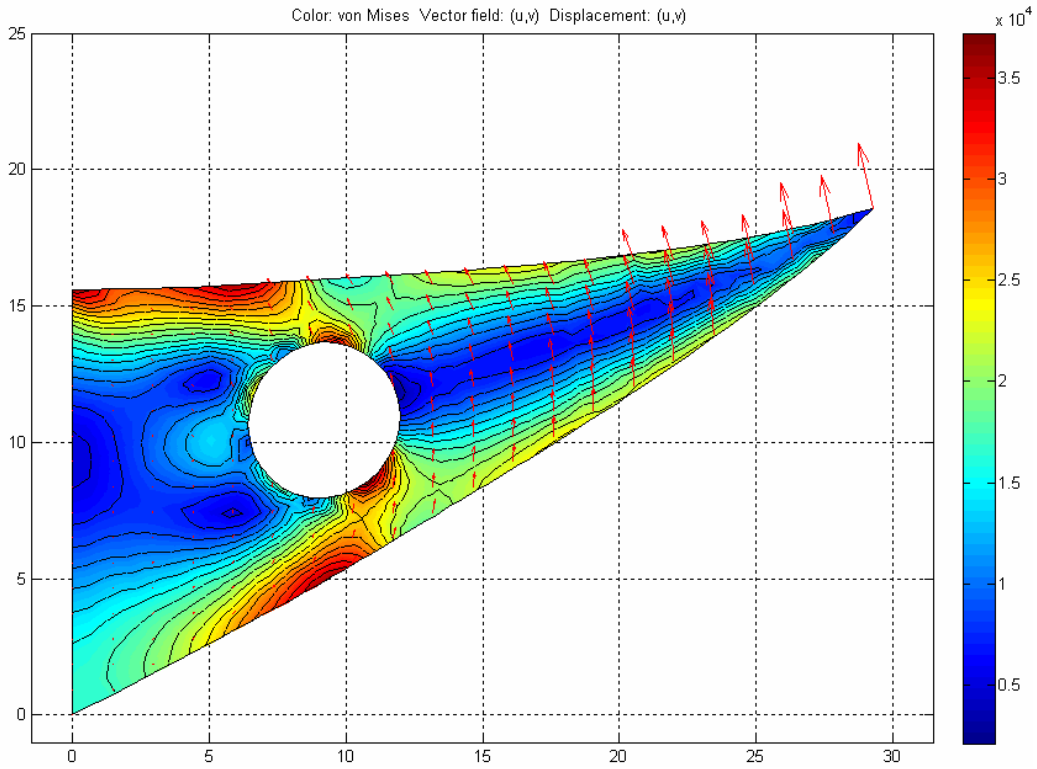

Figure 5.58 von Mises stress distribution for optimal design for quadrangular plate with a circular hole with unspecified center location

5.12 Discussions on the Results

In this chapter, the feasibility of applying the proposed scheme for structural optimization has been demonstrated successfully. Except for a few instances, the proposed method outperformed MATLAB built-in optimization function *fmincon* in terms of finding the better optimum designs and the number of function evaluations requirements. The definition of the ten example problems solved in this research and the experimental combinations of different RSM models and LDS sequences are listed in Table 5.1 and Table 5.2 respectively. In the first problem all the combinations of radial

basis functions and sequencing methods produced the same optimum results. Although direct *fmincon* also produced the same optimum result for the minimum volume, the center location of the hole is not symmetric along the length of the plate. Moreover, it took more function evaluations (45 function evaluations) than the response surface optimization (22 function evaluations).

Table 5.1 Definitions of Solved Example Problems

No	Problem Definition
1	Determining the optimal location and radius of a hole for minimum weight design of a rectangular plate with one circular hole.
2	Determining the optimal location and radius of a hole for minimum weight design of a rectangular plate with two circular holes.
3	Stress minimization of a rectangular plate with three circular holes by finding the optimal locations for the holes.
4	Shape optimization of a five stepped cantilever beam.
5	Minimum weight design of a trapezoidal plate.
6	Weight minimization of a trapezoidal plate with one circular hole by finding the heights of two parallel sides and the radius of the hole.
7	Weight minimization of a trapezoidal plate with one circular hole by finding the heights of two parallel sides and the optimal location and radius of the hole.
8	Minimum weight design of a quadrangular plate.
9	Determination of the length of three sides and the radius of the hole for minimum weight design of a quadrangular plate with one circular hole.
10	Determination of the length of three sides and the location and radius of the hole for minimum weight design of a quadrangular plate with one circular hole.

Again in the second problem, all the combinations of radial basis functions and sequencing methods produced the same optimum results. In this case direct *fmincon* optimization required equal number of function evaluations (22 function evaluations) to

end up with the same results. In seventh and tenth problem, direct *fmincon* optimization produced better results than response surface optimization method. However, in both the cases, response surface optimization method reached very close (0.038 % for seventh problem and 2.595 % for tenth problem) to the optimum results achieved by direct *fmincon* optimization with a less number of function evaluations. The list of best performing RBF models and DOE methods are presented in Table 5.3.

Table 5.2 List of Experimental Combinations

No.	Model	Method	DOE Level*	No.	Model	Method	DOE Level*
1	Halton	MQI	1	13	Sobol	GaussI	1
2	Halton	MQI	2	14	Sobol	GaussI	2
3	Halton	MQR	1	15	Sobol	GaussR	1
4	Halton	MQR	2	16	Sobol	GaussR	2
5	Halton	GaussI	1	17	Faure	MQI	1
6	Halton	GaussI	2	18	Faure	MQI	2
7	Halton	GaussR	1	19	Faure	MQR	1
8	Halton	GaussR	2	20	Faure	MQR	2
9	Sobol	MQI	1	21	Faure	GaussI	1
10	Sobol	MQI	2	22	Faure	GaussI	2
11	Sobol	MQR	1	23	Faure	GaussR	1
12	Sobol	MQR	2	24	Faure	GaussR	2

DOE Level:

1. *For 9th and 10th problems, initial DOE points 20, for all other problems, initial DOE points 10.*
2. *For 9th and 10th problems, initial DOE points 40, for all other problems, initial DOE points 30.*

Table 5.3 Best Performing RSM Models and DOE Methods for the Solution of Example Problems

Problem	No. of Design Variables	RSM Model	DOE Method
1	3	All	All
2	2	All	All
3	6	MQI & GuassI	Faure
4	5	MQR	Halton
5	2	MQI	Faure
6	3	GuassI	Halton
7	5	MQR	Sobol
8	3	MQI	Halton
9	4	MQI	Halton
10	6	MQI	Halton

For the ten problems solved in this research, contributions of the response surface models and the sequencing methods for achieving the best optimal results are shown in Table 5.4 and Table 5.5 respectively. From the results, it is evident that Multiquadric Interpolation (MQI) model and Halton sequencing method contributed more number of times for producing best optimum results. However, all other RBF models and sequencing methods also demonstrated their capability of producing good results for the problem solved in this research. It is to be noted here that, as discussed in chapter 3, literature survey indicates the ability of Sobol sequencing method to demonstrate more uniform space mapping in higher dimension than Halton and Faure sequencing methods. In this research the maximum number of design variables was six.

Hence, due to this small dimension, all the sequencing methods demonstrated acceptable performance in this research. It would certainly be interesting to see the performance of these methods for generating design of experiments for structural optimization with large number of design variables.

Table 5.4 Contribution of Response Surface Models for Achieving Best Optimal Design

Response Surface Model	No. of Instances Contributed to the best Optimal Design
Multiquadric Interpolation (MQI)	7
Multiquadric Regularization (MQR)	4
Gauss Interpolation (GaussI)	3
Gauss Regularization (GaussR)	3

Table 5.5 Contribution of Sequencing Methods for Achieving Best Optimal Design

Low Discrepancy Sequencing Methods	No. of Instances Contributed to the best Optimal Design
Halton	7
Faure	4
Sobol	3

For some of the problems, optimization of the actual function by *fmincon* and response surface optimization scheme were used together to investigate the effect on the final optimal designs. For these cases, initially the problems were solved by response

surface optimization and then the actual function is optimized by *fmincon*, considering the optimum results of the response surface optimization as the initial input for the design variables and optimum results of the response surface optimization ± X as the range for the design variables. Where, X is a number which would define a very narrow upper and lower bounds for the design variables. This combined technique showed some improvements of the final results than that achieved by using *fmincon* or response surface optimization individually. The comparison of results by RSM, *fmincon* and hybrid method are presented in Table 5.6.

Table 5.6 Comparison of Results by RSM, *fmincon* and Hybrid Method

Problem	Solution by RSM		Solution by *fmincon*		Solution by Hybrid Method	
	Best Objective Function	No. of Functional Evaluations	Best Objective Function	No. of Functional Evaluations	Best Objective Function	No. of Functional Evaluations
1	398.9381 $inch^3$	22	398.9381 $inch^3$	45	--	--
2	373.8053 $inch^3$	22	373.8053 $inch^3$	22	--	--
3	6002.8299 Psi	42	6111.1 Psi	506	--	--
4	14.8820 Hz	42	13.1653 Hz	1005	14.9598 Hz	1005
5	273.3937 $inch^3$	22	277.542 $inch^3$	22	270.3715 $inch^3$	19
6	406.4515 $inch^3$	42	408.8521 $inch^3$	114	400.8658 $inch^3$	54
7	316.8925 $inch^3$	42	316.7711 $inch^3$	285	300.2922 $inch^3$	326
8	223.4073 $inch^3$	42	243.1761 $inch^3$	68	215.9669 $inch^3$	77
9	224.8266 $inch^3$	52	239.3363 $inch^3$	153	221.5685 $inch^3$	298
10	221.5929 $inch^3$	52	215.9873 $inch^3$	516	210.59 $inch^3$	260

Although this hybrid technique could improve the final design to some extant, this has some problems also. When the optimal result of the response surface optimization is very near or on the border of the design space, using that optimal result as the initial input and defining the range of the design variable based on that could change the final dimensions of the structure that was initially intended due to the changes in the design space. Again, this combined technique could be very time consuming as in the second phase, *fmincon* might require large number of function evaluations before the solution is converged.

CHAPTER 6

CONCLUSIONS AND RECOMMENDATIONS

6.1 Conclusions

In this research, an effective and simple structural optimization scheme based on response surface methodology (RSM) and design of experiments (DOE) has been successfully developed and implemented for solving computationally expensive design optimization problems. For this purpose a design optimization code was written in MATLAB. Four different radial basis function models namely, Multiquadric Interpolation, Multiquadric Regularization, Gauss Interpolation, and Gauss Regularization were utilized for constructing the meta models and three different Quasi-Monte Carlo sequencing methods known as Halton sequence, Faure sequence, and Sobol sequence were used to generate the design of experiments. MATLAB Partial Differential Equation Toolbox was used for finite element model development and determining the true response of the design problems.

Ten different design optimization problems have been solved successfully using the proposed optimization scheme. The results thus obtained have been compared to that achieved by solving the same problems using MATLAB optimization function *fmincon*. It was observed that the RSM based optimization scheme produced better results than *fmincon* function in most of the cases. Only for two problems *fmincon* achieved better optimum results than the proposed method. However, even for those

two problems the proposed method was very close to the results obtained by *fmincon*. Moreover, except for the second and fifth problems where the number of function evaluations were equal for both the problems, the number of function evaluations and the computation time were significantly less for the proposed RSM based optimization scheme.

This research demonstrated the applicability of the various types of radial basis functions for response surface creation/ meta modeling purpose and the use of different Quasi-Monte Carlo sequencing method for generation of design of experiments for structural design optimization. Based on the results obtained in this research, it can be said that, it is not wise to recommend any specific radial basis function for meta modeling and any specific sequencing method for design of experiment purpose for all design optimization problems. Performance of any particular radial basis function and sequencing method is rather problem dependent and all the radial basis function models and sequencing methods studied in this research demonstrated their applicability for design optimization purpose. It is recommended to use more than one radial basis functions and sequencing methods if possible while solving any specific problem so that the best suited combinations could be determined by comparing their results.

6.2 Recommendations for Future Work

The following studies are suggested to extend the applications of the proposed optimization scheme:

1. In this study, MATLAB optimization function *fmincon* was used to perform the response surface optimization, which is a local optimizer. Instead of *fmincon*, a global search technique can be utilized for response surface optimization.
2. Problems associated with large dimension of design variables should be studied to examine the performance of the Quasi-Monte Carlo sequencing methods used for the generation of design of experiments with higher dimensions.
3. The proposed optimization algorithm can be modified and extended to solve multi objective structural optimization problems.
4. Instead of using MATLAB Partial Differential Equation Toolbox which is capable of only two dimensional modeling, the performance of the proposed optimization scheme can be studied by using it with a more powerful finite element code, capable of handling three dimensional modeling of complex structures.
5. This method can be studied to solve more complex problems involving large non-linear characteristics, topology optimization etc.

APPENDIX A

DERIVATION OF THE SHORTEST DISTANCE FROM THE CENTER OF THE CIRCLE TO THE EDGE OF THE TRAPIZOIDAL/QUADRANGULAR PLATE

A1. Derivation of the shortest distance, d from the center of the circle, P to the edge AB of the trapezoidal plate:

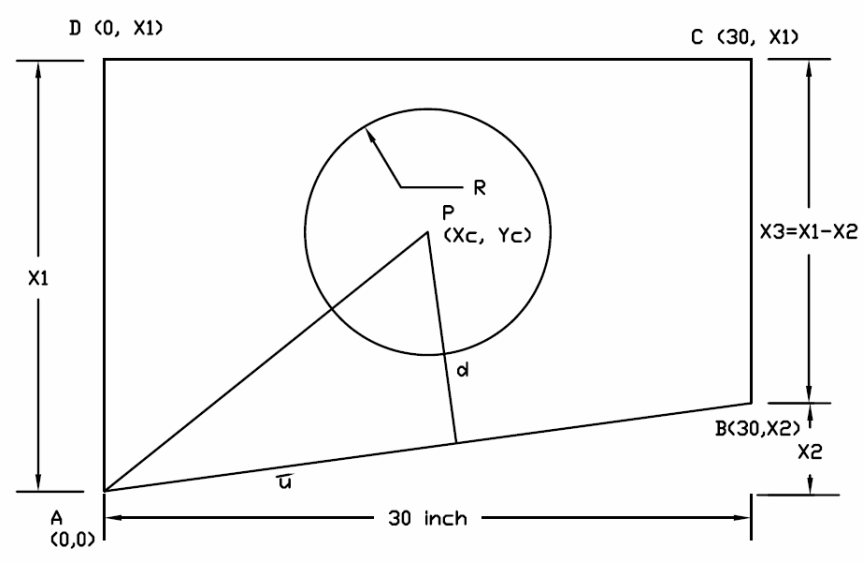

Figure A1 Derivation of the shortest distance from the center of the circle to the edge AB of the trapezoidal plate

$$\overrightarrow{AP} = Xc.\hat{i} + Yc.\hat{j}$$

$$\overrightarrow{AB} = 30.\hat{i} + X2.\hat{j}$$

$$\hat{u} = \frac{\overrightarrow{AB}}{\left|\overrightarrow{AB}\right|} = \frac{30.\hat{i} + X2.\hat{j}}{\sqrt{(30)^2 + X2^2}} = \frac{30}{\sqrt{900 + X2^2}}\hat{i} + \frac{X2}{\sqrt{900 + X2^2}}\hat{j}$$

$$d.\hat{k} = \left|\hat{u} \times \overrightarrow{AP}\right| = \begin{vmatrix} \hat{i} & \hat{j} & \hat{k} \\ \frac{30}{\sqrt{900 + X2^2}} & \frac{X2}{\sqrt{900 + X2^2}} & 0 \\ Xc & Yc & 0 \end{vmatrix} = \left[\frac{30.Yc}{\sqrt{900 + X2^2}} - \frac{X2.Xc}{\sqrt{900 + X2^2}}\right].\hat{k}$$

$$\therefore d = \frac{30.Yc}{\sqrt{900 + X2^2}} - \frac{X2.Xc}{\sqrt{900 + X2^2}}$$

A2. Derivation of the shortest distance, d1 and d2 from the center of the circle, P to the edge AB and BC respectively of the quadrangular plate:

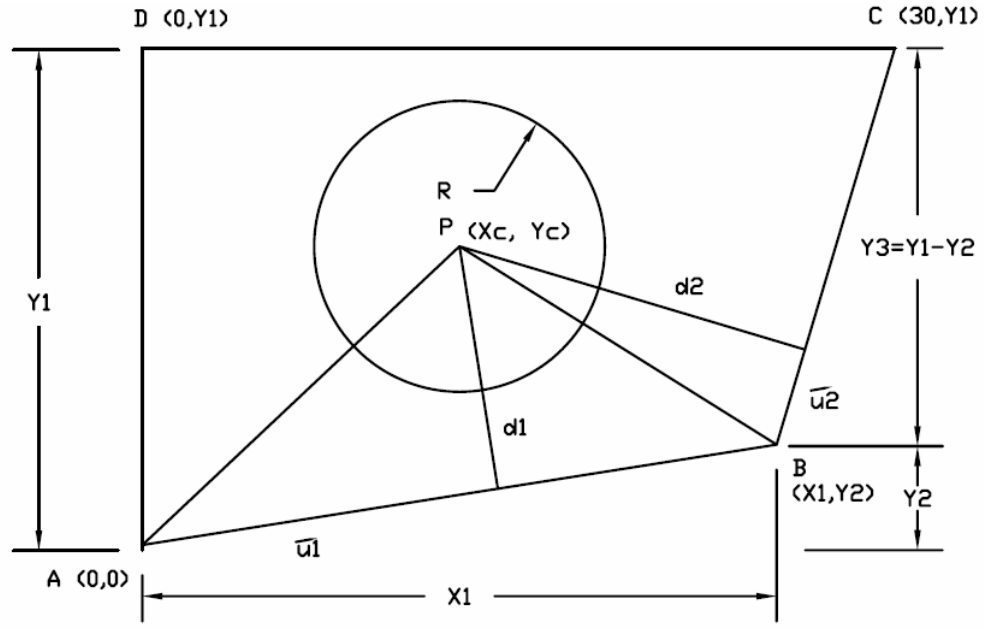

Figure A2 Derivation of the shortest distance from the center of the circle to the edge AB and BC of the quadrangular plate

$$\overrightarrow{AP} = Xc.\hat{i} + Yc.\hat{j}$$

$$\overrightarrow{BP} = (Xc - X1).\hat{i} + (Yc - Y2).\hat{j}$$

$$\overrightarrow{AB} = X1.\hat{i} + Y2.\hat{j}$$

$$\overrightarrow{BC} = (30 - X1).\hat{i} + (Y1 - Y2).\hat{j}$$

$$\hat{u1} = \frac{\overrightarrow{AB}}{\left|\overrightarrow{AB}\right|} = \frac{X1.\hat{i} + Y2.\hat{j}}{\sqrt{X1^2 + Y2^2}} = \frac{X1}{\sqrt{X1^2 + Y2^2}}\hat{i} + \frac{Y2}{\sqrt{X1^2 + Y2^2}}\hat{j}$$

$$\hat{u}2 = \frac{\overrightarrow{BC}}{\left|\overrightarrow{BC}\right|} = \frac{30 - X1}{\sqrt{(30 - X1)^2 + (Y1 - Y2)^2}}\hat{i} + \frac{Y1 - Y2}{\sqrt{(30 - X1)^2 + (Y1 - Y2)^2}}\hat{j}$$

$$d1.\hat{k} = \left|\hat{u}1 \times \overrightarrow{AP}\right| = \begin{vmatrix} \hat{i} & \hat{j} & \hat{k} \\ \dfrac{X1}{\sqrt{X1^2 + Y2^2}} & \dfrac{Y2}{\sqrt{X1^2 + Y2^2}} & 0 \\ Xc & Yc & 0 \end{vmatrix} = \left[\frac{X1.Yc}{\sqrt{X1^2 + Y2^2}} - \frac{Y2.Xc}{\sqrt{X1^2 + Y2^2}}\right].\hat{k}$$

$$\therefore d1 = \frac{X1.Yc}{\sqrt{X1^2 + Y2^2}} - \frac{Y2.Xc}{\sqrt{X1^2 + Y2^2}}$$

$$d2.\hat{k} = \left|\hat{u}2 \times \overrightarrow{BP}\right| = \begin{vmatrix} \hat{i} & \hat{j} & \hat{k} \\ \dfrac{30 - X1}{\sqrt{(30 - X1)^2 + (Y1 - Y2)^2}} & \dfrac{Y1 - Y2}{\sqrt{(30 - X1)^2 + (Y1 - Y2)^2}} & 0 \\ Xc - X1 & Yc - Y2 & 0 \end{vmatrix}$$

$$= \left[\frac{(30 - X1).(Yc - Y2)}{\sqrt{(30 - X1)^2 + (Y1 - Y2)^2}} - \frac{(Y1 - Y2).(Xc - X1)}{\sqrt{(30 - X1)^2 + (Y1 - Y2)^2}}\right].\hat{k}$$

$$\therefore d2 = \frac{(30 - X1).(Yc - Y2)}{\sqrt{(30 - X1)^2 + (Y1 - Y2)^2}} - \frac{(Y1 - Y2).(Xc - X1)}{\sqrt{(30 - X1)^2 + (Y1 - Y2)^2}}$$

REFERENCES

[1] G. Mastinu, M. Gobbi, and C. Miano, "Optimal Design of Complex Mechanical Systems with Applications to Vehicle Engineering", Springer-Verlag, Berlin, Heidelberg, 2006

[2] A. A. Mullur and A. Messac, "Extended Radial Basis functions: More Flexible and Effective Metamodeling", AIAA Journal, Vol. 43, No. 6, June 2005, pp.1306-1315

[3] W. J. Roux, N. Stander, and R.T. Haftka, "Response Surface Approximations for Structural Optimization", Int. J. Numer. Meth. Engng. **42**, 1998, pp. 517-534

[4] T.W. Simpson, A. J. Booker, D. Ghosh, A. A. Giunta, P. N. Koch, and R.-J. Yang, "Approximation Methods in Multidisciplinary Analysis and Optimization: A Panel Discussion", Struct Multidisc Optim, 27, 2004, pp. 302-313

[5] A. D. Belegundu, and T. R. Chandrupatla, "Optimization Concepts and Applications in Engineering", Prentice Hall, New Jersey, 1999

[6] U. Kirsch, "Structural Optimization – Fundamentals and Applications", Springer-Verlag, Berlin Heidelberg, 1993

[7] G. N. Vanderplaats, "Approximation concepts for Structural Design Optimization", In: Geometry and Optimization Techniques for Structural

Design, S. Kodiyalam, and M. Saxena (Eds.), 1994, Computational Mechanics Publications, Elsevier Applied Science, pp. 289-317

[8] Y. S. Ong, P. B. Nair, A. J. Keane, and K. W. Wong, "Surrogate-Assisted Evolutionary Optimization Frameworks for High-Fidelity Engineering Design Problems", In: Knowledge Incorporation in Evolutionary Computation, J. Yaochu (Ed.), Springer, 2004, pp. 307-332

[9] S. Kodiyalam, "Structural Shape Optimization", In: Geometry and Optimization Techniques for Structural Design, S. Kodiyalam, and M. Saxena (Eds.), 1994, Computational Mechanics Publications, Elsevier Applied Science, pp. 318-339

[10] Optimization Toolbox 4 - User's Guide, 2008

[11] R. H. Myers, A. I. Khuri, and W. H. Carter, "Response Surface Methodology: 1966-1988", Technometrics, Vol. 31, No.2, 1989, pp. 137-157

[12] J.-F.M. Barthelemy, and R. T. Haftka, "Approximation Concepts for Optimum Structural Design – A Review", Structural Optimization, 5, 1993, 129-144

[13] R. Jin, W. Chen and T. W. Simpson, "Comparative Study of Metamodeling Techniques under Multiple Modeling Criteria", AIAA – 2000-4801

[14] J. Auzins, and R. Rikards, "Approximation Techniques for Response Surface Method in Structural Optimization", In: Proceedings of Fourth World Congress of Structural and Multidisciplinary Optimization (WCSMO – 4), Dalian, China, June 4-8, 2001,

[15] T. W. Simpson, J. D. Peplinski, P. N. Koch, and J. K. Allen, "Metamodels for Computer-based Engineering Design: Survay and Recommendations", Engineering with Computers, 17, 2001, pp. 129-150

[16] R. L. Hardy, "Multiquadratic Equations of Topology and Other Irregular Surfaces", J. Geophys. Res., 76, 1971, pp. 1905-1915

[17] S. Ripa, "An Algorithm for Selecting a Good Value for the Parameter C", Advances in Computational Mathematics 11 (1999) 193-210

[18] B .P. Wang, "Parameter Optimization in Radial Basis Function Response surface Approximation", AIAA – 2002-1344

[19] B. P. Wang, "Parameter Optimization in Multiquadric Response Surface Approximations", Structural and Multidisciplinary Optimization, 26, 2004, pp. 219-223.

[20] S. Wang and M. Y. Wang, "Radial Basis Functions and Level Set Method for Structural Topology Optimization", Int. J. Numer. Meth. Engng 2006; **65:** 2060-2090

[21] C. Harpham, C. W. Dawson, "The Effect of Different Basis Functions on a Radial Basis Function Network for Time Series Prediction: A Comparative Study", Neurocomputing, 69, 2006, pp. 2161-2170

[22] H. Fang, M. R. Rohani, and M. F. Horstemeyer, "Multiobjective Crashworthiness Optimization with Radial Basis Functions", AIAA – 2004-4487

[23] R. Frank, “Scattered Data Interpolation: Tests of Some Methods”, Math. Comput., Vol. 38, No. 157, 1982, pp. 181-200

[24] E. J. Kansa, “Multiquadrics – a Scattered Data Approximation Scheme with Applications to Computational Fluid Dynamics”, I. Comput. Math. Appl., 19, 127-145, 1990.

[25] A. A. Giunta, S. F. Wojtkiewicz Jr., and M. S. Eldred, “Overview of Modern Design of Experiments Methods for Computational Simulations”, AIAA – 2003-649

[26] T. W. Simpson, D. K. J. Lin, and W. Chen, “Sampling Strategies for Computer Experiments: Design and Analysis”, International Journal of Reliability and Applications, August, 2001

[27] U. M. Diwekar and J. R. Kalagnanam, “Efficient Sampling Technique for Optimization under Uncertainty”, AIChE Journal, Vol. 43, No. 2, 1997, pp. 440-447

[28] L. Kocis and W. J. Whiten, “Computational Investigations of Low-Discrepancy Sequences”, ACM Transactions on Mathematical Software, Vol. 23, No. 2, 1997, pp. 266-294

[29] F. Levi, M. Gobbi, and G. Mastinu, “An Application of Multi-Objective Stochastic Optimization to Structural Design”, Struct. Multidisc. Optim. 29, 2005, 272-284

[30] A. Nelson, J. J. Alonso, and T. H. Pulliam, “Multi-Fidelity Aerodynamic Optimization Using Treed Meta-Models”, AIAA – 2007-4057

[31] C.-H. Tho, and B. P. Wang, "Improved Structural Impact Performance Using Sequential Multiquadric Regression with Output Space Mapping", AIAA – 2007-1899

[32] S. Galanti, and A. Jung, "Low-Discrepancy Sequences: Monte Carlo Simulations of Option Prices", Journal of Derivatives, Fall 1997, pp. 63-83

[33] Partial Differential Equation Toolbox for Use with MATLAB – User's Guide, Version 1, 2006

[34] J.-Q. Min, and M. Jixie, "Numerical Simulation of Straight Fins Heat Conduction Based on PDE Tool", Coal Mine Machinery, Vol. 27, No. 1, 2006, pp. 48-50

[35] S. Makarov, "MoM Antenna Simulations with Matlab: RWG Basis Functions", IEEE Antennas and Propagation Magazine, Vol. 43, No. 5, 2001, pp. 100-107

[36] M. D. Magistris, "A MATLAB-Based Virtual Laboratory for Teaching Introductory Quasi-Stationary Electromagnetics", IEEE Transaction on Education, Vol. 48, No. 1, 2005, pp. 81-88

[37] M. J. L. Orr, "Introduction to Radial Basis Function Networks", Center for Cognitive Science, University of Edinburgh, Scotland, 1996

BIOGRAPHICAL INFORMATION

Faisal Tanveer Mosharrof, the eldest son of Mosharrof Hossain and Shaheen Mosharrof, was born in February 25, 1981, in Dhaka, Bangladesh. He earned his Bachelor of Science in Mechanical Engineering Degree in February, 2004 from Bangladesh University of Engineering and Technology (BUET), Dhaka, Bangladesh. After his undergraduate studies, he joined in Navana CNG Limited, the leading compressed natural gas service provider in Bangladesh in May, 2004 and worked there till April, 2006 as an Assistant Manager.

He started his graduate studies in the University of Texas at Arlington in May, 2006 and earned Master of Science in Mechanical Engineering Degree in August, 2008. During Masters studies, Faisal conducted his research on the development and implementation of a structural optimization scheme using radial basis function based response surface model and MATLAB Partial Differential Equation Toolbox under the supervision of Dr. Bo Ping Wang.